

**Stratigraphy of the Parguera Limestone exposed in Cerro de
Abra, Guánica, Puerto Rico, Late Cretaceous of Southwestern
Puerto Rico**

by

RAFAEL J. MORALES FERNÁNDEZ

Thesis submitted in partial fulfillment of the requirements for the degree of

MASTER IN SCIENCE
in
GEOLOGY

UNIVERSITY OF PUERTO RICO
MAYAGÜEZ CAMPUS
2017

Approved by:

Hernán Santos Mercado, Ph.D.
President, Graduate Committee

Date

James Joyce, Ph.D.
Member, Graduate Committee

Date

Wilson R. Ramírez, Ph.D.
Member, Graduate Committee

Date

Evi De La Rosa Ricciardi, Ph.D.
Representative of Graduate Studies

Date

Lizzette Rodríguez, Ph.D.
Director of the Department

Date

ABSTRACT

A sequence stratigraphic and facies distribution model was developed by performing stratigraphic and lithofacies analyses of the Late Cretaceous volcano-sedimentary rock succession exposed at Cerro de Abra, north of the Bahía de Guánica. These rocks are part of the Parguera Limestone, specifically the lower and middle members, Bahía Fosforescente and Punta Papayo Members respectively. The stratigraphic section represents a geologic record from Santonian to Middle Campanian. The depositional sequence starts with deposition of the Bahía Fosforescente Member represented by a transgressive system tracts (TST) at the base and a highstand system tract (HST) during the Santonian, similar to the deposits of the Cotuí Limestone, north of the Lajas Valley. This is followed by a relative drop in sea level and up-dip volcanism that resulted in deposition of volcanic arenites with limestone intraclasts and planktonic foraminifera, and slumped blocks close to the base of the unconformity. These deposits are interpreted as result of a forced regression, and represents the start of deposition of the Punta Papayo Member of the Parguera Limestone during the Campanian. These deposits are interpreted to be stratigraphically equivalent to the Sabana Grande Formation north of the Lajas Valley. The deposits above the unconformity are interpreted to represent a forced regression, LST, TST, followed by a HST characterized by bedded, fine grained carbonates. This bedded fine-grained carbonates are equivalent to the Yauco Formation exposed north of the Lajas Valley. The models, based on lithology, fossil content and facies interpretation, integrated fieldwork and laboratory data that helped reconstruct the paleofacies and paleoenvironment of these members. This interpretation established a better stratigraphic

correlation of the lower and middle members of the Parguera Limestone with the stratigraphy of the Cotuí Limestone, Sabana Grande Formation, Guaniquilla Limestone, and Yauco Formation exposed north of this area.

RESUMEN

Un modelo de estratigráfica secuencial y de distribución de facies fue elaborado ejerciendo un análisis de la estratigrafía y las litofacies de las sucesiones de roca volcano-sedimentarias expuestas en el Cerro de Abra al norte de la Bahía de Guánica. Estas rocas son parte de las Calizas Parguera, específicamente de los miembros bajo y medio, Bahía Fosforescente y Punta Papayo respectivamente, expuestas al sur del Valle de Lajas. La sección estratigráfica representa un registro geológico del Santoniano al Campaniano medio. La secuencia deposicional comienza con el Miembro Bahía Fosforescente representado por un “transgressive system tracts” (TST) en la base y un “highstand system tract” (HST) durante el Santoniano, similar a los depósitos de las Calizas Cotuí, al norte del Valle de Lajas. A esta le sigue una baja relativa en el nivel del mar y volcanismo en zonas próximas resultando en la deposición de areniscas volcánicas con intraclastos de caliza y foraminíferos planctónicos, y bloques deslizados cerca de la base de la disconformidad. Estos depósitos se interpretan como el resultado de un “forced regression” y representan el comienzo de la deposición del Miembro Punta Papayo de las Calizas Parguera durante el Campaniano. Estos depósitos son interpretados como estratigráficamente equivalentes a la Formación Sabana Grande al norte del Valle de Lajas. Los depósitos estratigráficamente por encima de la disconformidad se interpretan como “forced regression”, LST, TST, seguidos por HST caracterizados por sedimentos finos de carbonato estratificados. Estos carbonatos estratificados son equivalentes a la Formación Yauco al norte del Valle de Lajas. Los modelos, basados en litología, contenido de fósiles

e interpretación de facies, integrados por trabajo de campo y de laboratorio, ayudaron a reconstruir las paleofacies y paleoambientes de estos miembros. Esta interpretación establece una mejor correlación estratigráfica de los miembros bajo y medio de las Calizas Parguera con la estratigrafía de las Calizas Cotuí, la Formación Sabana Grande, las Calizas Guaniquilla y la Formación Yauco, expuestas al norte de esta área.

© Rafael J. Morales-2017

A mi familia y amigos, por su desinteresado apoyo, amor incondicional,
tolerancia y aceptar los hechos...

ACKNOWLEDGEMENTS

During the development of my graduate studies in the University of Puerto Rico several persons collaborated directly and indirectly with my research. Without their support, it would've been impossible for me to finish my work. That is why I wish to dedicate this section to recognize their support.

I want to start expressing a sincere acknowledgement to my advisor, Dr. Hernán Santos, for always believing in me, your guidance and never-ending patience. For being a friend and becoming family. For the opportunity of guiding me to grow as a professional. I would also like to extend this recognition to Dr. James Joyce, also for being a friend and becoming family. For finding time at every occasion we've met to teach me more about geology and life. Also, this recognition should be extended to Dr. Wilson Ramirez for his advice in the study of carbonate rocks, many life lessons and tales, and constant support. Thanks to all the faculty of the Department of Geology, they were primordial part in my development as a student. Dr. Johannes Schellekens, thank you for everything, you will never be forgotten. Very special appreciation to the never-ending encouragement of Alex Soto, for pushing me to finish this degree and guiding me through many other phases as a professional.

Prime recognition to my wife Denise Echávez who's been always here by my side, with patience, at every crazy step I take, and for the never-ending help provided. Kind appreciations to all my friends that helped me during these years: Leandro Addarich, Arnaldo Hernández, Edgar Vélez Montes, John Conway, Keith Wilson, José R. Fonseca and Walter Soler. I would also like extend my appreciation to Marsha Irizarry and

Catherine Pérez for helping me resolve an array of situations throughout these years. Last but not least, this research would not have been possible without the never-ending support of my parents and family. I love you all and may this be another accomplishment I share with you.

TABLE OF CONTENTS

ABSTRACT	ii
RESUMEN	iv
ACKNOWLEDGEMENTS	viii
LIST OF TABLES	xi
LIST OF FIGURES	xi
LIST OF PHOTOGRAPHS	xv
CHAPTER 1.....	1
INTRODUCTION.....	1
1.1 Objective.....	4
1.2 Study Area	6
1.3 Literature Review.....	6
1.3.1 General Geology of Puerto Rico.....	6
1.3.2 Tectonic Setting of the Puerto Rico Southwest Igneous Providence	7
1.3.3 Cretaceous Volcano-sedimentary Stratigraphy.....	10
1.3.4 Previous Work.....	11
CHAPTER 2.....	15
METHODOLOGY	15
2.1 Field Work.....	15
2.2 Petrographic Analysis	16
2.3 Limestone Classification	17
2.4 Stratigraphic Correlation	20
2.5 Sequence Stratigraphy.....	20
CHAPTER 3.....	28
RESULTS.....	28
3.1 PR 116 Section.....	28
3.2 Stratigraphic Section.....	37
3.3 Cerro de Abra Type Area.....	38

CHAPTER 4	39
INTERPRETATION	39
4.1 Stratigraphy	39
4.2 Bahía Fosforescente and Punta Papayo Members depositional history	44
CHAPTER 5	48
DISCUSSION	48
5.1 Sequence Stratigraphy	48
5.2 Correlation with Previous Work.....	49
5.3 Correlation with the Stratigraphy of the Cabo Rojo-Sabana Grande Block	50
CHAPTER 6	55
CONCLUSION	55
REFERENCES	56

LIST OF TABLES

Table 1: Classification of Limestone (Dunham, 1962).....	18
Table 2: Expanded Classification of Limestone (Embry and Klovan 1971).....	18
Table 3: Folk's (1962) Classification	19

LIST OF FIGURES

Figure 1: Extract from the Geologic Map of the Parguera Area in Southwestern Puerto Rico (Almy, 1965) showing the study area.....	2
Figure 2: Geologic Map with a summary chart of the stratigraphic sequences of the Late Cretaceous of Southwestern Puerto Rico (after Santos, 1999).....	5
Figure 3: Summary chart of the stratigraphic sequences of the Late Cretaceous of southwestern Puerto Rico, as viewed by different authors (extract from Santos, 1999)	8
Figure 4: Google Earth image showing the area of study.....	9

Figure 5: Tectonic map of the Caribbean region. Plate motion and velocities are after Mann et al. (1991).....	10
Figure 6: Geologic map of Puerto Rico, GV: Guanajibo Valley, LV Lajas Valley (After Schellekens, 1993)	12
Figure 7: Basic limestone types of Folk's (1959) limestones classification	19
Figure 8: Parasequence sets (Emery & Myer, 1996; after Van Wagoner et al., 1988)	25
Figure 9: Carbonate Sequence Stratigraphy model (after, Tucker and Wright, 1990)	26
Figure 10: Forced Regression after Posamentier & Vail (1999)	27
Figure 11: Generalized Stratigraphy, Cerro de Abra Type Area	47
Figure 12: Stratigraphic correlation of this study with the rest of the studies in SW-PR	51
Figure 13: Stratigraphic Column from 0 to 26.25 m	61
Figure 14: Stratigraphic Column from 26.25 to 52.5 m	62
Figure 15: Stratigraphic Column from 52.5 to 78.75 m	63
Figure 16: Stratigraphic Column from 78.75 to 105 m	64
Figure 17: Stratigraphic Column from 105 to 131.25 m	65
Figure 18: Stratigraphic Column from 131.25 to 157.5 m	66
Figure 19: Stratigraphic Column from 157.5 to 183.75 m	67
Figure 20: Stratigraphic Column from 183.75 to 210 m	68
Figure 21: Stratigraphic Column from 210 to 236.25 m	69
Figure 22: Stratigraphic Column from 236.25 to 262.5 m	70
Figure 23: Stratigraphic Column from 262.5 to 288.75 m	71
Figure 24: Stratigraphic Column from 288.75 to 315 m	72
Figure 25: Stratigraphic Column from 315 to 341.25 m	73
Figure 26: Stratigraphic Column from 341.25 to 367.5 m	74
Figure 27: Stratigraphic Column from 367.5 to 393.75 m	75
Figure 28: Stratigraphic Column from 393.75 to 420 m	76

Figure 29: Stratigraphic Column from 420 to 446.25 m	77
Figure 30: Stratigraphic Column from 446.25 to 472.5 m	78
Figure 31: Stratigraphic Column from 472.5 to 498.75 m	79
Figure 32: Stratigraphic Column from 498.75 to 525 m	80
Figure 33: Stratigraphic Column from 525 to 551.25 m	81
Figure 34: Stratigraphic Column from 551.25 to 577.5 m	82
Figure 35: Stratigraphic Column from 577.5 to 603.75 m	83
Figure 36: Stratigraphic Column from 603.75 to 630 m	84
Figure 37: Stratigraphic Column from 630 to 656.25 m	85
Figure 38: Stratigraphic Column from 656.25 to 682.5 m	86
Figure 39: Stratigraphic Column from 682.5 to 708.75 m	87
Figure 40: Thin section images of sample from 52.9 m (10/26/11_1), grayish skeletal wack-packstone, some rudists fragments, coralline algae, few mud between grains	89
Figure 41: Thin section images of sample from 53.6 m (10/26/11_2), grayish skeletal packstone, some rudists fragments	90
Figure 42: Thin section images of sample from 97.1 m (11/25/11_1), brownish very fine grained volcanic arenite with skeletal fragments, intraclasts and planktonic foraminifera, sub-rounded to sub-angular, some high relieve minerals, micriticized	91
Figure 43: Thin section images of sample from 98.4 m (11/25/11_2), brownish very fine grained sandstone to siltstone with very few skeletal fragments, rounded to sub-angular	92
Figure 44: Thin section images of sample from 100.25 m (11/25/11_3), volcanic arenite, intraclasts, volcanic grains, angular to sub-rounded.....	93
Figure 45: Thin section images of sample from 102.05 m (11/25/11_4), volcanic arenite, intraclasts, volcanic grains, angular to sub-rounded.....	94
Figure 46: Thin section images of sample from 112.3 m (11/25/11_7), andesitic volcanic flow, feldspars, few intraclasts	95
Figure 47: Thin section images of sample from ~223 m (CJ1), columnar joints	96
Figure 48: Thin section images of sample from 551.38 m (3/21/12_1), grayish skeletal packstone, red algae present	97

Figure 49: Thin section images of sample from 552.16 m (3/21/12_2), grayish skeletal packstone	98
Figure 50: Thin section images of sample from 553.96 m (3/21/12_3), grayish skeletal wack-packstone	99
Figure 51: Thin section images of sample from 553.96 m (3/21/12_4), grayish skeletal packstone, few planktonic foraminifera	100
Figure 52: Thin section images of sample from 554.32 m (3/21/12_5), grayish planktonic rich packstone	101
Figure 53: Thin section images of sample from 556.07 m (3/28/12_1), grayish skeletal packstone, few foraminifera	102
Figure 54: Thin section images of sample from 557.08 m (3/28/12_2), planktonic foraminifera rich packstone, few Echinoderm fragments.....	103
Figure 55: Thin section images of sample from 557.86 m (3/28/12_3), grayish skeletal packstone, spicule rich with lithics	104
Figure 56: Thin section images of sample from 560.06 m (3/28/12_4), grayish skeletal packstone, few planktonic foraminifera	105
Figure 57: Thin section images of sample from 563.27 m (3/28/12_5), grayish skeletal packstone, some planktonic foraminifera and volcanic grains.....	106
Figure 58: Thin section images of sample from 565.76 m (3/28/12_6), grayish skeletal grainstone, some planktonic foraminifera and volcanic grains	107
Figure 59: Thin section images of sample from 574.52 m (4/6/12_1), grayish skeletal grainstone, some planktonic foraminifera, spicules and volcanic grains, some skeletal fragments with microborings	108
Figure 60: Thin section images of sample from 576.87 m (4/6/12_2), grayish skeletal grainstone, some planktonic foraminifera, spicules and volcanic grains	109
Figure 61: Thin section images of sample from 602.42 m (4/13/12_1), grayish skeletal grain-packstone, some volcanic grains	110
Figure 62: Thin section images of sample from 605.99 m (4/26/12_1), olivine basalt, sub-aerial.....	111
Figure 63: Thin section images of sample from 606.71 m (4/26/12_2), olivine basalt, zeolites, slightly altered	112

Figure 64: Thin section images of sample from 606.98 m (4/26/12_3), olivine basalt, feldspar porphyry, sub-aerial	113
Figure 65: Thin section images of sample from 608.54 m (4/13/12_2), grayish skeletal grain-packstone, some red algae and spicules	114
Figure 66: Thin section images of sample from 618.09 m (4/20/12_1), grayish skeletal grainstone, some skeletal fragments with microborings	115
Figure 67: Thin section images of sample from 697.76 m (5/4/12_3b), grayish skeletal packstone, few red algae and few planktonic foraminifera	116
Figure 68: Thin section images of sample from 697.76 m (5/4/12_8), grayish skeletal packstone, few red algae and few planktonic foraminifera	117
Figure 69: Thin section images of sample from 698.16 m (5/4/12_7), grayish skeletal packstone, some rudists and planktonic foraminifera fragments.....	118
Figure 70: Thin section images of sample from 698.25 m (5/4/12_6), grayish skeletal packstone, some lithics and planktonic foraminifera fragments.....	119
Figure 71: Thin section images of sample from 698.53 m (5/4/12_5), grayish skeletal packstone, some lithics and planktonic foraminifera fragments.....	120
Figure 72: Thin section images of sample from 698.67 m (5/4/12_4), grayish skeletal packstone, some lithics and planktonic foraminifera fragments.....	121
Figure 73: Thin section images of sample from 698.94 m (5/4/12_3), grayish skeletal wack-packstone.....	122
Figure 74: Thin section images of sample from 699.51 m (5/4/12_2), grayish skeletal packstone, some lithics and planktonic foraminifera fragments.....	123
Figure 75: Thin section images of sample from 699.90 m (5/4/12_1), grayish skeletal packstone, some lithics and planktonic foraminifera fragments.....	124

LIST OF PHOTOGRAPHS

Image 1: Basaltic andesite sub-rounded clasts present near the base of the massive Limestone. Very coarse sand size and gravel size clasts can be seen as well	126
Image 2: <i>Barrettia</i> and <i>Antillosarcolites</i> sp.	126

Image 3: <i>Bournonia sp.</i> seen in the massive Limestone of the Bahía Fosforescente Member.....	127
Image 4: <i>Stellacaprina nov. gen.</i> seen in the massive Limestone of the Bahía Fosforescente Member.....	127
Image 5: <i>Durania sp.</i> seen in the massive Limestone of the Bahía Fosforescente Member.....	128
Image 6: <i>Actaeonella sp.</i> gastropods seen in the massive Limestone of the Bahía Fosforescente Member.....	128
Image 7: View towards the Northeast of the outcrops of the massive Limestone and upper volcanic arenites. This location is an abandoned quarry	129
Image 8: View of the first deposits on top of the seen in the massive Limestone of the Bahía Fosforescente Member, brown medium grained sandstone with eroded limestone grains and planktonic foraminifera	129
Image 9: View of the calcarenite block slumped in the brown medium grained sandstone at around 85 m	130
Image 10: Volcanic arenite with limestone intraclasts. Near the start of the first Lowstand System Tract at 113 m	130
Image 11: Volcaniclastic event, very coarse sand and pebble size sediments, sub-rounded, little to no matrix at around 300 m	131
Image 12: Volcaniclastic event, very coarse sand and pebble size sediments, sub-rounded, little to no matrix, sample from 300 m	131
Image 13: Volcaniclastic event, some local stratification at 385 m	132
Image 14: View of the change in stratigraphy at 548.68 m.....	132
Image 15: View of the rock that outcrops around 564.56 m. The rock was first described as a very fine grained sandstone with lithics but refined with thin sections as alternating skeletal packstone to grainstone with some lithics.....	133
Image 16: View of the outcrop where the section from 615.78 m to 621.72 m was measured	133
Image 17: View of the dark gray fine volcaniclastic sandstone at 615.78 m. At 0.8m higher the reddish altered silicified material, red siliceous mudstone	134
Image 18: View of the rock at 616.81 m described as a very fine to fine sandstone	134

Image 19: View of the outcrop at the end of the section. It encompasses from 659.02 m to 700.81 m of the stratigraphic section 135

LIST OF APPENDICES

Appendix A – Stratigraphic Column.....	60
Appendix B – Thin Sections	88
Appendix C – Field Photographs	125

CHAPTER 1

INTRODUCTION

The Parguera Limestone is exposed south of the Lajas Valley in southwest Puerto Rico between the towns of Cabo Rojo and Guánica. This limestone was originally described by Mattson in his general recognition of the area in 1960. It was further subdivided by Almy (1965) into three members: the Bahía Fosforescente, the Punta Papayo and the Isla Magueyes Members (Figure 1). Mattson (1960) determined the age of the Parguera Limestone from microfaunas of foraminifera ranging from Turonian to Early Maastrichtian. Almy (1965) suggested an age range from Late Santonian through Early Maastrichtian using contained foraminifera.

The Bahía Fosforescente Member (lowest member) consists of massive and bedded limestone that in many areas is composed of a foraminiferal mudstone. Almy (1965) described the Bahía Fosforescente Member as a tan calcarenite with an important non-carbonate clastic component at the base that decreases upwards and a very coarse-grained, bioclastic, somewhat lenticular and pure carbonate limestone. As described by Volckmann (1984a and 1984d) it consists chiefly of bedded calcarenite, locally with volcanic lithic clasts, foraminiferal mudstone, thin lenses of glauconite, and beds of massive bioclastic limestone. Its age was determined by contained foraminifera to be Santonian through Early Campanian (Almy, 1965). Volckmann (1984d) agreed with Almy and used the same age range in his work when he mapped the Parguera Limestone.

Although Volckmann (1984d) proposed the same age range for the Parguera Limestone as Almy (1965), while mapping the Cabo Rojo and Parguera quadrangles (Volckmann, 1984a

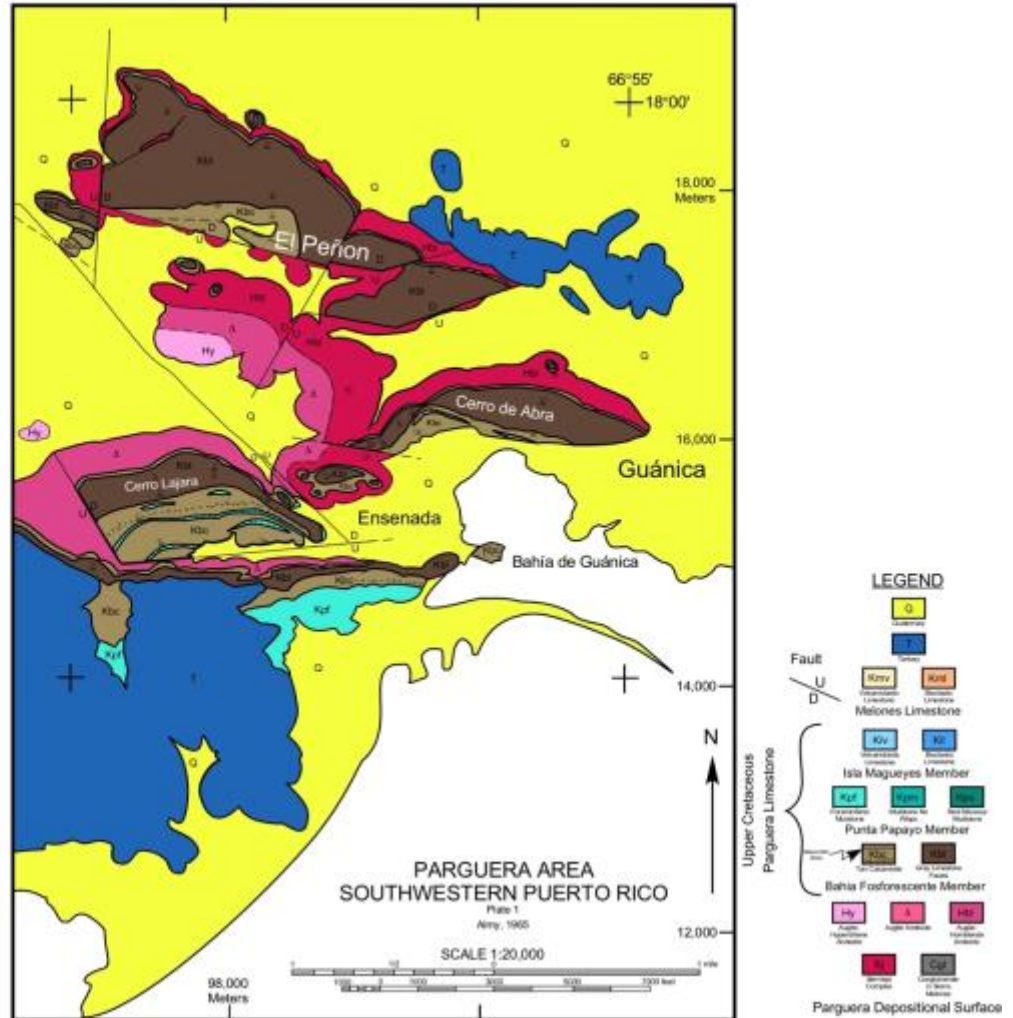


Figure 1: Extract from the Geologic Map of the Parguera Area in Southwestern Puerto Rico (Almy, 1965) showing the study area

and 1984d), he couldn't consistently separate lithofacies assigned by Almy (1965) to the Bahía Fosforescente and Punta Papayo Members. Volckmann (1984a and 1984d) then referred to both members as the lower member of the Parguera Limestone and the upper member to the Isla Magueyes. This is probably the result of using different mapping

techniques. Almy (1965) based his work on field mapping of distinctive rock types or suites of rock types, then augmented the distinctions with thin sections, paleontology, combined with carbonate petrography, to provide information on the environment of deposition. Volckmann (1984a and 1984d) couldn't find any difference between the Bahía Fosforescente and Punta Papayo Members while using lithofacies to map the members and little paleontology. However, recent studies suggest that the Bahía Fosforescente member is Santonian in age (Santos, personal communication 2016-17). Santos (1999) while studying the Late Cretaceous strata in the Cabo Rojo-San Germán structural block in southwestern Puerto Rico, found some *Barretia gigas* rudists, which are of Middle Campanian in age, at the base of the Punta Papayo member. No detailed stratigraphic or paleofacies analysis has been performed in the Parguera Limestone. This study uses the nomenclature assigned by Almy (1965) to the Bahía Fosforescente and Punta Papayo Members.

The hills north of the Bahía de Guánica, named Cerro de Abra (Figure 1), along PR116 and trending E-W, contain exposures of the Bahía Fosforescente and Punta Papayo Members. To resolve some of the uncertainties of the stratigraphy a reconstruction of the paleofacies and paleoenvironment with a stratigraphic, lithofacies, and paleoecologic analyses of these members of the Parguera Limestone was prepared. The relationship between stratigraphy and facies changes helped to stratigraphically correlate the Bahía Fosforescente and Punta Papayo Members of the Parguera Limestone to other units such as the Cotuí Limestone, Sabana Grande Formation, Guaniquilla Limestone, and Yauco Formation for the regional stratigraphy of southwestern Puerto Rico. This study produced

a stratigraphic column portraying the data gathered in the field along with a facies distribution model, an interpretation in a sequence stratigraphic framework with a correlation with other Late Cretaceous rocks in southwestern Puerto Rico. A facies interpretation is attempted to achieve an improved stratigraphic correlation of the Parguera-Ensenada structural block with the Cabo Rojo-San Germán structural block.

1.1 Objective

The purpose of this study was to make detailed stratigraphic, lithofacies, and paleoecologic analyses to reconstruct the depositional history of the Parguera Limestone exposed in the Cerro de Abra area. Determine the relationship between stratigraphy, and facies changes of the Parguera-Ensenada structural block with those in the Cabo Rojo-San Germán structural block. This will enhance the stratigraphic resolution in the Late Cretaceous distal deep-water carbonate successions of southwest Puerto Rico. The stratigraphic section discussed in this study was named as the *Cerro de Abra section*.

This study of the Parguera Limestone provides data that helps to stratigraphically correlate it to other units like the Cotuí Limestone, Sabana Grande Formation, Guaniquilla Limestone, and Yauco Formation for the regional stratigraphy of southwestern Puerto Rico (Figures 2 and 3).

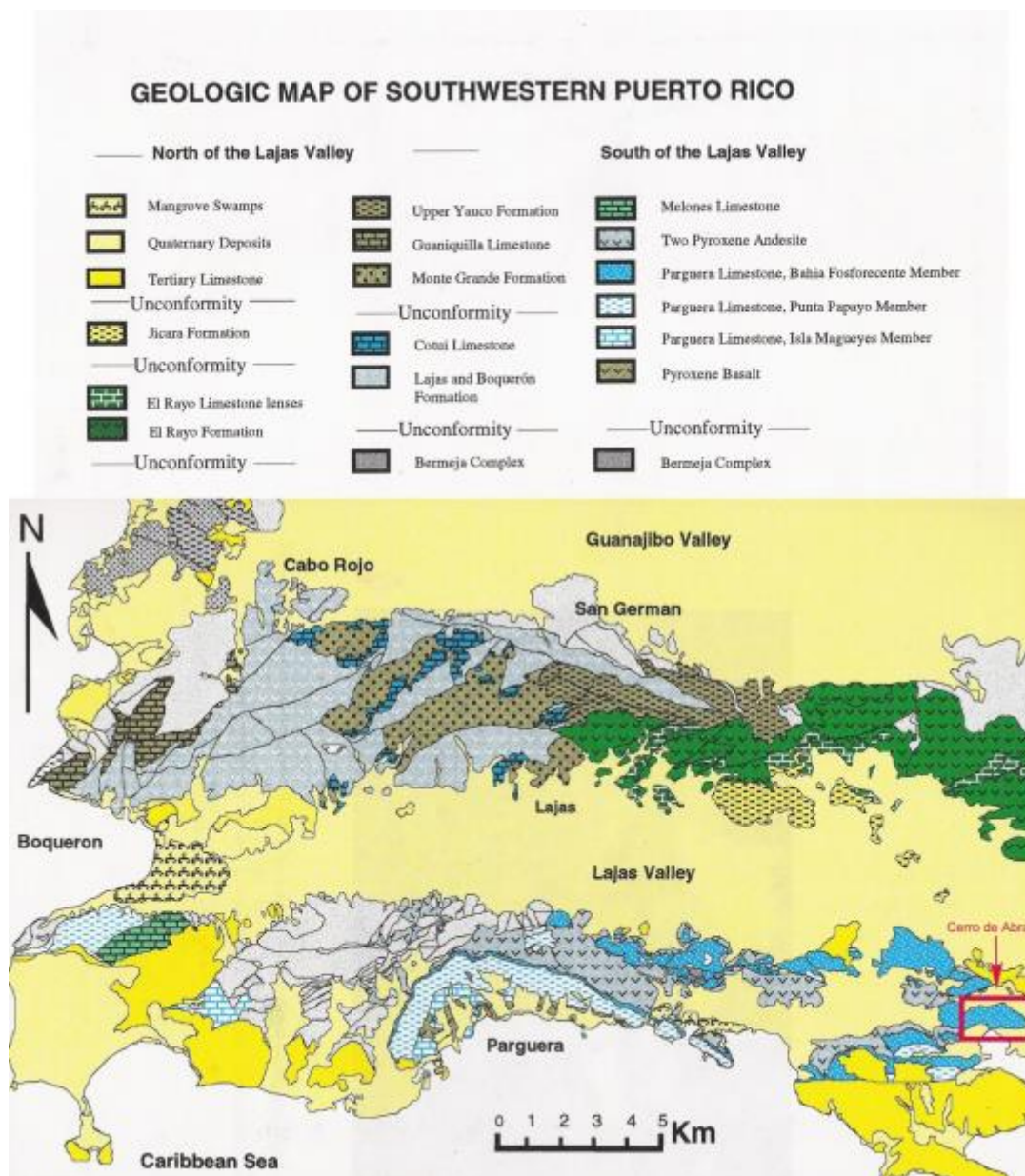


Figure 2: Geologic Map with a summary chart of the stratigraphic sequences of the Late Cretaceous of Southwestern Puerto Rico (after Santos, 1999)

1.2 Study Area

The study area is located south of the easternmost part of the Lajas valley. The Cerro de Abra section is located north of Guánica along state road PR-116 from approximately road marker 21km to road marker 19km (Figure 4). Some parts of the section are covered by heavy vegetation or rock debris from anthropogenic activity. The best option to measure the stratigraphy of the basal rock is to access Cerro the Abra through the north-eastern side. The location of the Cerro de Abra section is at Latitude 17°58'33"N, Longitude 66°55'28"W. The Cerro de Abra section consists of massive limestone exposed by the quarry, volcanics and volcanoclastics, and bedded mudstones.

1.3 Literature Review

1.3.1 General Geology of Puerto Rico

Puerto Rico is a complex island arc terrane that forms part of the Caribbean Plate. It is the easternmost and smallest island of the Greater Antilles, and lies within the seismically active Caribbean-North American Plate boundary zone (Figure 5). It is part of a microplate that is defined to the north by the Puerto Rico Trench, to the south by the Muertos Trough, to the east by the Anegada Trough and to the west by the Mona Canyon that separates the island from the Hispaniola block.

The island consists of a basement of Late Jurassic metamorphic rocks to Early Tertiary volcanic, volcanoclastic, and sedimentary rocks, intruded by felsic plutons, and overlain by Oligocene to Miocene and younger sediments (Krushensky and Schellekens, 2001). The pre-Oligocene rocks are divided into three geographic igneous provinces; southwest,

central, and northeast, each with a distinctive geology and petrology (Schellekens *et al.*, 1993; Figure 6). The three igneous provinces are separated by NW-SE trending fault zones.

1.3.2 Tectonic Setting of the Puerto Rico Southwest Igneous Providence

The Southwestern Igneous Province is located in the west, southwest part of the island and is separated from the rest of the island by the Great Southern Puerto Rico Fault Zone (Figure 6). The province is represented by complex volcano-sedimentary cycles and ocean crust that has been dated using fossils or radiometric dating. The oldest basement units are part of the “Bermeja Complex” which represents obducted ocean crust and contains bodies of serpentinite, blocks of mafic metamorphic rocks, and cherts of Pliensbachian to Aptian age (Schellekens *et al.*, 1993; Montgomery *et al.*, 1994; Schellekens and Joyce, 1999).

The southwestern igneous province is divided by the east-west oriented Lajas and Guanajibo valleys (Figure 6) into three major structural blocks. The middle Cabo Rojo-San Germán structural block and the southern Parguera-Ensenada structural block are characterized by steep north-facing slopes rising above the Guanajibo and Lajas valleys (Santos, 1999). The northern Mayagüez-Sabana Grande block is in fault contact with the Las Mesas serpentinite belt to the north (Santos, 1999). Santos (1999) studied the Late Cretaceous exposures in the Cabo Rojo-San Germán structural block, southwestern Puerto Rico, a thick sequence of Cenomanian to Maastrichtian limestones and mudstones interbedded with volcanic rocks and cut by numerous small, high level, intermediate igneous intrusions, across the southwest of Puerto Rico that overlies the basement complex. Santos (1999) described three depositional cycles composed of: (1) intense volcanism and

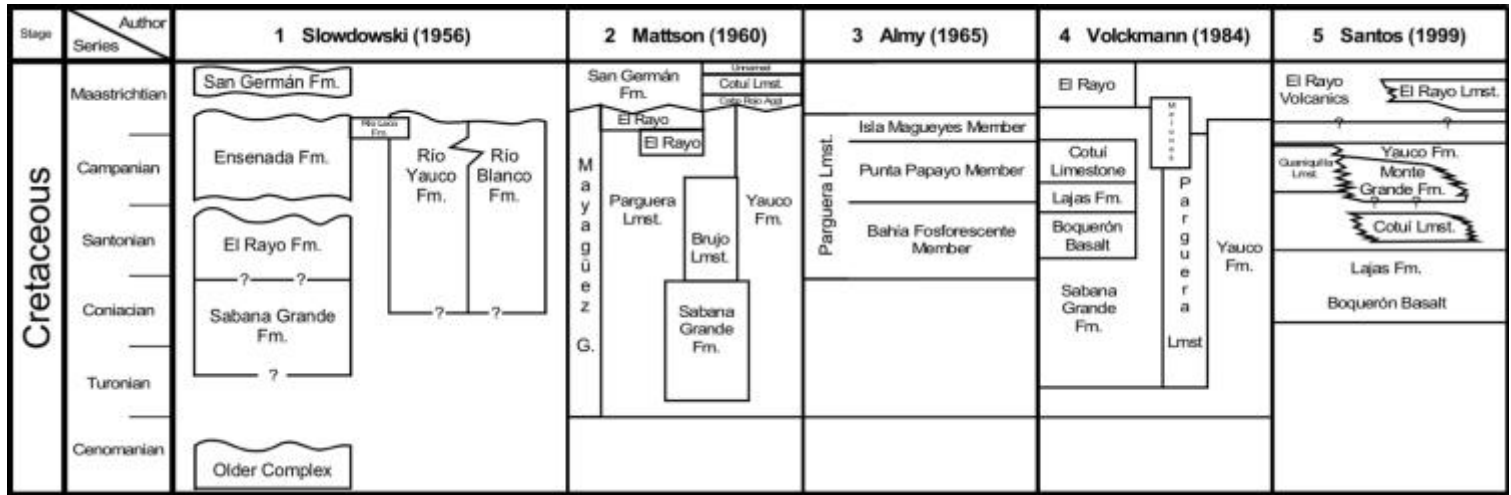


Figure 3: Summary chart of the stratigraphic sequences of the Late Cretaceous of southwestern Puerto Rico, as viewed by different authors (extract from Santos, 1999)



Figure 4: Google Earth image showing the area of study

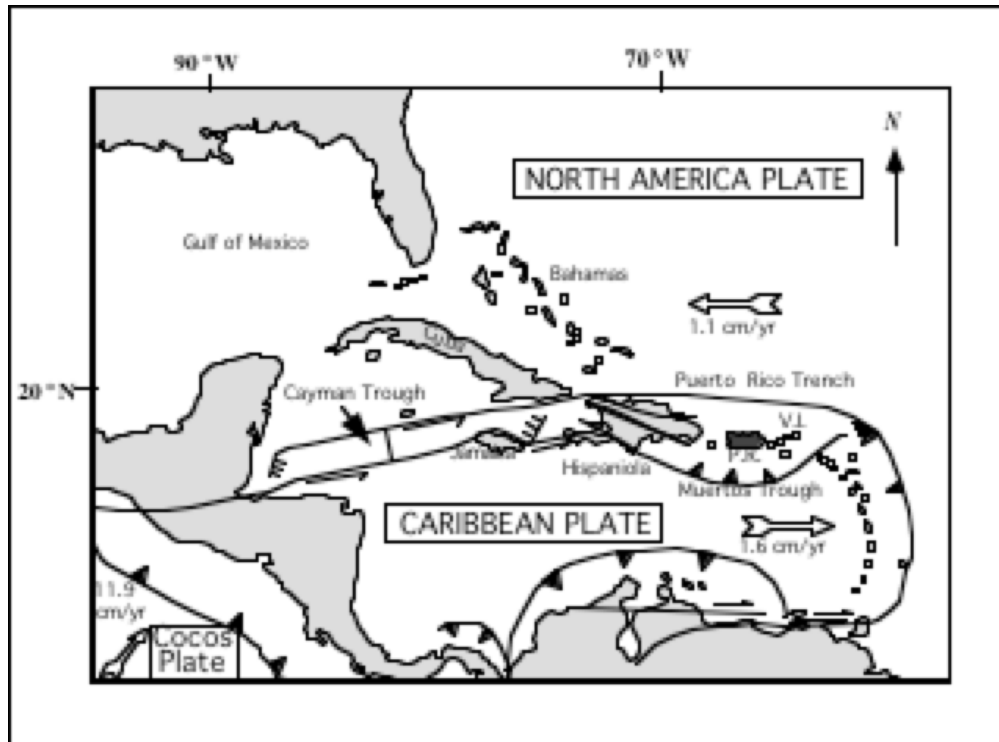


Figure 5: Tectonic map of the Caribbean region. Plate motion and velocities are after Mann et al. (1991)

volcaniclastic sedimentation during the Santonian to Campanian; (2) subsidence produced by decrease of volcano-tectonic activities during the Campanian; and (3) a short period of carbonate deposition during the Maastrichtian. The formations that reflect these events are the Cotuí Limestone, Sabana Grande Formation, Guaniquilla Limestone, Yauco Formation, El Rayo Volcanics, and El Rayo Limestone (see Figure 2).

1.3.3 Cretaceous Volcano-sedimentary Stratigraphy

The most recent work that sums up the geological history of Southwestern Puerto Rico is that of Santos (1999) (Figure 2). He interpreted that during the Late Santonian to Early Campanian, the rocks record three separate relative sea-level rises halted by volcanic/tectonic events. Most

of the deposition was controlled first by regional tectonic and volcanic events, and secondarily by eustatic sea-level changes (Santos, 1999).

1.3.4 Previous Work

Many studies have been made about the geology of the southwestern igneous province of Puerto Rico with the most recent made by Santos (1999, and references therein) which gives a stratigraphic and depositional history of the Late Cretaceous strata in the Cabo Rojo-San Germán structural block (Figure 2).

Mitchell (1922) described the exposures at Ensenada as the “Ensenada Shale”, his term for medium-bedded calcareous material. The unit was redefined because the Ensenada Formation as defined by Slodowski (1956) includes limestones and volcanic rocks. Slodowski (1956) described the Parguera Limestone as part of the Ensenada Formation within the “Younger Complex”. But, Mattson (1960) (Figure 3) later placed in the San Germán Formation of Maastrichtian in age. And defined the “Older Complex” alongside the Mayagüez Group, of Santonian to Maastrichtian in age, to units mapped strictly as lithofacies sequence bounded by unconformities.

Mattson (1960) studied the geology of the Mayagüez area and described the Parguera Limestone as a buff to gray medium-bedded calcilutite and medium-bedded to massive fragmental limestone (microcoquina) with less than 15 percent tuff and a slightly smaller amount of calcarenite. Thick-bedded and massive fragmental limestone, commonly with wavy bedding, found at the base of the unit and in some places near the top. Diagnostic features include the abundance of marly weathering calcilutite, the common presence of glauconite, and a general lack of noncalcareous debris.

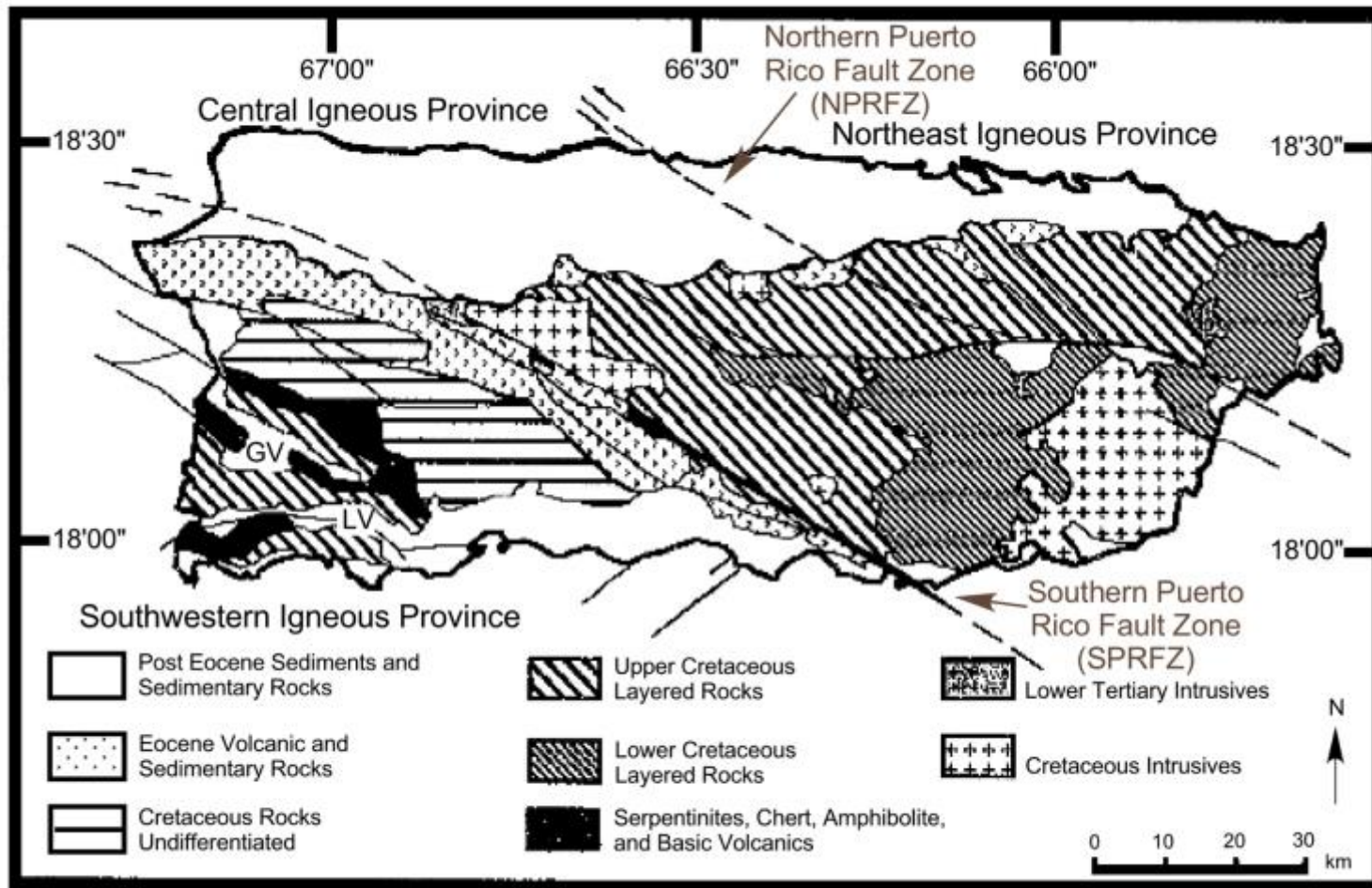


Figure 6: Geologic map of Puerto Rico, GV: Guanajibo Valley, LV Lajas Valley (After Schellekens, 1993)

Almy (1965) (Figures 1 and 3) divided the formation into three members; the Bahía Fosforescente, the Punta Papayo, and the Isla Magueyes Members. He described the Parguera Limestone as representing a shallow water bank under normal marine conditions with possible reefs deposits, open ocean deeper-water deposits, and near-shore deposits. It consists of a thick, basal, medium-grained calcarenite that decreases upward in non-carbonate clastic material; a fine-grained, foraminiferal mudstone; and a coarse-grained bioclastic limestone.

Later, Volckmann (1984a) mapped the same area as Almy (1965), the Cabo Rojo and Parguera quadrangles, but couldn't differentiate or consistently separate lithofacies assigned by Almy (1965) to the Bahía Fosforescente and Punta Papayo Members so he referred to them both as the lower member of the Parguera Limestone. The lower member consists, as described by Volckmann (1984a and 1984d), of chiefly bedded calcarenite, locally with volcanic lithic clasts; foraminiferal mudstone; thin lenses of glauconite; and beds of massive bioclastic limestone. A conglomerate, which contains sand- to cobble-size clasts of volcanic rock, chert, serpentinite, and amphibolite, is locally present. Calcarenite is the predominant lithic type in the lower part of the lower member, whereas calcareous mudstone is the predominant lithic type in the upper part of the lower member. The upper member consists of a coarse-grained massive bioclastic limestone, grading at the base into a volcanoclastic conglomerate. Gray to brown andesitic tuff is interbedded in the upper part of the upper member. Detailed descriptions of the Parguera Limestone are given by Mattson (1960), Almy (1965), and Volckmann (1984a and 1984d).

Addarich (2009) worked on the geologic mapping and history of the Guánica Quadrangle which encompass the present study site. He adopted the nomenclature and name designation assigned to the lower member of the Parguera Limestone as Volckmann (1984a and 1984d). He described three major events controlling the structural geology of the area. The post-Ponce Limestone deformation, the post-Juana Díaz Formation – pre-Ponce Limestone deformation and the pre-Juana Díaz Formation deformation.

Others studies have been made in the Southwestern Igneous Province of Puerto Rico with the carbonates found in the area. These studies where made for the Cotuí Limestone in Cerro Buena Vista (Bonilla, 2004; Pérez, 2004; Díaz, 2004), PR-100 (Díaz, 2004) and La Cuchilla area (Pérez, 2004). Bonilla (2007) made a detailed sequence stratigraphic analysis of the Cotuí Limestone that enhanced the stratigraphic resolution of the Late Cretaceous history of southwest Puerto Rico.

CHAPTER 2

METHODOLOGY

The methodology employed in this thesis research aligns with the techniques used in the field for identifying and measuring stratigraphic units and those used in the laboratory for detailing the rock descriptions. This chapter will feature the techniques employed in this study which lead to the interpretations and discussions later established.

2.1 Field Work

The area of study was visited several times before any description or measurement were taken to determine the best exposure that represents the best stratigraphic information. The best area to acquire the stratigraphic information was by accessing the northeastern end of Cerro de Abra through a cemetery and walking south towards the Cerro. From there you could see the nonconformity between the basaltic andesite and the Massive Limestone (Bahía Fosforescente member). A detailed stratigraphic section of 59.1m was measured. Accessing the rock exposures of the abandoned quarry, just south of the previously measured section, and moving west, the lithological successions can be followed and measured. A detailed stratigraphic section of a total of 641.7m was measured.

Structural data was collected were available and used to determining the true thickness of the lithostratigraphy. All of the measurements taken were georeferenced with the aid of a Global Positioning System (GPS) device and plotted using the available free platform provided by Google Earth (Figure 4).

The rocks were described following standard rock descriptions. For carbonate rock descriptions of hand specimens were made by using Dunham (1962) and its expanded version of classification of Embry and Klovan (1971) and, for thin sections descriptions were made by using Folk (1959, 1962). For siliciclastic rock descriptions of hand specimens were made by using Tucker (2001). And, for igneous rock descriptions of hand specimens were made by using Le Maitre (2002).

2.2 Petrographic Analysis

Collection of samples was a very significant factor in refining the rock descriptions made in the field. Without the recollection of this samples the interpretation and conclusions of this work would be incomplete. So, as part of the initial scope of the work it was crucial to have this component as part of the work to be accomplished. Samples were collected and further analyzed in thin section when their texture was not well understood in the field, further detail was needed, or where similar rocks were seen in a portion of the stratigraphy. Samples were labeled in reference to the time and number of samples taken (i.e. 11/25/11_4). A total of 66 samples were collected through the section. All of the samples taken and rock descriptions made were georeferenced with the aid of a Global Positioning System (GPS) device and plotted using the available free platform provided by Google Earth (Figure 4).

Samples taken went through a screening process before being sent for processing to acquire thin sections. Out of the 66 samples gathered, 44 were selected and sent to National Petrographic Service, Inc., of which 36 are presented in this manuscript (Figures 40 to 75). Samples were impregnated as needed in blue stained epoxy. After the thin sections were

received they were extensively reviewed under the petrographic microscope and the field descriptions were refined. The rocks were described using the classification scheme described before.

2.3 Limestone Classification

Limestones are classified by using the classification schemes established by Dunham (1962) and Folk (1959, 1962). These classifications aim towards the interpretation of depositional environments. The most commonly used, since their use apply to both field and laboratory analysis, are the Dunham's classification and its expanded version of Embry and Klovan (1971). Folk's classification restricts its use to laboratory analysis applied to thin sections and peels.

Dunham's classification (Table 1) model characterizes two major groups; carbonates which original components are organically bounded together during deposition, and those which are not organically bounded together. Components not organically bounded together during deposition are subdivided according to the material that support their components in two distinctive textures; mud-supported or grain-supported. Mud-supported textures are mudstones (less than 10% grains) and wackestones (more than 10% grain). Grain-supported textures are packstones (contains lime mud between the grains) and grainstones (lack of lime mud between the grains). Dunham's classification was expanded by Embry and Klovan (Table 2) by introducing the grains size aspect, with the differentiation of grains smaller or larger than 2 mm. The new categories were; floatstone (corresponding to wackestones texture with components greater than 2 mm) and rudstones (corresponding to grainstone texture with components greater than 2 mm).

Table 1: Classification of Limestone (Dunham, 1962)

DEPOSITIONAL TEXTURE RECOGNIZABLE					Depositional texture not recognizable
Original components not bounded together during deposition			Lacks mud and is grain supported	Original components were bounded together during deposition.	
Contains mud (particles of clay and fine silt size)		Grain supported			
Mud supported					
Less than 10% grains	More than 10% grains				
MUDSTONE	WACKESTONE	PACKSTONE	GRAINSTONE	BOUNDSTONE	CRYSTALLINE

Table 2: Expanded Classification of Limestone (Embry and Klovan 1971)

ALLOCHTHONOUS LIMESTONE ORIGINAL COMPONENTS NOT ORGANICALLY BOUND DURING DEPOSITION					AUTOCHTHONOUS LIMESTONE COMPONENTS ORGANICALLY BOUND DURING DEPOSITION			
Less than 10% > 2 mm components contains lime mud (<0.03 mm)		No lime mud	Greater than 10% >2 mm components		by organisms which			
Mud supported		Grains-supported		Matrix-supported	> 2 mm component supported	build a rigid framework		
Less than 10% grains	Greater than 10% grains					encrust and bind	act as baffles	
Mudstone	wackestone	packstone	grainstone	floatstone	rudstone	framestone	Bindstone	bafflestone

Folk's classification (Table 3) model is a practical technique for describing texture in thin sections and peels. Three main components in limestones were stated; allochem (grains), matrix (micrite) and sparite (cements). Folk's philosophy was that carbonate rocks are similar to siliciclastic rocks in their mode of transportation and deposition, because their textures are primarily controlled by the water energy in which are deposited. Folk differentiated the matrix of carbonate rocks deposited in calm water from those deposited in high water energy. Calm water deposits are likely to have a matrix composed of carbonate mud (lime mud or micrite) with or without grains (micrite, fossiliferous micrite

Table 3: Folk's (1962) Classification

Percent Allochems	Over 2/3 Lime Mud Matrix				Subequal Spar and Lime Mud	Over 2/3 Spar Cement		
	0 – 1%	1 – 10%	10 – 50%	Over 50%		Sorting poor	Sorting good	Rounded and abraded
Representative Rock Terms	Micrite	Fossiliferous Micrite	Sparse Biomicrite	Packed Biomicrite	Poorly washed Biosparite	Unsorted Biosparite	Sorted Biosparite	Rounded Biosparite
1959 Terminology	Micrite	Fossiliferous Micrite	Biomicrite		Biosparite			
Terrigenous Analogues	Claystone		Sandy Claystone	Clayey or Immature Sandstone		Submature Sandstone	Mature Sandstone	Supermature Sandstone

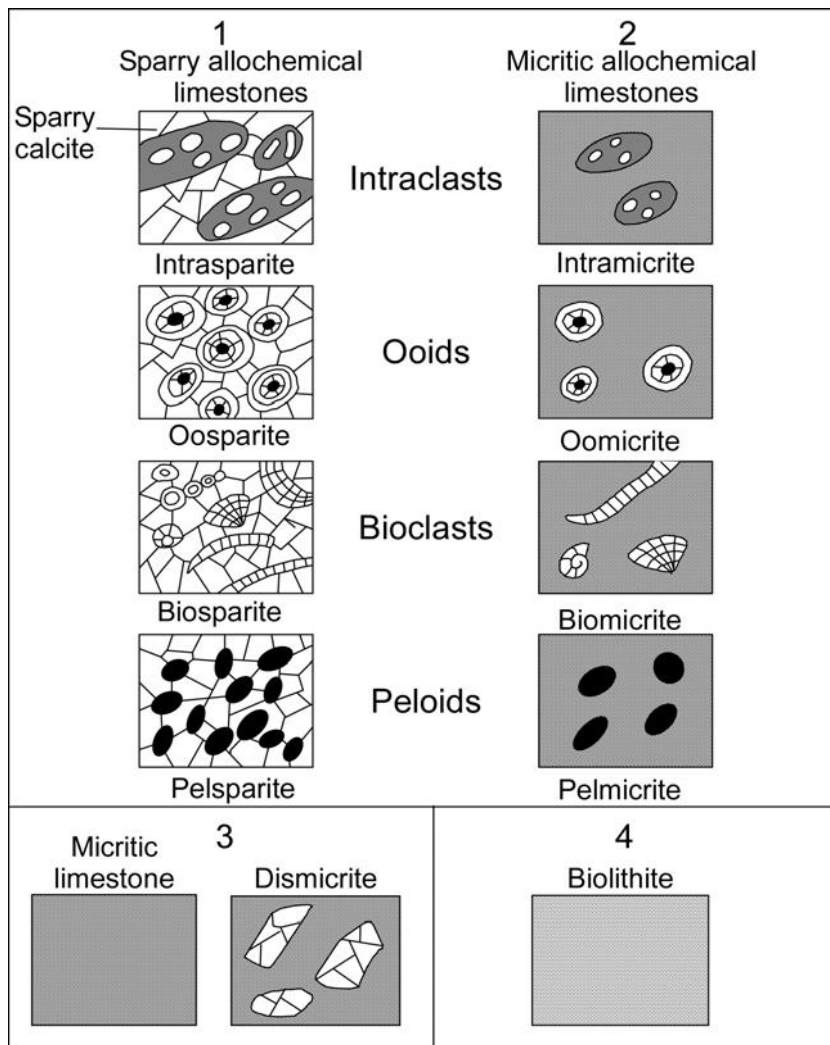


Figure 7: Basic limestone types of Folk's (1959) limestones classification

and biomicrite). High energy deposits support the deposition of winnowed sand with open pore spaces that are later filled with crystalline cements (biosparite). But the most important textural differences are those between limestone with lime mud matrix and calcite cement (poorly washed biosparite). These deposits represent areas where the water energy becomes turbulent enough to wash out the lime mud and carry it out to areas of low water energy. Folks (1959) also provided a system to classify limestone based on the compositional constituents (Figure 7); intraclasts, ooids, bioclasts and peloids.

2.4 Stratigraphic Correlation

All the data gathered from the field as rock descriptions, lithological thicknesses, structural features and georeferenced locations, and from the laboratory was analyzed to create a representative stratigraphic column that embodies the history of the deposition of the rocks on the area of study. The data was condensed and with the aid of the drawing computer program Canvas Draw 3 the figures, representing the depositional history of this study, were made and presented. The stratigraphic columns were plotted following an analog of a template for a graphic sedimentary log presented by Nichols (1999) but, modified to fit the purpose of presenting the data as analyzed, suitable for the discussion and portraying the story as interpreted. Most of the figures presented were modified using Canvas Draw 3 program.

2.5 Sequence Stratigraphy

Emery and Myer (1996) defined *sequence stratigraphy* as the “subdivision of sedimentary basin fills into genetic packages bounded by unconformities and their correlative conformities”. These genetic packages are chronostratigraphic markers that describe

periods of relative sea-level changes. Vail *et al.* (1997) and, Mitchum *et al.* (1976) pioneered works in sequence stratigraphy of siliciclastic sediments and to characterize the deposition of these depositional packages as the result of sea-level changes. The conception of the sequence stratigraphy model was influenced by the following geological disciplines: *seismic stratigraphy*, *chronostratigraphy*, *biostratigraphy* and *sedimentology*. Mitchum *et al.* (1977) defined the term *sequence*, as applied in *sequence stratigraphy*, as “a stratigraphic unit composed of a relatively conformable succession of genetically related strata bounded at its top and base by unconformities or their correlative conformities”. Different episodes of deposition occurring in periods of relative falling and rising of the sea-level are represented by *sequences*. These *sequences* are affected by the rate of sediment supply and the relative sea-level change resulting in three major architectures. The recognized major architectures are *progradational*, *aggradational*, and *retrogradational* geometries (Emery and Myer, 1996). *Progradational* geometry occurs with high sedimentation in a stagnant relative sea-level scenario, and the facies belt migrate basinward, hence occurring when sediment supply exceeds the rate of creation of topset accommodation volume. *Aggradational* geometry occurs when the sediment deposition and the sea-level change are in balance, consequently the facies belt stack vertically, hence occurring when sediment supply and the rate of creation of topset accommodation volume are roughly balanced. While *retrogradational* geometry occurs when the sediment deposition is less than the rate in which the relative sea-level raise and the facies belt migrate landward, hence occurring when sediment supply is less than the rate of creation of topset accommodation volume.

These sequences have deposits associated that occur in depositional packages known as *systems tracts* (Emery and Myer, 1996). *System tracts* are characterized by different phases of deposition in a third order sea-level change. The three main systems tracts (Emery and Myer, 1996) are; *lowstand system tract (LST)*, *transgressive system tract (TST)* and *highstand system tract (HST)*. *Lowstand system tract* consist of submarine fans deposited during a fall in the sea-level that passes the offlap break. The deposits associated with this system tract are characterized by a progradation that becomes an aggradation during the slow relative sea-level raise. *Transgressive system tract* consists of sedimentary packages in a retrogradational pattern deposited during a sea-level rise that outcompeted sedimentation. *Highstand system tract* is deposited during the deceleration rate of sea-level raise resulting initially of aggradations becoming progradations as the sea-level rise continue decreasing and sediment fill the accommodation space.

During TST and HST, shallow marine sediments are typically arranged as upward-coarsening units with shoaling-upward facies succession separated by fine sediments that represent a deeper facies succession (Emery & Myer, 1996). These depositional sequences are known as *parasequences* and represent the smallest building blocks of the system tracts. Van Wagoner *et al.* (1990) defined them as relatively conformable successions of genetically related beds or bedsets bounded by marine flooding surfaces and their correlative surfaces. The parasequence sets (Figure 8) were described by Van Wagoner *et al.* (1990) as; *progradational parasequence set*, *aggradational parasequence set* and *retrogradational parasequense set*. The *progradational*

parasequence set are typical in highstand system tract and lowstand prograding wedge. The *aggradational parasequence set* are distinctive in shelf- margin system tract. While the *retrogradational parasequence set* are characteristic in transgressive system tract. For carbonate rocks the sequence stratigraphy model was modified and applied by Sarg (1988). He described the depositional sequences of platforms and carbonate shelf margins. Following carbonates sequence stratigraphy models were developed by Calvet et al. (1990), Tucker and Wright (1990), Hunt and Tucker (1993) and Tucker et al. (1993). General concepts remained the same, however fundamental differences were influenced by sediment supply. Carbonate sedimentation occurs being strongly influenced by environmental factors controlled by biogenic production. The rate of carbonate production is contingent of water depth, temperature, and water chemistry, while siliciclastic sedimentation is ruled on the sediment influx from continental margin. In brief, carbonate sequence stratigraphy records fluctuations in sea-level, changes in carbonate sedimentation and distinctive environmental factors (Flügel, 2004).

Models for both limestones and siliciclastic rocks are very similar in that an ideal sequence is divided by system tracts (Figure 9); highstand system tract (HST) “still stand”, transgressive system tract (TST) “sea-level rise” and lowstand system tract (LST) “sea-level fall” (Flügel, 2004). But, most carbonate sedimentation has been reported in the TST and HST. Carbonate deposition in the LST is restricted to narrow areas and is characterized by abundant siliciclastic input and exposure surface of carbonates platforms. The TST is portrayed by deepening-upward successions with progressive open marine condition. The HST tend to produce thick bedded or massive carbonate deposition, often with light colored

rock, abundant marine biota, shoaling upward patterns and changes from open to restricted marine conditions.

Parasequences are relative conformable successions of genetically related beds bounded by surfaces that represent abrupt changes in water depth and make up in, small scale (meters to tens of meters in thickness), the system tracks. They consist of small scale shallowing upward successions (Flügel, 2004). As in siliciclastic sediments, in carbonate sediments the parasequences are often organized in *parasequence sets* that indicate trends of shallowing, deepening or no change in the sea-level. The parasequences in shallow marine environment are composed by shoaling upward successions with an upper boundary that indicates rapid flooding or increase in the water depth. The inner carbonate platform parasequences consists of shallow lime sands or muds, capped by tidal flat deposits and exposure surfaces. In slightly deeper water, parasequences show coarsening upward changing from lime mud deposit to interbedded mud and sand.

Forced Regression as defined by Catuneanu (2002) (Figure 10) is a type of regression occurring during stages of base level fall, when the shoreline is forced to regress by the falling base level irrespective of the sediment supply. It triggers erosional processes in both the nonmarine and shallow marine settings adjacent to the coastline thus, fluvial incision can be accompanied by the progradation of offlapping shoreface deposits. Forced regressive sediments are those sediments that collect during a forced regression that display diagnostic progradational and downstepping stacking patterns.

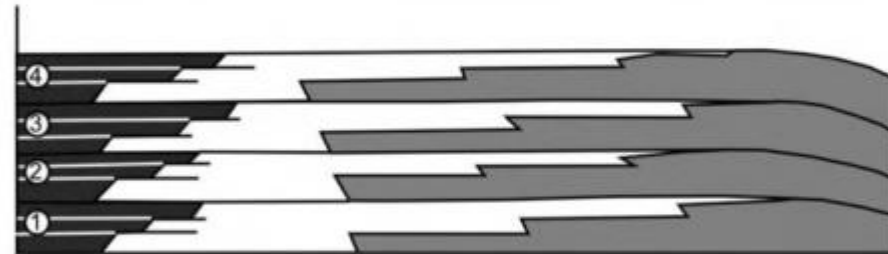
PROGRADATIONAL PARASEQUENCE SET

- Net basinwards movement of the shoreline
- Characteristic of highstand systems tract and lowstand prograding wedge



AGGRADATIONAL PARASEQUENCE SET

- No net movement of the shoreline
- Characteristic of shelf-margin system tract



RETROGRADATIONAL PARASEQUENCE SET

- Net landwards movement of the shoreline
- Characteristic of transgressive system tract

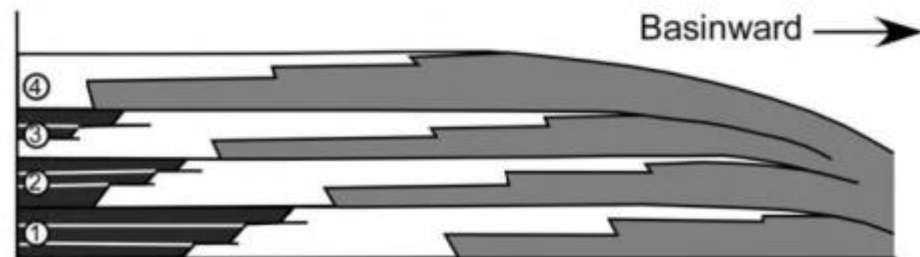


Figure 8: Parasequence sets (Emery & Myer, 1996; after Van Wagoner et al., 1988)

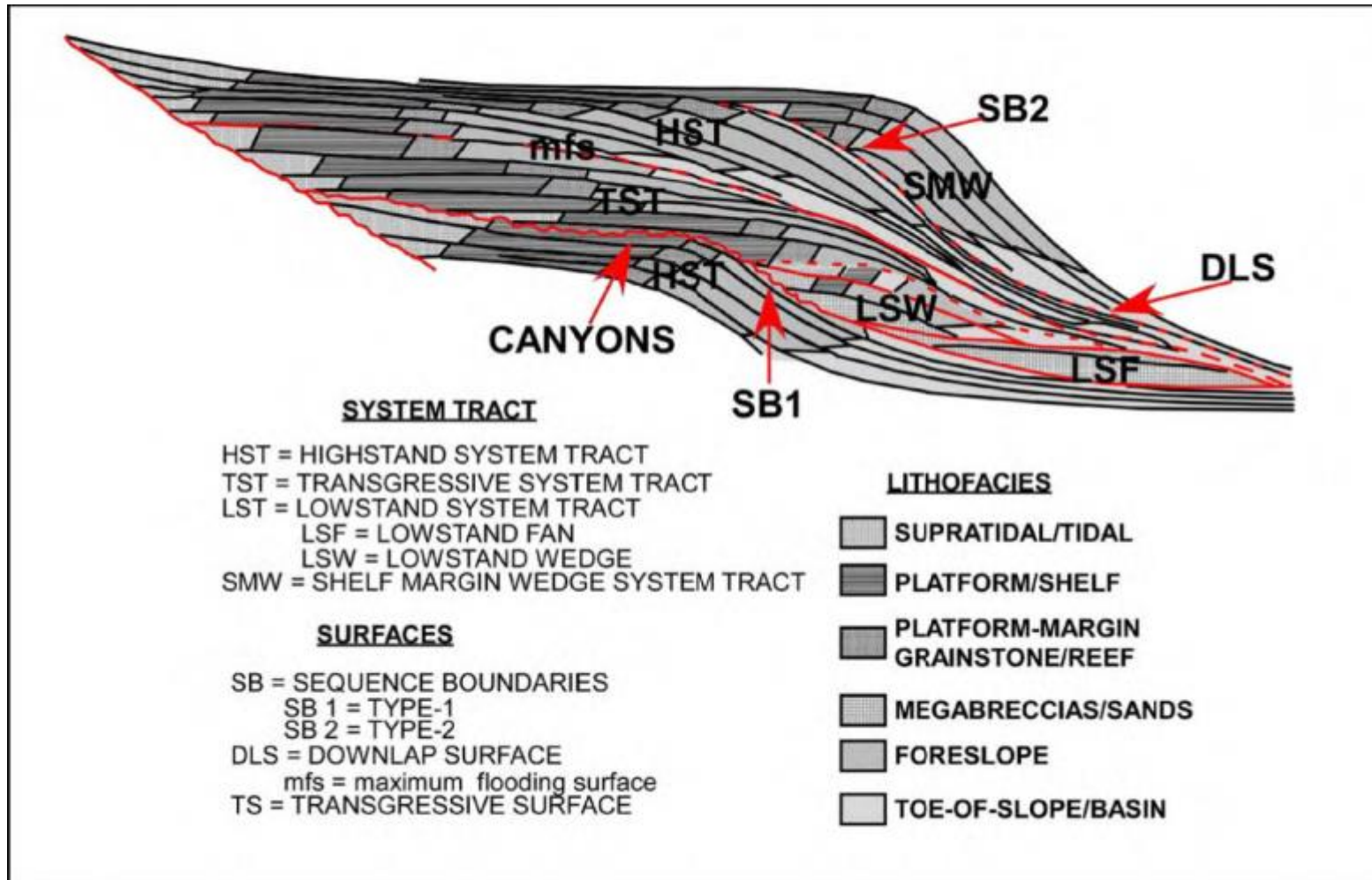


Figure 9: Carbonate Sequence Stratigraphy model (after, Tucker and Wright, 1990)

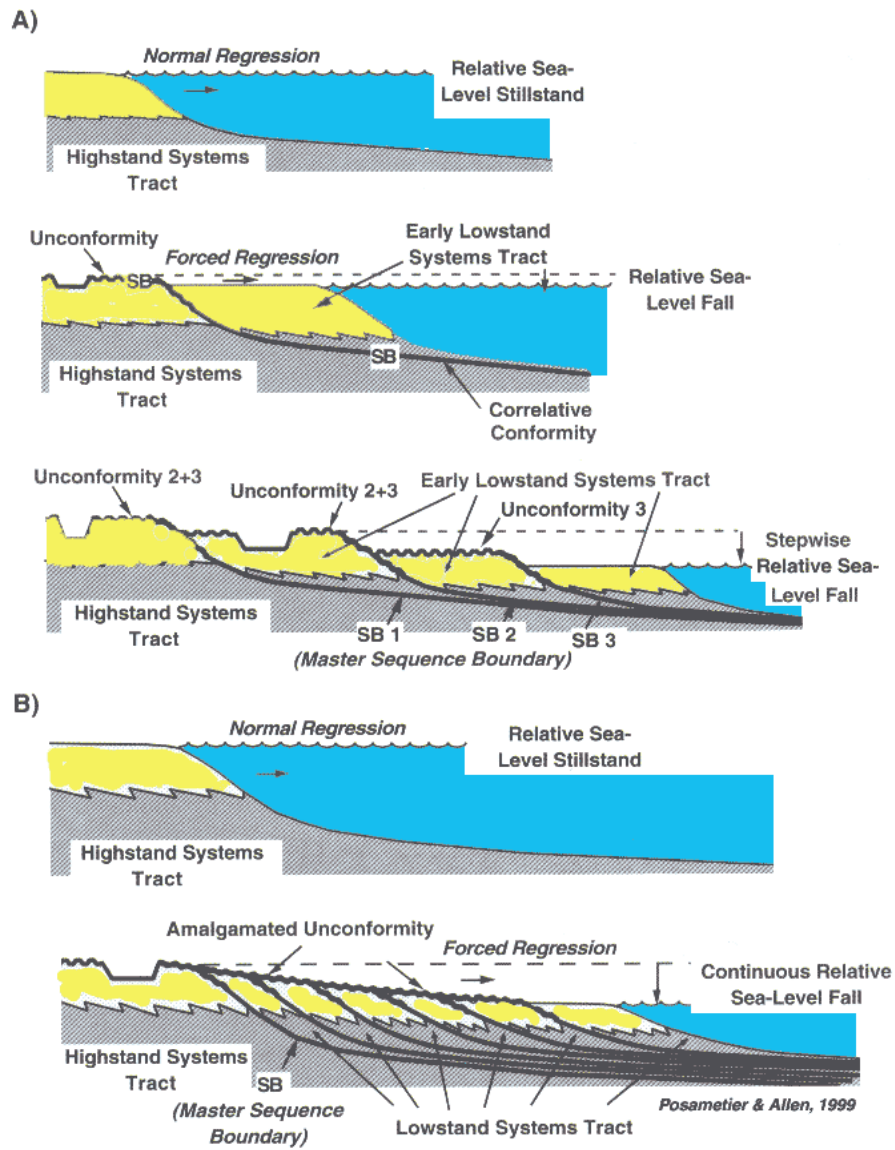


Figure 10: Forced Regression after Posamentier & Vail (1999)

CHAPTER 3

RESULTS

This chapter discusses the lithology described in this study for the Cerro de Abra area. The description of the units allowed for the development of a stratigraphic section for visualizing and recognizing the history of deposition, the components that made up our study site, and to discuss important changes of the vertical succession. Some of the field data was refined with the aid of thin sections prepared from samples gathered. A discussion of the grain constituents and their significance was performed to provide the microscopic view onto the big scenario and refining the field rock classifications. Furthermore, a brief discussion proposing that the stratigraphic history studied would become known as a type section for the Bahía Fosforescente and Punta Papayo Member (Almy, 1965), lower member (Volckmann, 1984a and 1984d), of the Parguera Limestone.

3.1 PR 116 Section

The area of study along State Road PR-116 is 2.18 Km long. Cerro de Abra is an east-west trending ridge, bounded to the east by State Road PR-331 where it's relieve levels out to the same elevation as the valley, to the west it's relieve also levels out to the same elevation as the valley. At this location about approximately 700.81 m of stratigraphic history were successfully measured. For visual reference of the upcoming discussion see Figures 13 to 39.

Samples were collected to refine the descriptions of the rock classifications made in the field. Included in this report are 36 (Figures 40 to 75) images illustrating a view under a

petrographic microscope of part of the grain constituents that made up the rocks of this study area and their locations stratigraphically. First measurements and descriptions of the stratigraphic section were started from the oldest rocks stratigraphically, the grayish limestone facies or “massive Limestone”, that outcrops at the easternmost end of the ridge. The nonconformity with the basal basaltic andesite was not seen at the exposures and open faces of the abandoned quarry. The best option to start measuring the stratigraphy from the basal rock is to access Cerro the Abra through the north-eastern side not from the abandoned quarry. While looking for the non-conformity some out of place blocks were seen of the same massive Limestone that contained the following rudists: *Barrettia* and *Antillosarcolites sp.* (see Image 2), *Bournonia sp.* (see Image 3), *Stellacaprina* nov. gen. (Mitchell, 2013 and personal communication; see Image 4), *Durania sp.* (see Image 5), and *Actaeonella sp.* (see Image 6).

0-59.10 m – After finding the nonconformity contact the recollection of data was initiated. A fining upward section of 6.50 m was measured of a grayish skeletal grainstone with a few angular and sub-prismoidal to spherical very coarse sand and fine pebble sized basaltic andesite grains, to a grayish skeletal wackestone with few coarse pebbles to cobble sized clasts of basaltic andesite (see Image 1). Some *Actaeonella sp.* gastropods were seen (see Image 6) in this section. It coarsens to a grayish skeletal grainstone of 50 cm in thickness but, it then gets covered for about 15 m. The only option at the moment in the field was to move up topographically and stratigraphically, no other exposures were found nearby for 25 m on each side. Resuming with data recollection from 22 m a series of coarsening upward lithological packages (15 in total) were measured for a total of 37.10 m. The total

thickness of the grayish limestone facies is 59.10 m. Figure 40 is representative of stratigraphic unit at 52.90 m (sample 10/26/11_1), described in the field as a grayish skeletal wack-packstone. Refined as grayish sparse biomicrite, with some rudist fragments and coralline algae, few mud between the grains. Figure 41 is representative of stratigraphic unit at 53.60 m (sample 10/26/11_2), described in the field as a grayish skeletal packstone. Refined as grayish sparse biomicrite, with some rudist fragments, little mud between the grains.

59.10-107.60 m – A volcanic arenite follows that is comprised of two intercalated different sandstones: one described as a brownish sandstone ranging in grain size from very fine to medium sand, later refined with the thin sections to be a brownish very fine to medium grained sandstone with skeletal fragments, planktonic foraminifers and intraclasts, sub-rounded to sub-angular, some high relieve minerals, micriticized; and another described as a grayish sandstone ranging in grain size from fine to coarse sand, later refined with thin sections descriptions to be a grayish fine to coarse grained sandstone with intraclasts and sub-rounded to angular volcanic clasts. Figure 42 is representative of stratigraphic unit at 97.10 m (sample 11/25/11_1), described in the field as a brownish very fine to fine grained sandstone. Refined as brownish very fine volcanic arenite with intraclasts and planktonic foraminifera, some high relieve minerals, micriticized. Figure 43 is representative of stratigraphic unit at 98.40 m (sample 11/25/11_2), described in the field as a brown fine to medium grained volcanic sandstone, moderately-poorly sorted. Refined as brownish very fine sandstone with few skeletal fragments, intraclasts and planktonic foraminifera. Figure 44 is representative of stratigraphic unit at 100.25 m (sample 11/25/11_3), described in the

field as a grayish medium to coarse grained volcanic sandstone, poorly sorted, with some coarse grained black lithics. Refined as grayish volcanic arenite, few intraclasts, angular to sub-rounded, and few volcanic grains. Figure 45 is representative of stratigraphic unit at 102.05 m (sample 11/25/11_4), described in the field as a grayish medium grained volcanic sandstone, moderately sorted. Refined as volcanic arenite, some skeletal constituents with intraclasts.

107.60-112.30 m – An andesitic flow was described as seen on the thin sections. In the field and hand samples this 4.70 m unit was described as a gray fine grained volcanic sandstone. Figure 46 is representative of stratigraphic unit at 112.30 m (sample 11/25/11_7), described in the field as a grayish fine grained volcanic sandstone. Refined as andesitic volcanic flow, feldspars, few intraclasts.

112.30-114.39 m – A volcanic arenite follows that is comprised of two intercalated different sandstones: one described as a brownish volcanic sandstone ranging in grain size from fine to medium sand; and another described as a grayish volcanic sandstone ranging in grain size from fine to medium sand.

114.39-131.25 m – Columnar joints are exposed.

131.25-221.69 m – Volcaniclastic sediments are exposed. Figure 47 is representative of stratigraphic unit at 200.95 m (sample CJ1), described in the field as columnar joints, basaltic flow. Description confirmed in the thin sections.

221.69-240.11 m – Volcaniclastic sediments section becomes covered.

240.11-308.91 m – Volcaniclastic arenite outcrops and is described as a brown medium to coarse grained volcaniclastic sandstone. For 18.93 m this unit was covered and it was assumed that the same lithology continues.

308.91-548.68 m – A volcaniclastic arenite resumes, only becoming slightly finer, very fine to fine grained sand sized, for an additional 124.90 m. It continues to be exposed for an additional 90.84 m, coarsening upward. And it continues to be exposed for an additional 5.10 m, fining upward.

548.68-554.32 m – An erosional surface is exposed showing a change from volcaniclastic sandstone to limestone. The limestone is composed of 5.64 m, grayish skeletal packstone to wackestone, with the top 0.14 m composed of a planktonic rich packstone. Figure 48 is representative of stratigraphic unit at 551.38 m (sample 3/21/12_1), described in the field as a grainstone with ooliths, some skeletal fragments, well rounded grains. Refined as grayish sparse biomicrite, red algae. Figure 49 is representative of stratigraphic unit at 552.16 m (sample 3/21/12_2), described in the field as a grayish pack-wackestone, with pellets, very dirty limestone. Refined as grayish sparse biomicrite (skeletal packstone). Figure 50 is representative of stratigraphic unit at 553.96 m (sample 3/21/12_3), described in the field as a grayish grain-packstone. Refined as grayish sparse biomicrite. Figure 51 is representative of stratigraphic unit at 553.96 m (sample 3/21/12_4), described in the field as a grayish grain-packstone. Refined as grayish sparse biomicrite (skeletal wack-packstone), few planktonic foraminifera.

554.32-554.80 m – A thin layer, 0.48 m, of a brown fine grained sandstone with few lithics clasts of very coarse sand sized is exposed. Figure 52 is representative of stratigraphic unit

at 554.32 m (sample 3/21/12_5), described in the field as a grayish grainstone with some lithics. Refined as grayish packed biomicrite, planktonic rich.

554.80-578.57 m – More limestone was being deposited, a grayish skeletal grainstone to packstone, for a thickness of 23.77 m. Figure 53 is representative of stratigraphic unit at 556.07 m (sample 3/28/12_1), described in the field as a grayish grainstone. Refined as grayish packed biomicrite (grainstone), few skeletal fragments. Figure 54 is representative of stratigraphic unit at 557.08 m (sample 3/28/12_2), described in the field as a grayish packstone. Refined as grayish sparse biomicrite, planktonic foraminifera, few echinoderm fragments. Figure 55 is representative of stratigraphic unit at 557.86 m (sample 3/28/12_3), described in the field as a grayish grain-packstone. Refined as grayish sparse biomicrite, spicule rich with lithics. Figure 56 is representative of stratigraphic unit at 560.06 m (sample 3/28/12_4), described in the field as a grayish pack-grainstone. Refined as grayish sparse biomicrite, few planktonic foraminifera. Figure 57 is representative of stratigraphic unit at 563.27 m (sample 3/28/12_5), described in the field as a brownish very fine sandstone. Refined as grayish sparse biomicrite, some planktonic foraminifera and volcanic material. Figure 58 is representative of stratigraphic unit at 565.76 m (sample 3/28/12_6), described in the field as a grayish grainstone, some lithics. Refined as grayish packed biomicrite, some planktonic foraminifera and volcanic material. Figure 59 is representative of stratigraphic unit at 574.52 m (sample 4/6/12_1), described in the field as a grayish volcanoclastic sandstone with medium grained lithics of mafics. Refined as grayish packed biomicrite, some skeletal grains, planktonic foraminifera, spicules and volcanic grains, Echinodermata grains, fragments with microborings. Figure 60 is

representative of stratigraphic unit at 576.87 m (sample 4/6/12_2), described in the field as a grayish grainstone with some lithic flows, ooliths and skeletal fragments. Refined as grayish packed biomicrite, some planktonic foraminifera, spicules and volcanic grains.

578.57-584.67 m – Coarser sediments were deposited in a unit of 6.10 m in thickness, described as brownish fine grained sandstone.

584.67-600.85 m – A change in lithology occurs shifting into a feldspar porphyry basalt that probably represents a volcanic flow. This volcanic event is represented by a thickness of 16.18 m.

600.85-605.00 m – Limestone deposition follows the volcanics, a grayish skeletal grain-packstone to grainstone, for a thickness of 4.15 m. Figure 61 is representative of stratigraphic unit at 602.42 m (sample 4/13/12_1), described in the field as a grayish grainstone with some lithics, ooliths and skeletal fragments of medium grained sand sized. Refined as grayish packed biomicrite, some skeletal fragments and volcanic grains.

605.00-605.59 m – Coarser clastic sediments are over imposed and deposited in a unit of 0.59 m in thickness, described as brownish very fine to fine grained sandstone.

605.59-606.98 m – A change in lithology occurs with the deposition of a feldspar porphyry basaltic flow. This volcanic event is represented by a 1.39 m thick deposit. Figure 62 is representative of stratigraphic unit at 605.99 m (sample 4/26/12_1), described in the field as a grayish brown coarse to fine sandstone. Refined as olivine basalt. Figure 63 is representative of stratigraphic unit at 606.71 m (sample 4/26/12_2), described in the field as a grayish brown coarse to very coarse sandstone, few clasts. Refined as olivine basalt. Figure 64 is representative of stratigraphic unit at 606.98 m (sample 4/26/12_3), described

in the field as a grayish brown layered medium to fine sandstone. Refined as feldspar porphyry basalt.

606.98-615.74 m – Limestone deposition, a grayish skeletal grainstone, resumed with a thickness of 8.76 m. Figure 65 is representative of stratigraphic unit at 608.54 m (sample 4/13/12_2), described in the field as a grayish grainstone with some allochthonous material and skeletal fragments. Refined as grayish packed biomicrite, some red algae and spicules.

615.74-616.30 m – A dark gray fine volcanoclastic sandstone with some medium to coarse sand sized mafic grains is exposed, with a thickness of 0.56 m.

616.30-616.81 m – A reddish “altered/silicified” layer was exposed, with a thickness of 0.51 m. This layer was described in the field as a red siliceous mudstone (see Image 16 and Image 17).

616.81-618.09 m – A thin unit of limestone was again deposited at 616.81 m with a thickness of 1.28 m. Figure 66 is representative of stratigraphic unit at 618.09 m (sample 4/20/12_1), described in the field as a grayish grainstone. Refined as grayish packed biomicrite, skeletal fragments with microborings.

618.09-618.86 m – A brownish red siliceous mudstone is exposed, of 0.77 m in thickness (see Image 18), which is intermixed with brecciated mudstone clasts.

618.86-619.36 m – An additional thin unit of limestone, grayish grainstone, was deposited of about 0.5 m.

619.36-620.01 m – Dirtier sediments were deposited on top, starting with a reddish mudstone with what appeared to be magnetite, with a thickness of 0.65 m.

620.01-659.11 m – Deposition of a brownish fine to medium grained sandstone with some medium to very coarse sand grained mafics, with a thickness of 39.01 m.

659.11-659.02 m – A big change in structure was seen and logged. The stratigraphic section measurement was interrupted by a normal fault.

659.02-700.66 m – Unit descriptions resumed in younger rocks. A limestone facies was measured with a total of 41.64 m in thickness. The limestone was described as tan pack-wackestone with some skeletal constituents, mostly planktonic foraminifera as seen in the thin sections. As further studied with the thin sections, the entire unit is a skeletal packstone with some planktonic foraminifera, few lithics and, with red algae and rudist fragments at the bottom. Figure 67 is representative of stratigraphic unit at 697.76 m (sample 5/4/12_3b), described in the field as a yellowish tan wack-packstone with some skeletal fragments. Refined as tannish brown sparse biomicrite, few red algae and planktonic foraminifera. Figure 68 is representative of stratigraphic unit at 697.76 m (sample 5/4/12_8), described in the field as a yellowish tan wack-packstone with some skeletal fragments. Refined as tannish brown sparse biomicrite, few red algae and planktonic foraminifera. Figure 69 is representative of stratigraphic unit at 698.16 m (sample 5/4/12_7), described in the field as a yellowish tan pack-wackestone with some skeletal fragments. Refined as tannish brown sparse biomicrite, some rudists and planktonic foraminifera fragments. Figure 70 is representative of stratigraphic unit at 698.25 m (sample 5/4/12_6), described in the field as a yellowish tan wackestone. Refined as tannish brown sparse biomicrite, some lithics and planktonic foraminifera fragments. Figure 71 is representative of stratigraphic unit at 698.53 m (sample 5/4/12_5), described in the field as

a yellowish tan wackestone. Refined as tannish brown sparse biomicrite, some lithics and planktonic foraminifera fragments. Figure 72 is representative of stratigraphic unit at 698.67 m (sample 5/4/12_4), described in the field as a yellowish tan wackestone. Refined as tannish brown sparse biomicrite, some lithics and planktonic foraminifera fragments. Figure 73 is representative of stratigraphic unit at 698.94 m (sample 5/4/12_3), described in the field as a yellowish tan wackestone. Refined as tannish brown sparse biomicrite. Figure 74 is representative of stratigraphic unit at 699.51 m (sample 5/4/12_2), described in the field as a yellowish tan pack-wackestone. Refined as tannish brown sparse biomicrite, some lithics and planktonic foraminifera fragments. Figure 75 is representative of stratigraphic unit at 699.90 m (sample 5/4/12_1), described in the field as a yellowish tan wack-mudstone with some fine grained intraclasts. Refined as tannish brown sparse biomicrite, some lithics and planktonic foraminifera fragments.

700.66-700.69 m – The unit was interrupted by a calichified surface.

700.69-700.81 m – It coarsened with the deposition of a grayish very fine sandstone of 0.12 m in thickness.

A total of three intervals within the entire vertical succession were encountered with sufficient soil or debris cover that obstructed their description. These would be from 7 m to 22 m (15m covered), 221.69 m to 240.11 m (18.42 m in covered) and 308.91 m to 327.84 m (18.93 m covered) for a total of 52.35 m of covered section.

3.2 Stratigraphic Section

As a result of the fieldwork the data collected was used to prepare a stratigraphic section (see Figures 13 to 39). This effort took most of the time for finishing this study but, the

presentation and interpretation of these figures are the base for the discussion and, presentation of the data and geologic history of the area of study.

The depositional sequence of the sediments that make up the area of study and that were discussed under Section 3.1 can be followed and better viewed with the aid of the figures presented in Appendix A. An additional condensed stratigraphic column was made (Figure 11). This condensed version will allow a general discussion of the depositional history of the site along with the comparison with the rocks North of the valley and within the same time frame. Another purpose would be that this condensed section be used as a model to propose for the section be called as a “Type Area”.

3.3 Cerro de Abra Type Area

The data gathered and reviewed accounts for a very busy geological history of the southwestern Puerto Rico region during the Late Cretaceous Epoch at this ridge in particular. While analyzing the data and comparing it briefly to the previous work done by Almy (1965) on the geologic history of the Parguera Area, we noticed that our study area gathers much of the information and geologic history of the Parguera Limestone, specifically the Bahía Fosforescente and Punta Papayo Members. Volckmann (1984a and 1984d) referred later to these two members as the lower member. With all of the information available, for these members of the Parguera Limestone, in this ridge “Cerro de Abra”, the studied stratigraphic history shall be known as the Cerro de Abra Type Area accounting for the geologic history of the Bahía Fosforescente and Punta Papayo Members of the Parguera Limestone.

CHAPTER 4

INTERPRETATION

The sedimentary units describe in the Cerro de Abra were further analyzed in sequence stratigraphic techniques. Depositional sequences and parasequences were identified based on their texture and depositional environment interpretation. These parasequences were grouped in parasequence sets (*progradational parasequence set*, *aggradational parasequence set* and *retrogradational parasequence set*) and portrayed as system tracts. The objective of this chapter was to construct the depositional history of the Bahía Fosforescente and Punta Papayo Members of the Parguera Limestone, correlate it to the Cotuí Limestone, Sabana Grande Formation, Guaniquilla Limestone, and Yauco Formation of the Southwest Igneous Province and, to detail the significance of the parasequence sets. For better visualizing the following interpretation reference to Figure 11 and Figures 13 to 75.

4.1 Stratigraphy

The initial deposits of the Parguera Limestone, the Bahía Fosforescente Member, occurred as a carbonate platform sequence deposited over a volcanic/tectonic surface during a Santonian transgressive event that evolve rapidly into an aggradational/progradational event of the platform. The subsequent deposits of the Parguera Limestone, the Punta Papayo Member, occurred after a relative drop in sea-level and up-dip volcanism resulting in deposition of volcanic arenites with limestone intraclasts and planktonic foraminifera, and slumped blocks close to the base of the unconformity during a Campanian rapid

transgressive event. These deposits resulted of a Forced Regression. They're followed by volcanism during a LST, deposition of volcanic arenites during TST, followed by a HST characterized by bedded, fine grained carbonates.

The Bahía Fosforescente and Punta Papayo Member are divided into the following parasequence sets:

0-6.5 m; units 1 to 4, retrogradational parasequence set: Fining-upward (deepening-upward) succession deposited by a relative sea-level rise. This represents that the sea-level was relatively rising permitting the deposition of these sediments. At this parasequence set we can distinct some volcanic clasts reworked from the basal volcanics. The parasequence ends in a unit of coarser material with absence of the volcanic clasts, representing a relative sea-level rise, with a drowning of the whole volcanic/tectonic surface. The system track for this parasequence set is interpreted as a TST.

6.5-59.1 m; units 5 to 46, aggradational/progradational parasequence set: Carbonate deposition continues with at least 15 parasequences of aggradational/progradational parasequence sets with at least 5 events of relative sea-level equilibrium by particularly having a balanced accretion of carbonates and relative sea-level rise. The system track for this parasequence set is interpreted as a HST.

59.1-107.6 m; units 47 to 55, forced regression parasequence set: Carbonate deposition ceased by a relative sea-level drop resulting from deposition of volcanic arenites on an unconformity. The first sequence boundary (SB1) was identified at the base of this event. The volcanic arenites described had along its constituents some limestone intraclasts and planktonic foraminifera, slumped blocks close to the base of the unconformity. Both

sightings were associated to having enough time for a platform to build-up while having sediment bypass and deposition. Then enough relative sea-level drop caused a shift in sediment deposition to a deeper setting, stopping the aggradation of the platform and to part of it to slump down slope to deposit below on the new setting. Several downstepping prograding deposits are recorded. The system track for this parasequence set is a forced regression.

107.6-112.48 m; unit 56, volcanic event: Volcanic event recorded, sea-level dropped. The second sequence boundary (SB2) was identified at the base of this event. The volcanic rock was classified as an andesite with some intraclasts of limestone. This andesitic flow was deposited sub-aerially given its tuffaceous appearance and the intraclasts, angular in shape, content.

112.48-114.39 m; units 57 to 60, forced regression parasequence set: Initiation of several downstepping prograding deposits by relative rise in sea-level is recorded. Deposition of volcanic arenites intermixed with intraclasts of limestone. A source of limestone was close to the area for it to be eroded and be deposited along with the arenite.

114.39-221.69 m; units 61 to 62, volcanic event: An additional volcanic event recorded, sea-level dropped. The third sequence boundary (SB3) was identified at the base of this event. Clear evidence of subaerial deposition is seen by the columnar jointing pattern that the basaltic flow acquired. The volcanic event continued for a longer amount of time by the continued deposition of volcanoclastic sediments. We can suggest the source of volcanism was fairly close.

221.69-240.11 m; covered: Stratigraphy was covered.

240.11-548.68 m; units 63 to 70, retrogradational parasequence set: Volcanism ceased and a relative rise in the sea-level occurred. Deposition of volcanoclastic sediments is recorded. Analysis of the rocks in the field showed no fair amount of matrix between grains, meaning that the source of this deposits was fairly close. The thickness of this system track is considerably large. A slow and steady relative sea-level rise is considered as the mechanism of such deposit to aggrade in that manner. TST is the system tract associated with this parasequence.

548.68-554.80 m; units 71 to 74, aggradational/progradational parasequence set: Carbonate deposition resumes, resulting in a disconformity, while relative sea-level rise continues. The fourth sequence boundary (SB4) was identified at the base of this event. A fining-upward succession is recorded. It is followed by a coarsening-upward succession. This resulted in the system tract to change from TST to HST. There's some bypass of terrigenous sediments in the unit that is intermixed with some planktonic foraminifera. This implicates that the carbonate deposition was happening at deep waters while some terrigenous sediments bypassed the platform and deposited at this location. Relative sea-level rise continues with more deposition of carbonates as a progradational parasequence in a coarsening-upward sequence. The coarsening-upward succession culminates with deposition of terrigenous sediments. The fifth sequence boundary (SB5) was identified at the base of this event.

554.80-584.67 m; units 75 to 82, progradational parasequence set: A coarsening-upward succession represented by 3 progradational parasequences. The system tract for this parasequence set is a HST. Carbonate deposition continues, relative sea-level rise

decelerates. Skeletal fragments of both deep and shallow water biota are seen mixed portraying an unstable basin.

584.67-600.85 m; unit 83, volcanic event: A volcanic event occurred, sea-level dropped. The six sequence boundary (SB6) was identified at the base of this event.

600.85-605.59 m; units 84 to 86, retrogradational parasequence set: The previous volcanic event concluded and a rapid relative sea-level rise occurred with the deposition of carbonates prograding into a terrigenous deposition. Carbonate deposition resumed in a coarsening-upward succession by a relative sea-level rise. The system tract for this parasequence set is a TST.

605.59-606.98 m; unit 87, volcanic event: A volcanic event with a sea-level drop is recorded. The seventh sequence boundary (SB7) was identified at the base of this event.

606.98-659.02 m; units 88 to 99, retrogradational to progradational parasequence set: Carbonate deposition resumed in a coarsening-upward succession by a relative sea-level rise represented by 3 progradational parasequences into deposition of terrigenous material. The system tract for this parasequence set is a TST prograding into a HST.

659.02 m; The stratigraphic section is interrupted by a normal fault. The eight sequence boundary (SB8) was identified at the base of this event.

659.02-698.25 m; units 100 to 101, aggradational/progradational parasequence set: Carbonate deposition is recorded in a coarsening-upward sequence and a relative sea-level rise as aggradational to progradational parasequence. The ninth sequence boundary (SB9) was identified at the base of the event where deposition of finer sediments, mudstones, occurred. The system tract for this parasequence set is a HST.

698.25-700.66 m; units 101 to 107, aggradational/progradational parasequence set: Carbonate deposition resumed, a coarsening upward sequence is seen, progradational parasequence, ending with a relatively drop in sea-level and an exposure surface (caliche) with some terrigenous sediments on top. The tenth sequence boundary (SB10) was identified at the base of the caliche surface. The system tract for this parasequence set is a HST.

4.2 Bahía Fosforescente and Punta Papayo Members depositional history

The Bahía Fosforescente Member initiated as transgressive system tract deposits in the lower portion of the platform, and a highstand system tract deposits at the top. It consists of high frequency and relative short period parasequences. Carbonate deposition starts as a TST by deposits characterizing landward migration of the facies belt. A HST continues with deposition at least 15 parasequences of aggradational/progradational parasequence sets, with at least 5 events of relative sea-level equilibrium. Deposition culminated by a relative drop in sea-level and exposure followed by a rapid transgression which left almost no evidence that the exposure happened.

The Bahía Fosforescente Member is set to be Santonian in age due to the contained the rudists: *Barrettia* and *Antillosarcolites sp.* (see Image 2), *Bournonia sp.* (see Image 3), *Stellacraprina* nov. gen. (Mitchell, 2013 and personal communication; see Image 4), *Durania sp.* (see Image 5), and *Actaeonella sp.*

This unconformity and rapid transgression marks the initiation of deposition of the Punta Papayo Member during the Campanian. This regression evolved into a forced regression

with the sediments that deposited on top. These sediments are characterized by volcanic arenites intermixed with intraclasts of an eroded carbonate platform, also some slumped boulders of previously deposited volcanic arenites, and, planktonic foraminifera.

A brief volcanic event occurred, an andesitic volcanic flow which dragged along some intraclasts of limestone, marking a relative drop in sea-level that was then followed by some drowning of the area with deposition of more volcanic arenites intermixed with limestone intraclasts.

Another volcanic event occurred characterized by some columnar joints. These columnar joints indicate a relative drop in sea-level, exposure of the platform with some sub-aerial deposition. This is an indication of a nearby volcanic source.

Volcaniclastic sediment deposition follows during a lowstand system tract. Relative sea-level stays low for a considerable span of time which is recorded in the amount of volcaniclastic sediment that was deposited on this basin floor. Hardly no matrix is seen between the grains of these deposits, an indication that they were mostly deposited at shallow waters and nearby the source.

Transgression initiates with deposition of volcaniclastic arenites, a relative sea-level rise began. Relative sea-level continues to rise and carbonate deposition starts with a recorded disconformity followed by a thinning-upward succession marking a change in the sequence to a highstand system tract.

Relative sea-level rise continues during a HST and is interrupted by a relative drop in sea-level with a volcanic event. This event is not as big as the previous one recorded. A small regression follows and is exposed with a coarsening-upward succession, that yet again is

interrupted by a volcanic event. This event is even smaller than the previous one, geologically recording that the basin is shifting away from the volcanic source.

Relative sea-level rise resumes with a transgression with carbonate deposition coarsening-upward to volcanic arenites. Then it starts to prograde with carbonate deposition coarsening-upward succession during a HST.

CHAPTER 5

DISCUSSION

5.1 Sequence Stratigraphy

Sequence Stratigraphy allowed a better discussion and understanding of the geologic history of the Parguera Limestone, specifically the Bahía Fosforescente and Punta Papayo Members. By applying this technique, a clear relationship between the depositional patterns and their characteristic deposits of TST, HST, Forced Regression and LST was established. The TSTs represented a period of relative sea-level rise were high enough subsidence occurred to produced migration of the facies belt in landward direction, recording a characteristic retrogradational geometry, probably resulting from an end in volcanism and subsidence. The HSTs represented a period of low relative sea-level rise, recording characteristic aggradational/progradational geometries. Most of the time HSTs ceased with an exposure of the platform by a relative drop in sea-level. During the HST in the proximal area carbonate platform progrades depositing grainstone to wackestone and, in the distal carbonate mud is deposited. The LST's represents a period of relative sea-level fall at the offlap break, and subsequent slow relative sea-level rise. It is characterized by deposits of submarine fans during falling sea-level and a topset system. The forced regressions represented periods were transgression initiated, some deposition of a platform was established, but a relative sea-level drop occurred. This relative sea-level drop moved the shoreline basinward, erosion of the exposed platform occurred causing for these sediments, along with the other terrigenous material that bypassed the platform, to be deposited alongside deeper sediments and microfauna (planktonic foraminifera). A number

of these cycles of relative sea-level drop were the cause of the major forced regression system tract recorded in this study.

5.2 Correlation with Previous Work

The limestones recorded at the exposures on the quarry, a grayish fossiliferous limestone, are equivalent to the “massive limestone” of the Bahía Fosforescente Member of Almy (1965). Deposition of this limestone facies concluded by a relative drop in sea-level and exposure, therefore an unconformity. This was followed by a rapid transgression depositing arenites during a forced regression system tract. This event is not recorded by Almy (1965). He includes the arenites as part of the Bahía Fosforescente Member. As a result, initiation of deposition of the Punta Papayo Member has been shifted to this geological event. Volcanic activity follows the forced regression deposits, adding a geological event to the Punta Papayo Member that was not previously recorded in southwestern Puerto Rico. After these volcanic deposits a considerable amount of volcanoclastic sediment was deposited on top during the evolution of the LST.

Volcanoclastic arenite deposition followed the LST as a result of a transgression, which then evolved into a HST represented by a grayish skeletal packstone. These rocks are recorded by Almy (1965) but, are included as part of the Bahía Fosforescente Member, upper and final sequence of deposition, as “upper calcarenite”. Carbonate deposition resumes with deposition of a grayish fossiliferous limestone prograding and ending with a volcanoclastic arenite deposition. We believe that Almy’s (1965) Punta Papayo Member, “interbedded calcarenite and mudstone”, on which he starts the depositional history of the member, is equivalent to the carbonate deposition described here. But, as mentioned

before, the geological depositional history of the Punta Papayo Member starts at the unconformity on top of the “massive limestone” in the quarry. The previous sequence culminates with a recorded volcanic event that resulted in a relative sea-level drop. This adds a geological event to the Punta Papayo Member that was not previously recorded by Almy (1965). Carbonate deposition follows, with some coarsening-upward successions prograding into coarser clastic sediments. In part of the section, around 616m to 620m, iron staining and silicified mudstones were identified. This part of the section corresponds to the “zone of iron staining” and “silicified mudstones” identified by Almy (1965) as part of the Punta Papayo Member.

Carbonate deposition continues on top with a few coarsening-upward successions of a tannish fossiliferous limestone. This is interpreted as the distal deposition during HST. This part of the section corresponds to the “foraminiferal mudstones” identified by Almy (1965) as part of the Punta Papayo Member. Refer to Figure 12 for a stratigraphic correlation of this study with Almy’s (1965) stratigraphy and, with the rest of the studies in SW PR.

5.3 Correlation with the Stratigraphy of the Cabo Rojo-Sabana Grande Block

The Parguera Limestone represents deposits of upper slope to slope characterized by volcanic/tectonic episodes, subsidence and relative sea-level rise in the Late Cretaceous of the rocks south of the Lajas Valley. Correlation with other units of the same age like the Cotuí Limestone and Sabana Grande Formation was very important into recognizing the mechanisms that were affecting the depositional environments. The limestones recorded at the exposures on the quarry, first a thinning-upward succession of a grayish fossiliferous

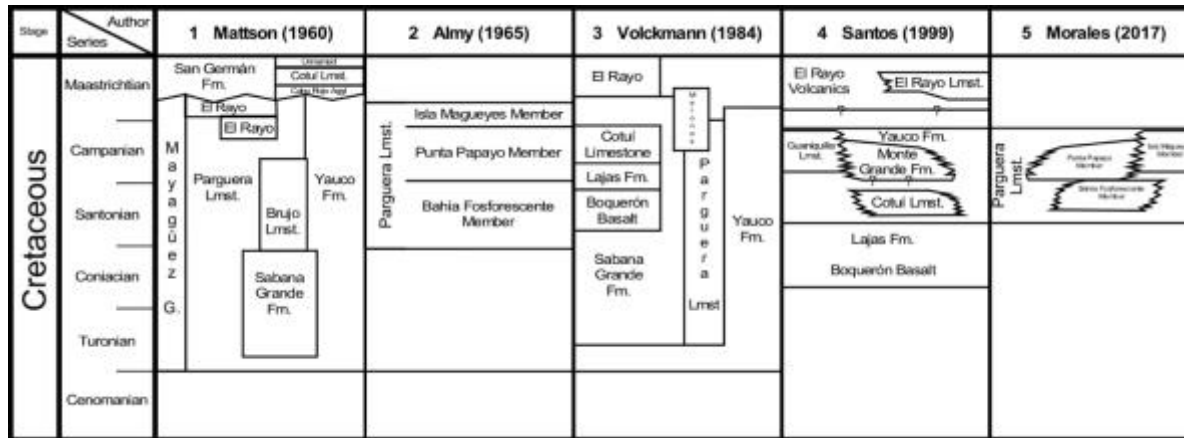


Figure 12: Stratigraphic correlation of this study with the rest of the studies in SW-PR

limestone (skeletal grainstones to packstones) with some basal volcanic clasts followed by coarsening-upward successions of a grayish fossiliferous limestone (skeletal grainstones to mudstones), equivalent to the Bahía Fosforescente Member of Almy (1965), correlate to the deposits of the Cotuí Limestone. The Bahía Fosforescente Member is characterized by a transgressive system tract deposits in the lower portion of the platform, and a highstand system tract deposits at the top similar to the Cotuí Limestone (Bonilla, 2007). The Bahía Fosforescente Member represents upper slope deposition occurring downslope of the Cotuí Limestone. Deposition of the Bahía Fosforescente Member concluded by a relative drop in sea-level and exposure, an unconformity. The previous described unconformity, followed by a rapid transgression with deposition, during a forced regression system tract, of volcanic arenites intermixed with intraclasts of the eroded carbonate platform including some slumped boulders of previously deposited volcanic arenites and, planktonic foraminifera marks the initiation of deposition of the Punta Papayo Member during the Campanian.

Sediments above the Cotuí Limestone have rip-up clasts that show soft sediment deformation and contain planktonic foraminifera as well rudist that are younger in age than the Cotuí Limestone (Santos, personal communication 2016-17). After the force regression started flows going into the area ripped-up the still soft sediment and deposited it over the Cotuí Limestone. As the force regression continued small carbonate platform developed but as the sea-level continued dropping the exposure of the not completely solidified sediment resulted in erosion and transportation of gravity blocks producing conglomerates and breccias. These are the limestone lenses of the Sabana Grande Formation mapped by

Volckmann (1984-b to -d) that included younger rudists. Thereafter, a relative rise in sea-level occurred and was accompanied by deposition of volcanoclastic sediments of the Sabana Grande Formation (Santos, 1999). This part of the stratigraphy, the initiation of the Punta Papayo Member correlates with the Sabana Grande Formation exposed in the Monte Grande area, yet again the Punta Papayo Member was in a deeper setting than the Sabana Grande Formation.

Volcanic activity is recorded followed by volcanoclastic sediment deposition in the Punta Papayo Member. Its analogous, the Sabana Grande Formation, during the same time frame, was recording some volcanic flows and deposition of volcanoclastic sediment with debris flows. A change in the settings of deposition is seen, the Punta Papayo Member becomes shallower than the Sabana Grande Formation. Volcanoclastic arenite deposition followed in the Punta Papayo Member. Its analogous, the Sabana Grande Formation, during the same time frame, was recording deposition of limestone and recycled volcanic debris. Also, at a shallower setting the Guaniquilla Limestone was being deposited and, at a deeper setting the Yauco Formation was being deposited as deeper slope sediments.

Carbonate deposition resumed, in the Punta Papayo Member, followed by deposition of a volcanoclastic arenite culminating with a recorded volcanic event. Analogous Sabana Grande Formation is recording volcanoclastic deposition of sediments that are being bypassed through the carbonate platform. Still, at a shallower setting the Guaniquilla Limestone was being deposited and, at a deeper setting the Yauco Formation was being deposited as deeper slope sediments. Carbonate deposition resumes, in the Punta Papayo Member, with lower slope sediments. Analogous Sabana Grande Formation is recording

volcaniclastic deposition of sediments that are being bypassed through the carbonate platform. Still, at a shallower setting the Guaniquilla Limestone was being deposited and, at a deeper setting the Yauco Formation was being deposited as deeper slope sediments.

CHAPTER 6

CONCLUSION

This thesis was devised to gather a better detailed stratigraphic and paleofacies analysis of the Parguera Limestone, specifically the Bahía Fosforescente and Punta Papayo Member. Cerro de Abra Type Area recollects most of the geology described by Almy (1965) from the gray limestone facies to the foraminiferal mudstone, accounting for a geologic history from Santonian to Middle Campanian. It is the most complete stratigraphic section to date of the lower member of the Parguera Limestone that presents the volcanic/tectonic episodes, subsidence and relative sea-level changes in the Late Cretaceous of the rocks south of the Lajas Valley. The study of the parasequences provided a better understanding of the geological depositional history and it also records the migration of the volcanic center, from southwest (Santonian) to east-northeast (Campanian). The data added value to the geologic history of the Southwest Igneous Province of Puerto Rico by reconstructing the stratigraphy, with the aid of sequence stratigraphy, and correlating it to other units like the Cotuí Limestone and Sabana Grande Formation of the same age. Further studies are encouraged in this rocks with the aid the additional tools that are provided under this discipline like the study of microfacies and isotopic dating.

REFERENCES

- Addarich, L., 2009, The geologic mapping and history of the Guánica Quadrangle, Southwestern Puerto Rico: Mayagüez, Puerto Rico, University of Puerto Rico, Mayagüez Campus, unpub. MS thesis.
- Almy, C. C., Jr., 1965, Parguera Limestone, Upper Cretaceous Mayagüez Group, Southwest Puerto Rico: Houston, Texas, Rice University, unpub. Ph.D. thesis.
- Bonilla, A., 2007, Sequence Stratigraphic Analysis of the Cotui Limestone, Upper Cretaceous of southwestern Puerto Rico: Mayagüez, Puerto Rico, University of Puerto Rico, Mayagüez Campus, unpub. MS thesis.
- Bonilla, A., 2004, Diagenetic Study of the Cements History of the Cotui Limestone, Upper Cretaceous of the South-West Puerto Rico: Mayagüez, Puerto Rico, University of Puerto Rico, Mayagüez Campus, Undergraduate research.
- Clavet, F., and Tucker, M.E., 1990, Carbonate Ramps, Sequence Stratigraphy and Depositional System Tracts; an example from Triassic Muschelkalk of the Catalan Basin, Spain: International Sedimentological Congress, vol. 13, p. 558- 559.
- Díaz, V., 2004, Isotopic Analysis of the upper Cotui and the Guaniquilla formation on road PR#100, Southwestern Puerto Rico: Mayagüez, Puerto Rico, University of Puerto Rico, Mayagüez Campus, Undergraduate research.
- Dunham, R.J., 1962, Classification of carbonate rocks according to depositional texture: American Association of Petroleum Geologist, Memoir 1, p. 108-121.
- Embry, A. F., and Klovan, J. E., 1971, A Late Devonian reef tract on Northeastern Banks Island, N.W.T: Canadian Petroleum Geology Bulletin, v. 19, p. 730-781.
- Emery, D., and Myers, K.J., 1996, Sequence Stratigraphy: Blackwell Science, Oxford. Chp 10, p. 211-237.
- Flügel, E, 2004, Microfacies of Carbonate Rocks, Analysis, Interpretation and Applications: Springer.
- Folk, R.L. ,1959, Practical petrographic classification of limestone: *Bul. Am. Ass. Petrol. Geol.* 43, p 1-38.
- Folk, R. L., 1962, Spectral Subdivision of Limestone Types, in W. E. Ham (ed.), Classification of carbonate rocks: American Association of Petroleum Geologists Memoir 1, p. 62-84.

- Hunt, D. and Tucker, M.E., 1993, The Middle Cretaceous Urganian Platform of Southeastern France: AAPG Memoir, vol. 56, p. 409-453.
- Krushensky, R. H. and J. H. Schellekens, 2001, Geology of Puerto Rico, p. 24-36. In W. J. Bawiec (compiler), Geology, geochemistry, geophysics, mineral occurrences and mineral resource assessment of the Commonwealth of Puerto Rico: U.S. Geological Survey Open File report 98-38.
- Le Maitre, R.W. 2002, Igneous Rocks: A Classification and Glossary of Terms, Recommendations of the International Union of Geological Science Subcommittee on the Systematics of Igneous Rocks, 2nd edition: New York, New York, Cambridge University Press, p. 236w
- Mann, P., Drapper, G., and Lewis, J. F., 1991 An overview of the geologic and tectonic development of Hispaniola: *in* Mann et al. Editors, Geologic and tectonic development of the North American-Caribbean plate boundary in Hispaniola: Geological Society of America Special Paper 262, p. 1-28.
- Mattson, P. H., 1960, Geology of the Mayagüez Area, Puerto Rico: Bulletin Geological Society of America. Vol. 71, No 3, p. 235-362.
- Mitchum, R.M., Vail, P.R., and Thompson, S., 1977, The depositional sequences as a basic unit for stratigraphic analysis: American Association of Petroleum Geologists Memoir 26, p. 53-62.
- Mitchell, G. J., 1922, Geology of the Ponce district, Porto Rico: N. Y. Acad. Sci., Scientific Survey of Porto Rico and the Virgin Islands, v. 1, p. 252.
- Mitchell, S.F., 2013, Revision of the Antilocaprinidae Mac Gillavry (Hippuritida, Bivalvia) and their position within the Caprinoidea d'Orbigny: Geobios Volume 46, n° 5, p. 438-440.
- Montgomery, H. M., Pessagno, E. A., and Pindell J. L., 1994, A 195 Ma Terrane in a 165 Ma Sea: Pacific origin of the Caribbean Plate: GSA Today, v. 4, p. 1-6.
- Nichols, G., 1999, Sedimentology & Stratigraphy, Blackwell Science Ltd., p. 71-73.
- Pérez, R., 2004, Stratigraphic and Carbon Isotope Analysis of the Cotui Limestone in the Cerro Buena Vista Area: University of Puerto Rico, Mayagüez Campus, unpub. Special topics class.

- Posamentier, H.W., Allen, G.P., 1999, Siliciclastic Sequence Stratigraphy: concepts and applications. SEPM Concepts in Sedimentology and Paleontology no. 7, p. 210.
- Santos, H., 1999, Stratigraphy and Depositional History of the Upper Cretaceous Strata in the Cabo Rojo-San Germán Structural Block, southwestern Puerto Rico: University of Colorado, unpub. Ph.D. thesis.
- Sarg, J.F., 1988, Carbonate Sequence Stratigraphy: Society of Economic Paleontologist and Mineralogist, Special Publication, 42, p. 155-181.
- Schellekens, J. H., 1993, Geochemical evolution of the volcanic rocks in Puerto Rico: unpub Ph.D. thesis, Syracuse University, Syracuse, New York, p. 289.
- Schellekens, J. H., Santos, H., Almy, C. C., and Jansma, P., 1993, Field Guide to the 12th Symposium on Caribbean Geology: University of Puerto Rico, Mayagüez, Puerto Rico, p. 65.
- Schellekens, J. H., and Joyce, J., 1999, Field Guide to the 18th Symposium on Caribbean Geology: University of Puerto Rico, Mayagüez, Puerto Rico, p. 2-6.
- Slodowski, T. R., 1956, Geology of the Yauco area, Puerto Rico: unpublished Ph.D. thesis, Princeton University, p. 31, 84-92, 122-124
- Tucker, M.E., and Wright, V.P., 1990, Carbonate sedimentology: Oxford, England, Blackwell.
- Tucker, M.E., 1993, Carbonate Sequence Stratigraphy, Diagenesis and Porosity Prediction: AAPG Bulletin, vol. 77, no 9, p. 1670.
- Tucker, M.E., 2001, Sedimentary Petrology, 3rd edition: Ames, Iowa, Blackwell Science, p. 262.
- Vail, P.R., Mitchum, R.M., Todd, R.G., Widmier, J.M., Thompson, S., Sangree, J.B., Bubb, J.N., Hatledid, W.G., 1977, Seismic stratigraphy—Application to hydrocarbons exploration: American Association of Petroleum Geologist Memoir, 26, p. 49-212.
- Van Wagoner, J.C., Mitchum, R.M., Jr., Campion, K.M. and Rahmanian, V.D. (1990) Siliciclastic Sequence Stratigraphy in Well Logs, Cores and Outcrops: Concepts for High Resolution Correlation of Time and Facies: American Association of Petroleum Geologist Methods in Exploration Series, Tulsa, p. 7-55

Volckmann, R. P., 1984a, Geologic map of the Cabo Rojo and Parguera quadrangles, southwest Puerto Rico: U.S. Geological Survey Miscellaneous Investigations Series Map I-1557, scale 1:20,000.

_____ 1984b, Geologic map of the San Germán quadrangle, southwest Puerto Rico: U.S. Geological Survey Miscellaneous Investigations Series Map I-1558, scale 1:20,000.

_____ 1984c, Geologic map of the Puerto Real quadrangle, southwest Puerto Rico: U.S. Geological Survey Miscellaneous Investigations Series Map I-1559, scale 1:20,000.

_____ 1984d, Upper Cretaceous Stratigraphy of southwest Puerto Rico: A revision. U.S. Geological Survey Bulletin, p. A73-A83.

Appendix A – Stratigraphic Column

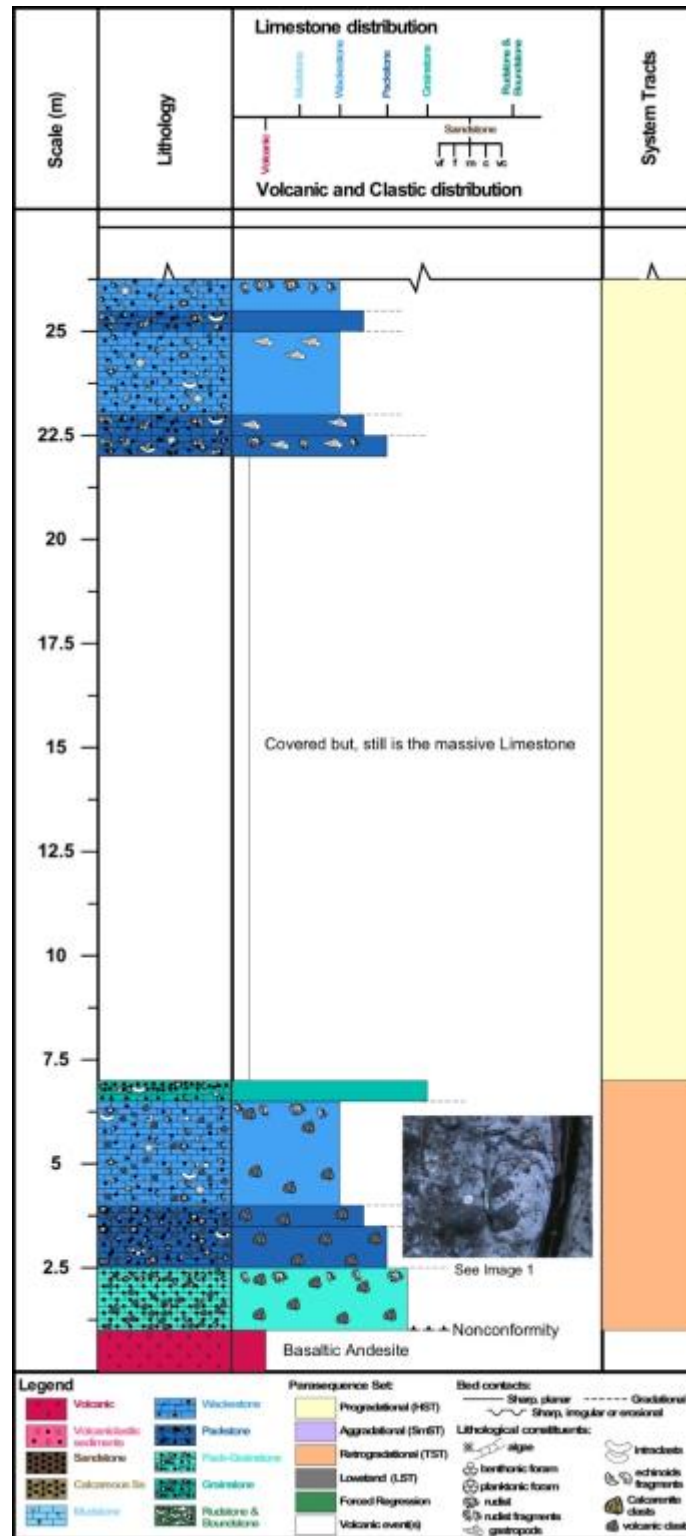


Figure 13: Stratigraphic Column from 0 to 26.25 m

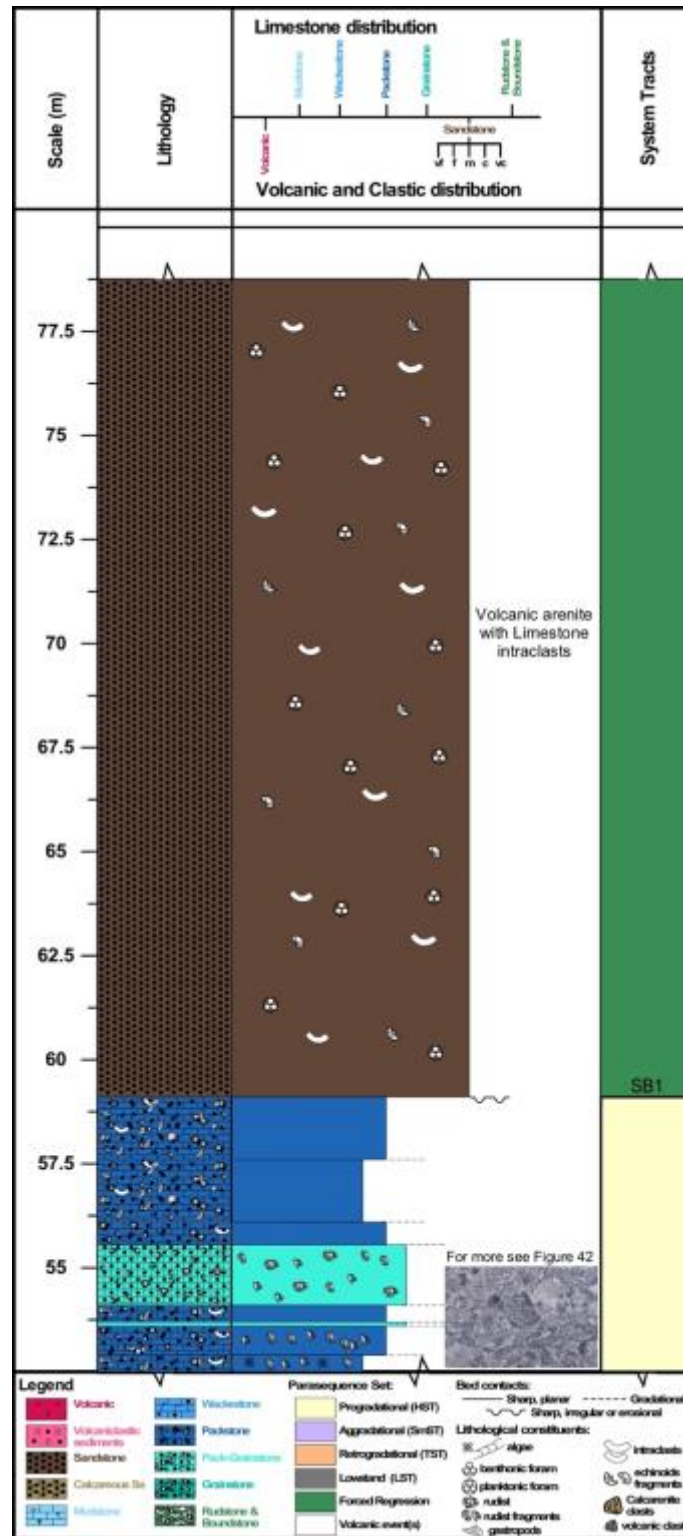


Figure 15: Stratigraphic Column from 52.5 to 78.75 m

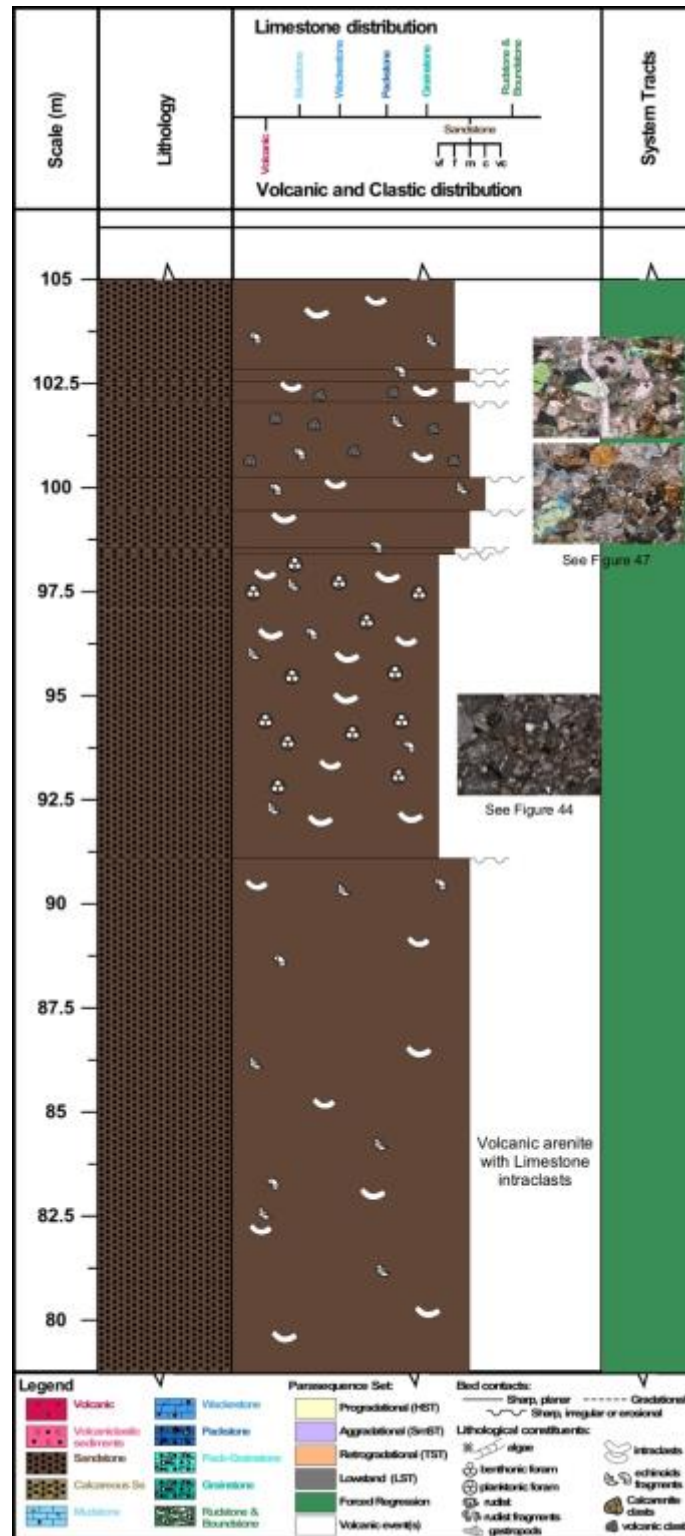


Figure 16: Stratigraphic Column from 78.75 to 105 m

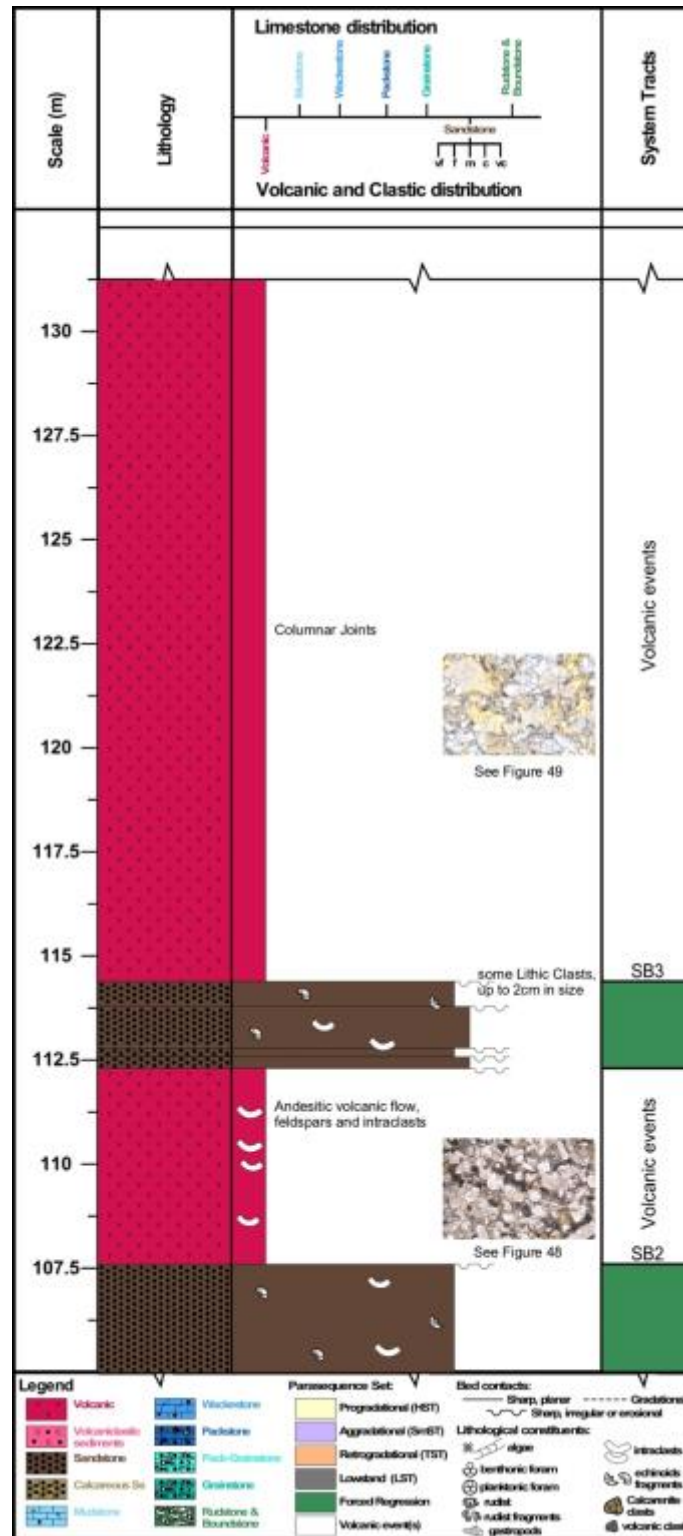


Figure 17: Stratigraphic Column from 105 to 131.25 m

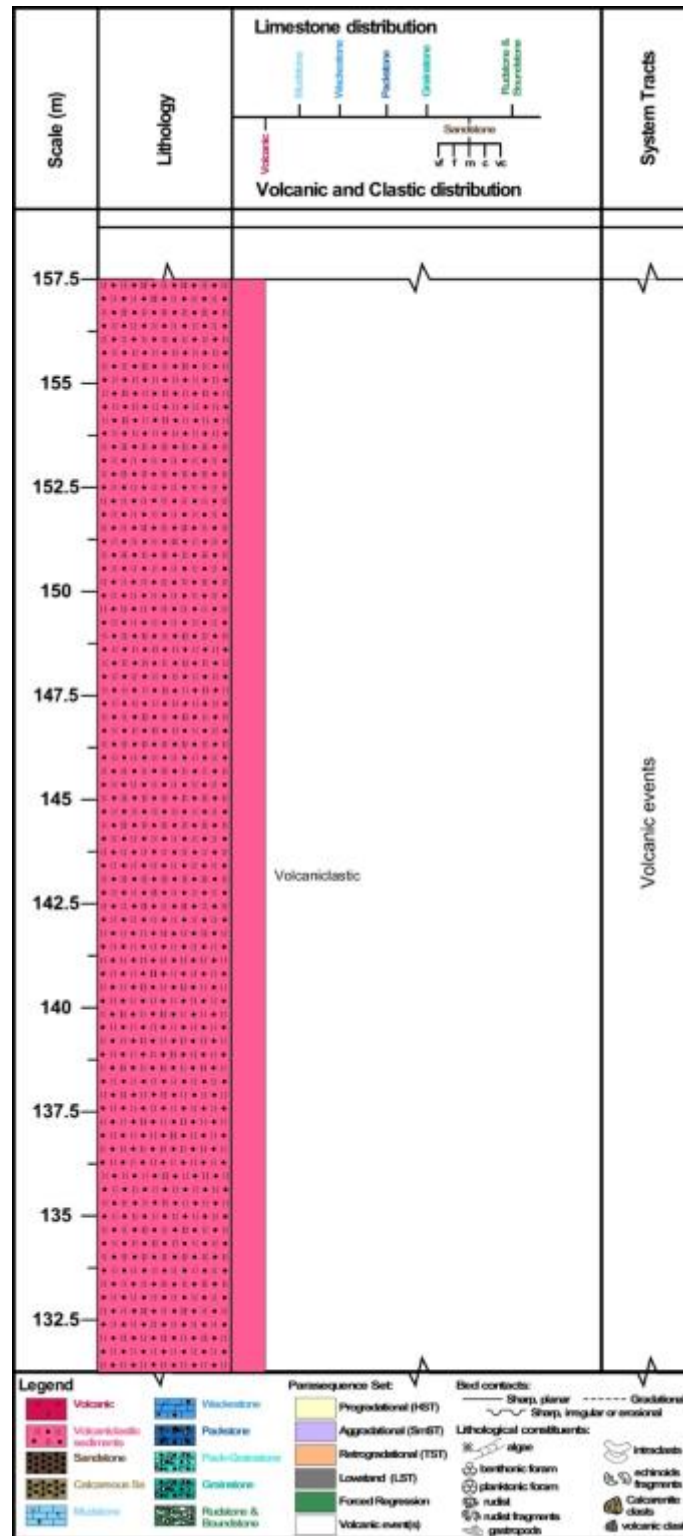


Figure 18: Stratigraphic Column from 131.25 to 157.5 m

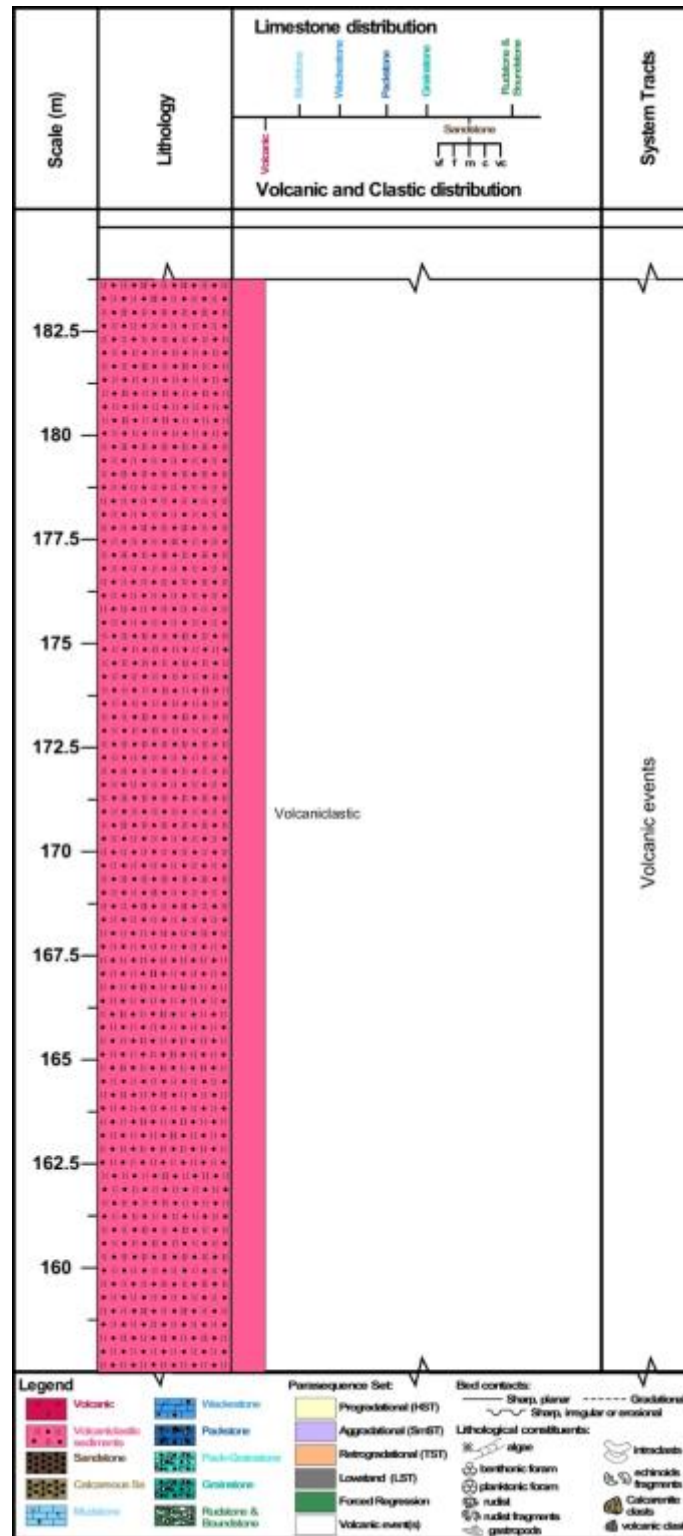


Figure 19: Stratigraphic Column from 157.5 to 183.75 m

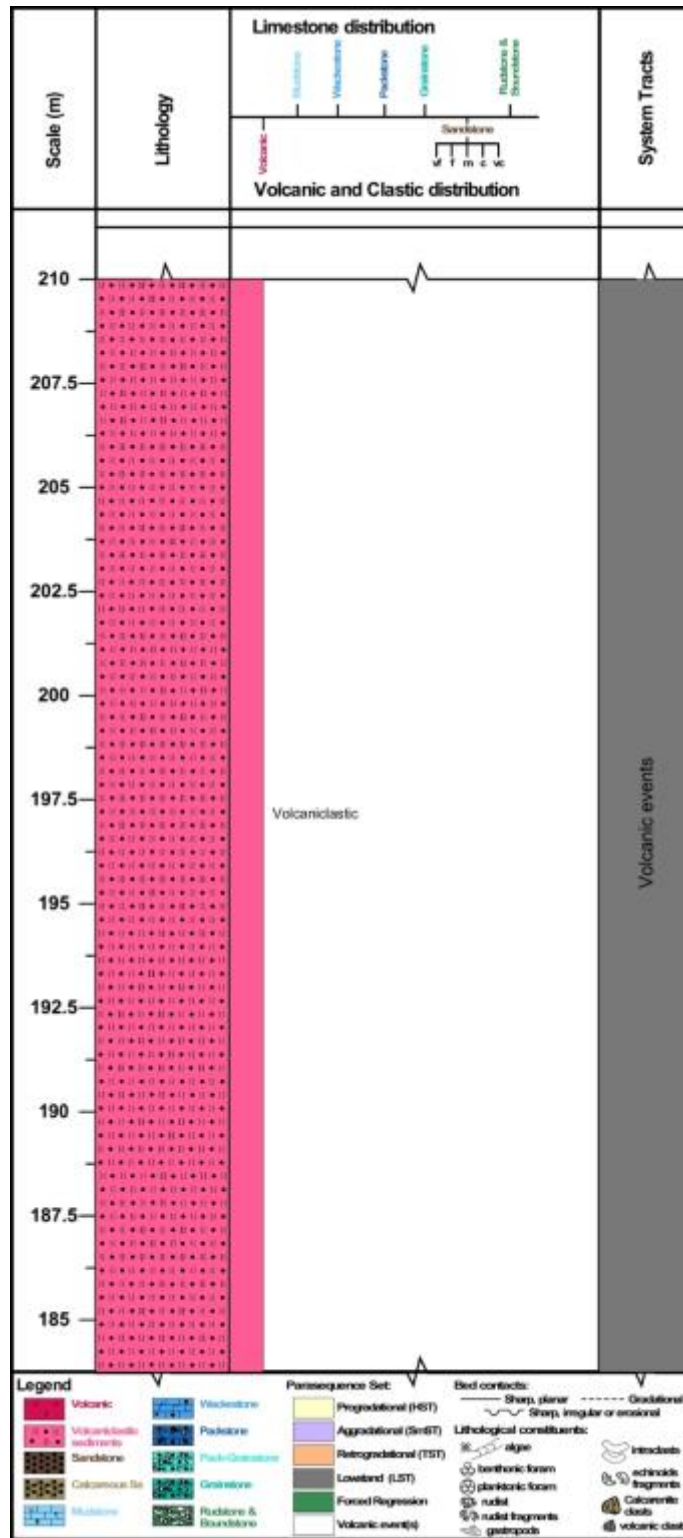


Figure 20: Stratigraphic Column from 183.75 to 210 m

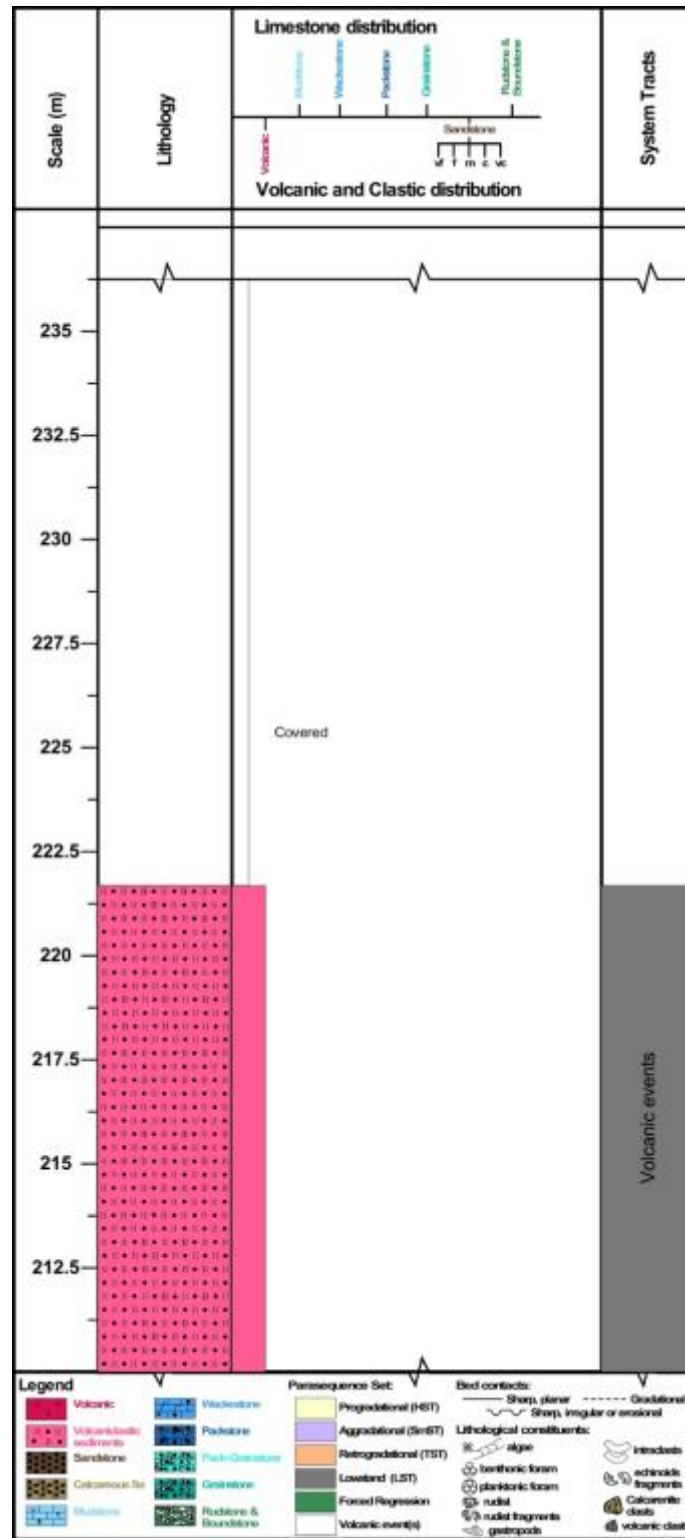


Figure 21: Stratigraphic Column from 210 to 236.25 m

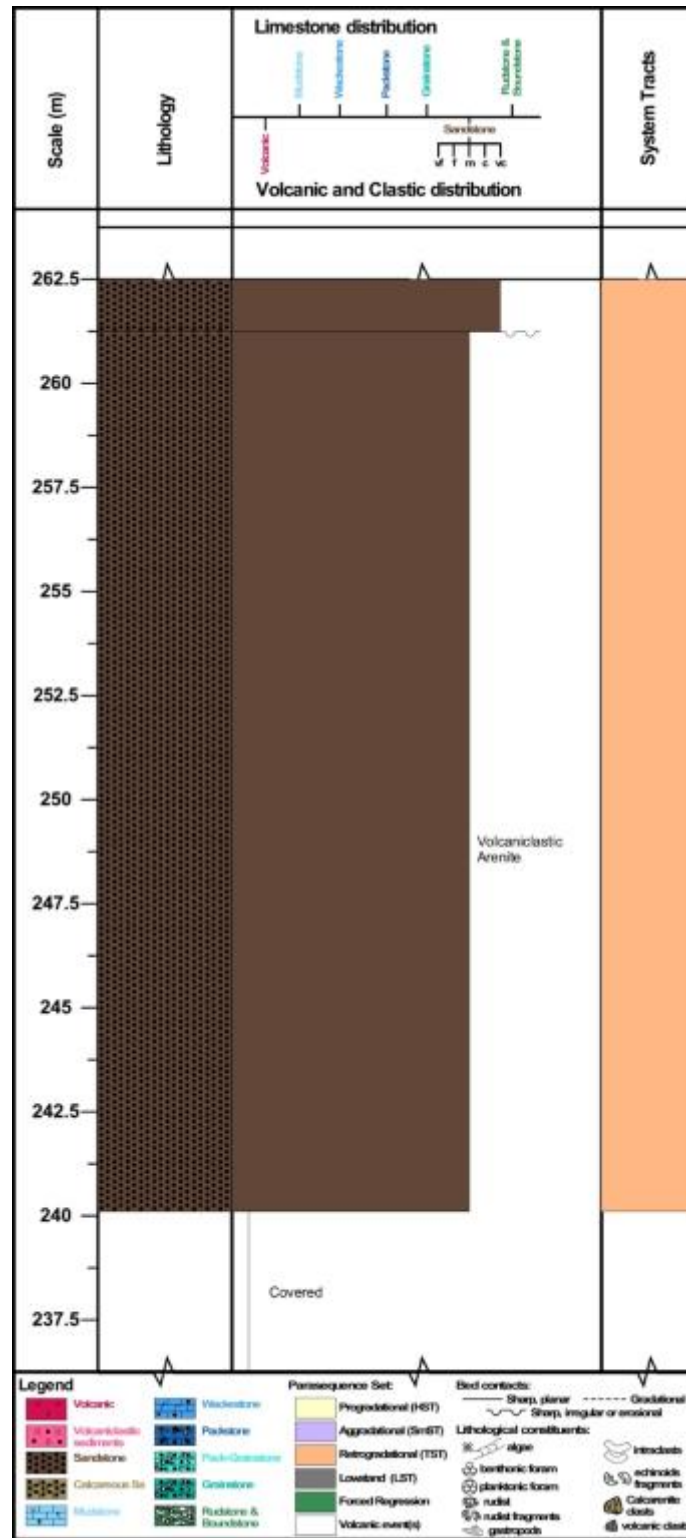


Figure 22: Stratigraphic Column from 236.25 to 262.5 m

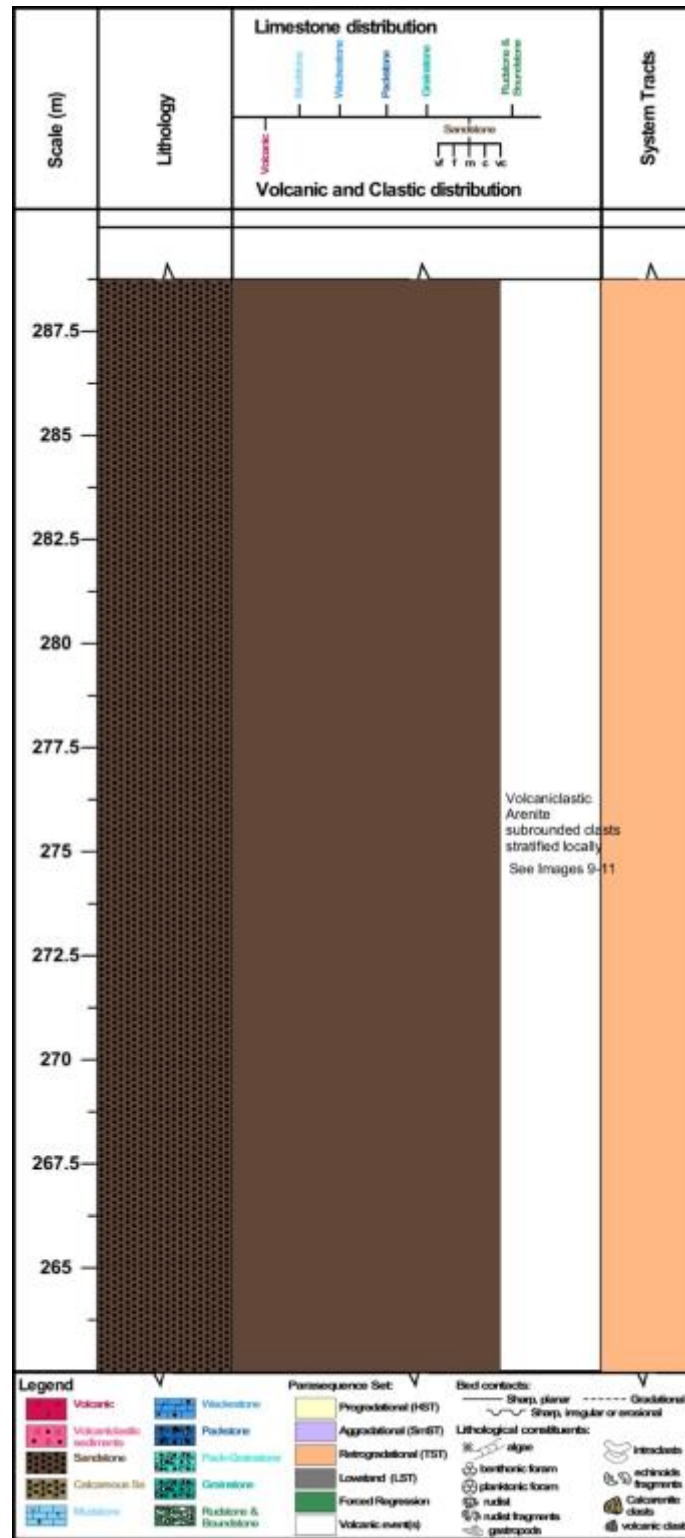


Figure 23: Stratigraphic Column from 262.5 to 288.75 m

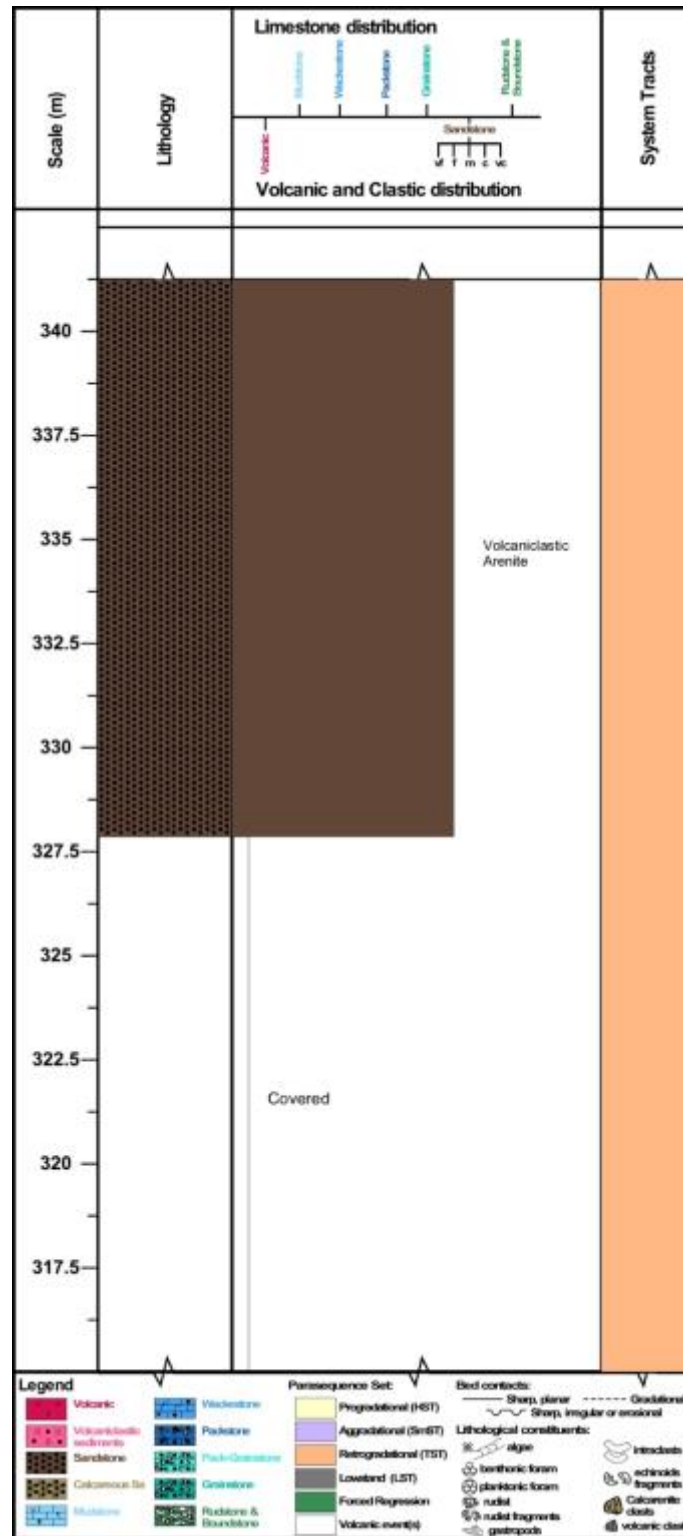


Figure 25: Stratigraphic Column from 315 to 341.25 m

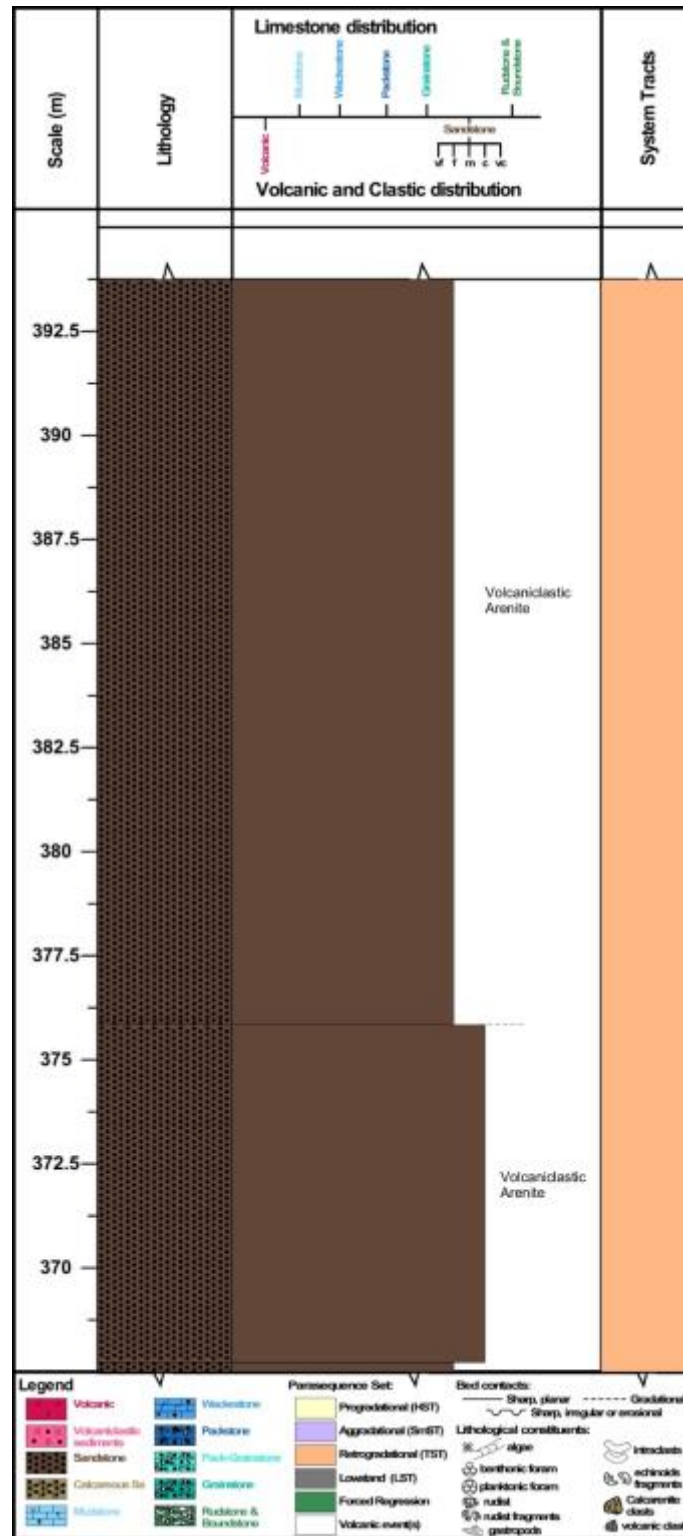


Figure 27: Stratigraphic Column from 367.5 to 393.75 m

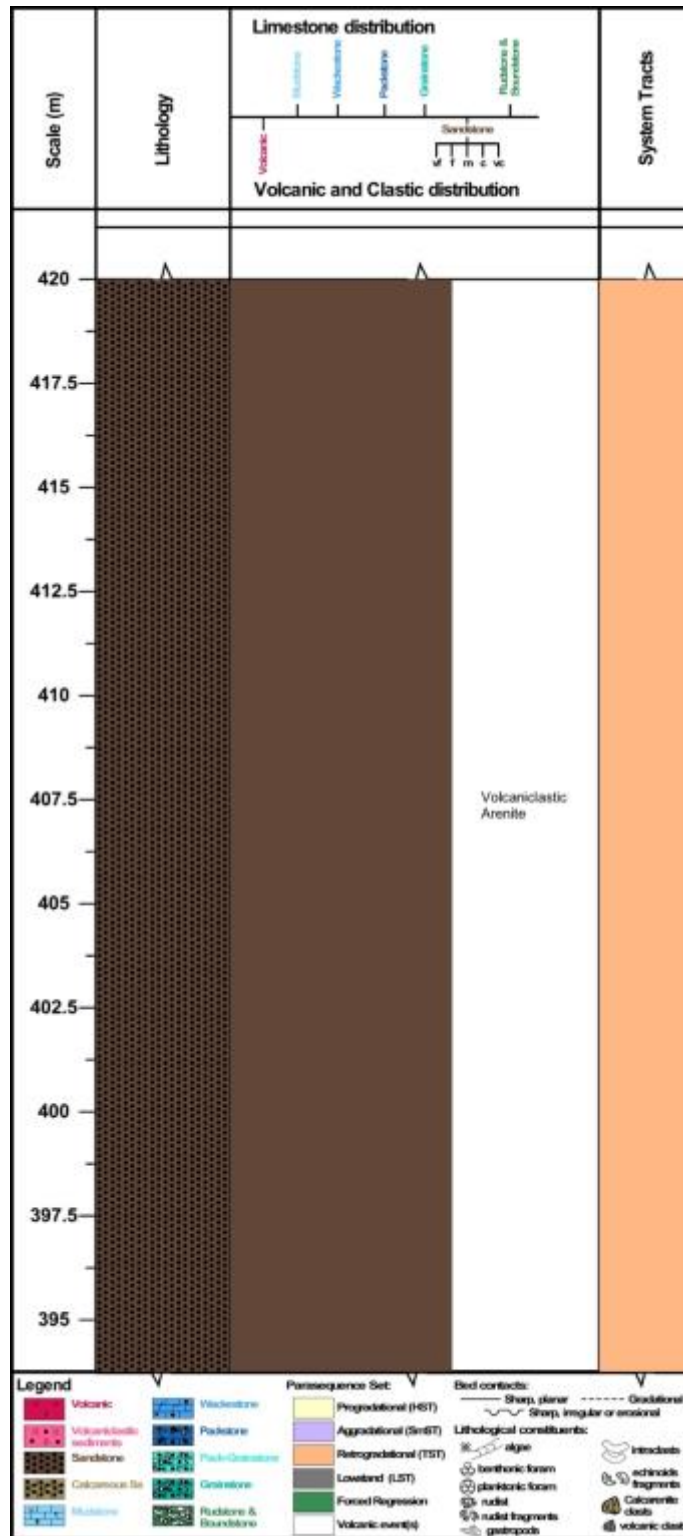


Figure 28: Stratigraphic Column from 393.75 to 420 m

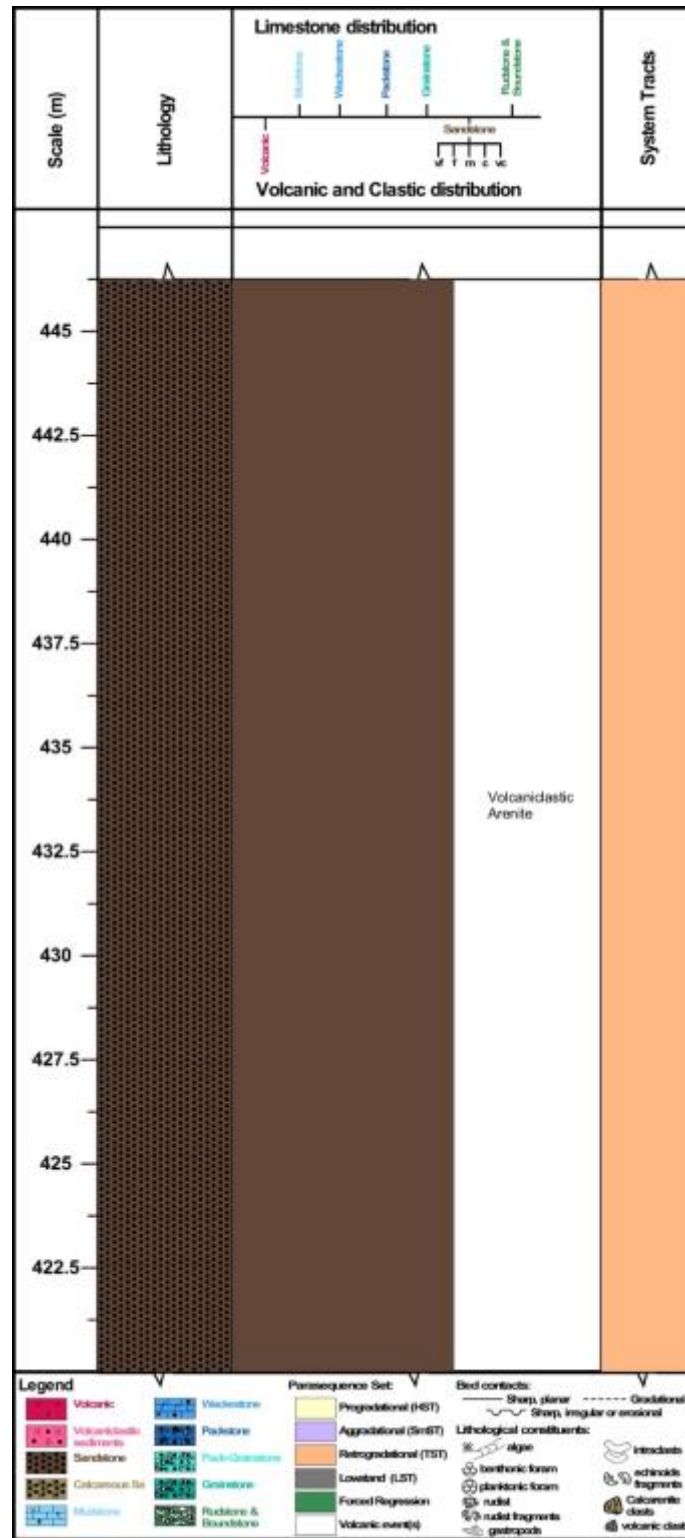


Figure 29: Stratigraphic Column from 420 to 446.25 m

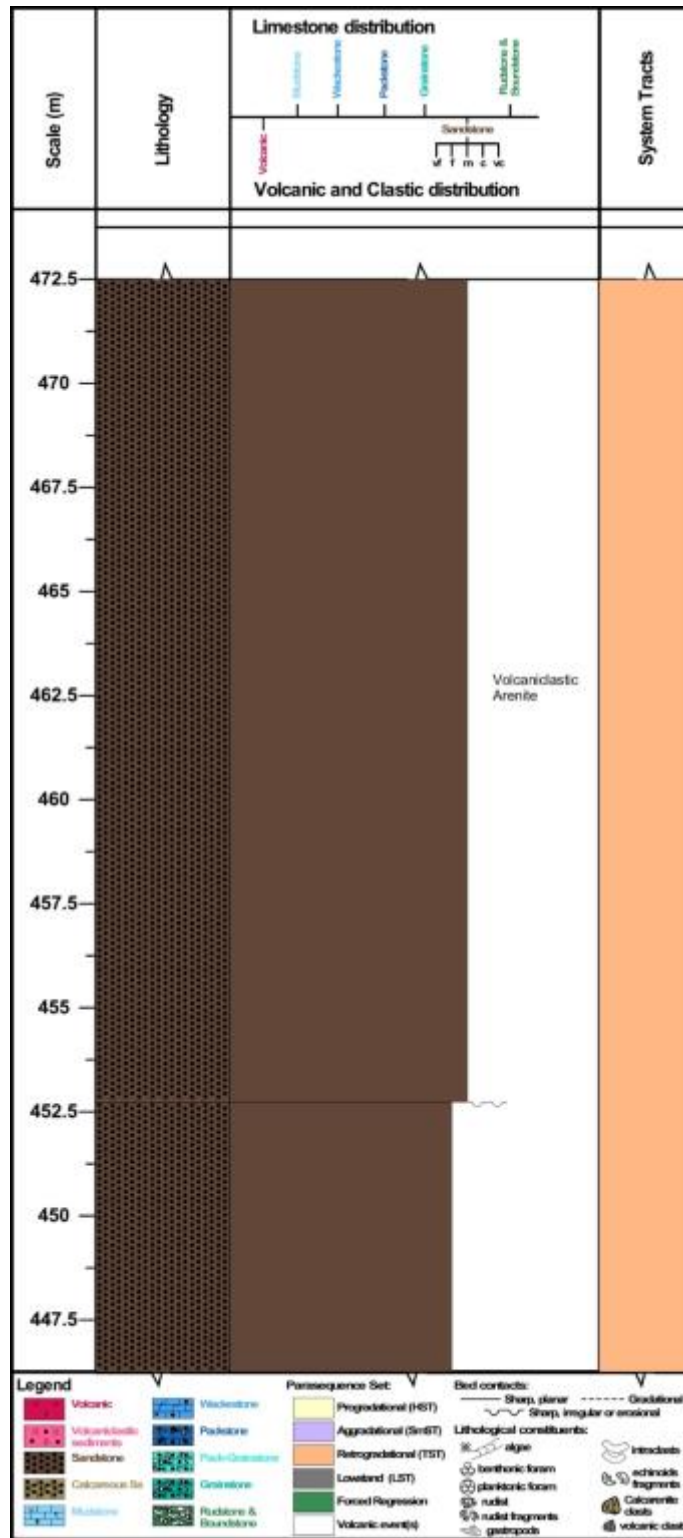


Figure 30: Stratigraphic Column from 446.25 to 472.5 m

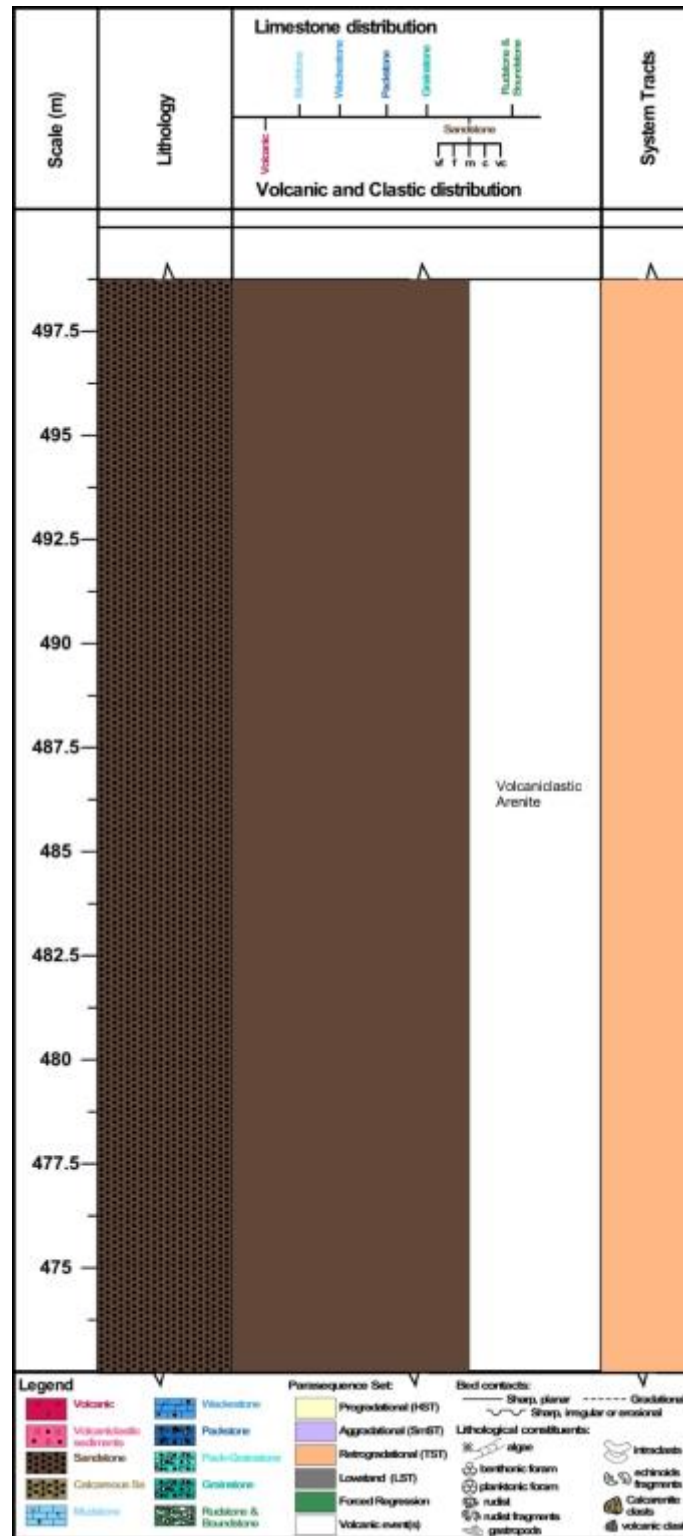


Figure 31: Stratigraphic Column from 472.5 to 498.75 m

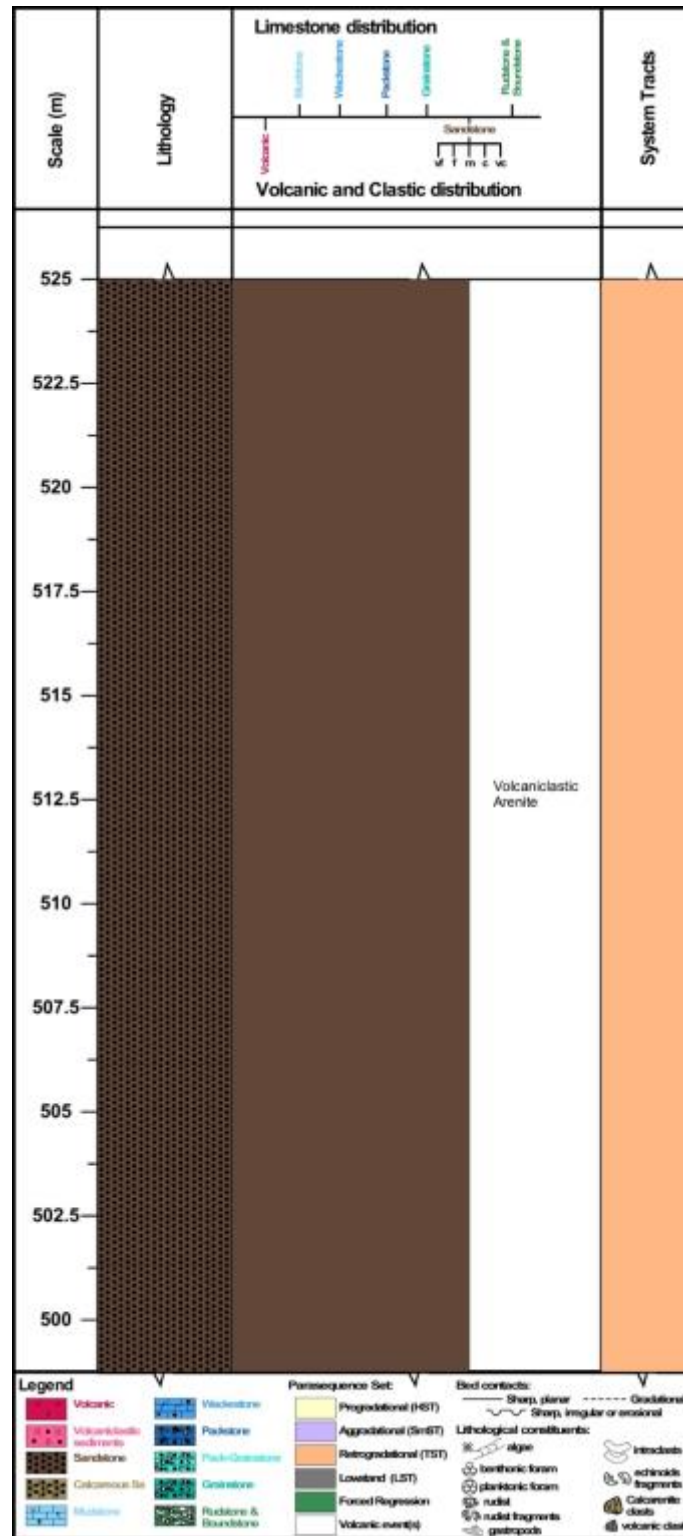


Figure 32: Stratigraphic Column from 498.75 to 525 m

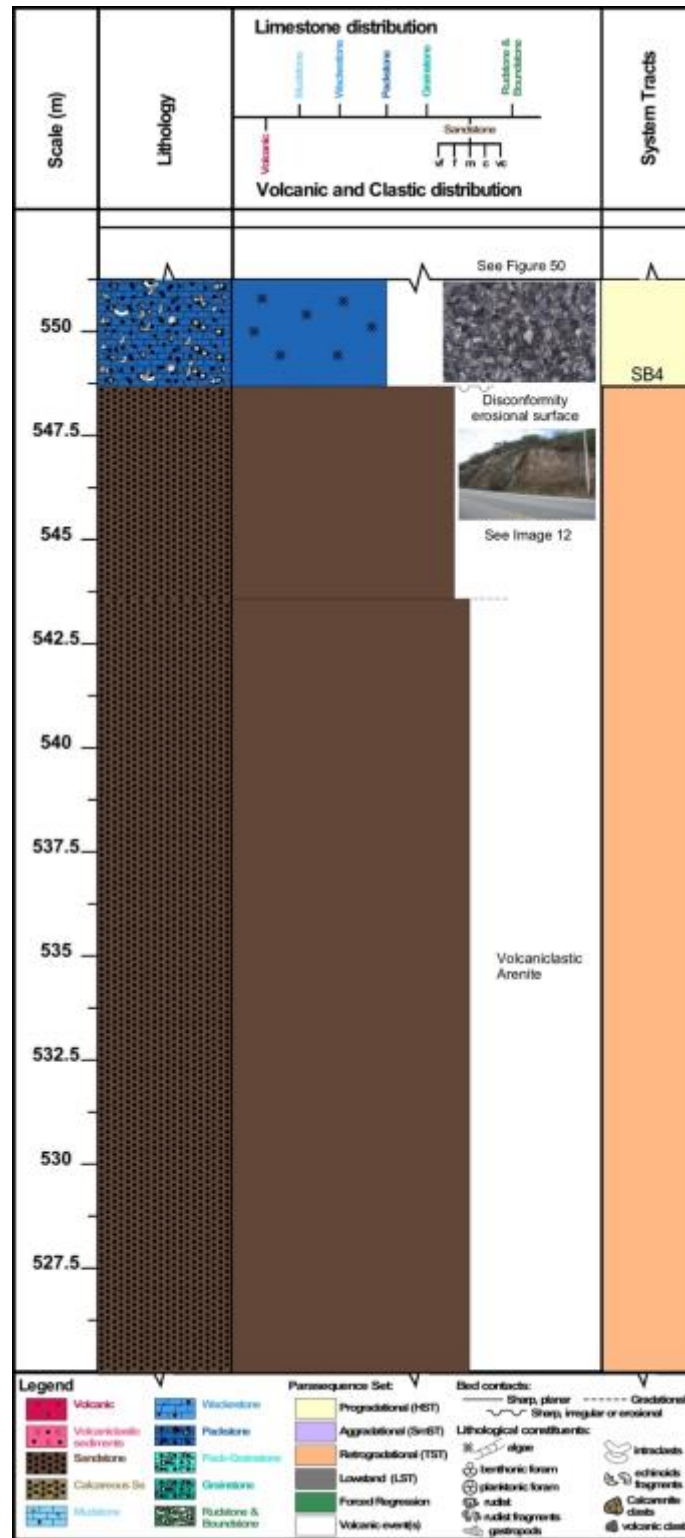


Figure 33: Stratigraphic Column from 525 to 551.25 m

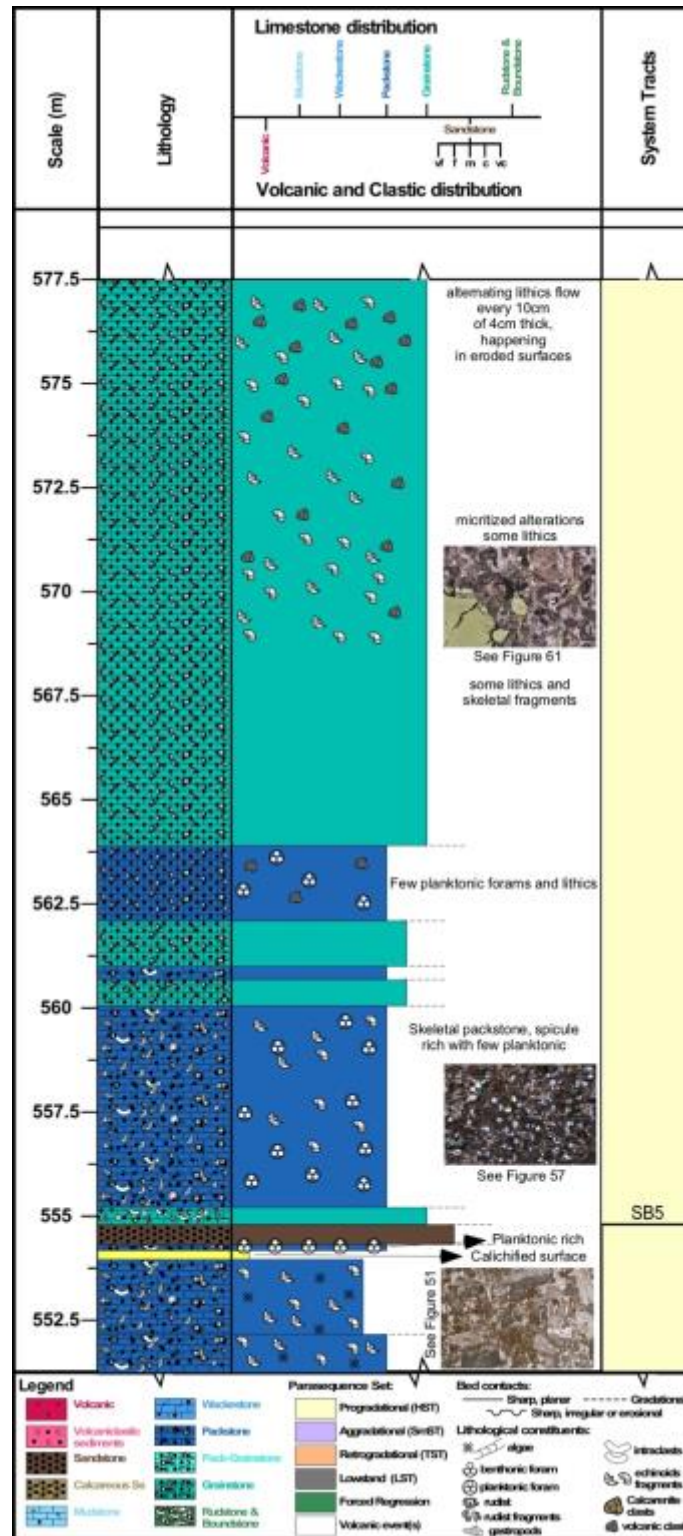


Figure 34: Stratigraphic Column from 551.25 to 577.5 m

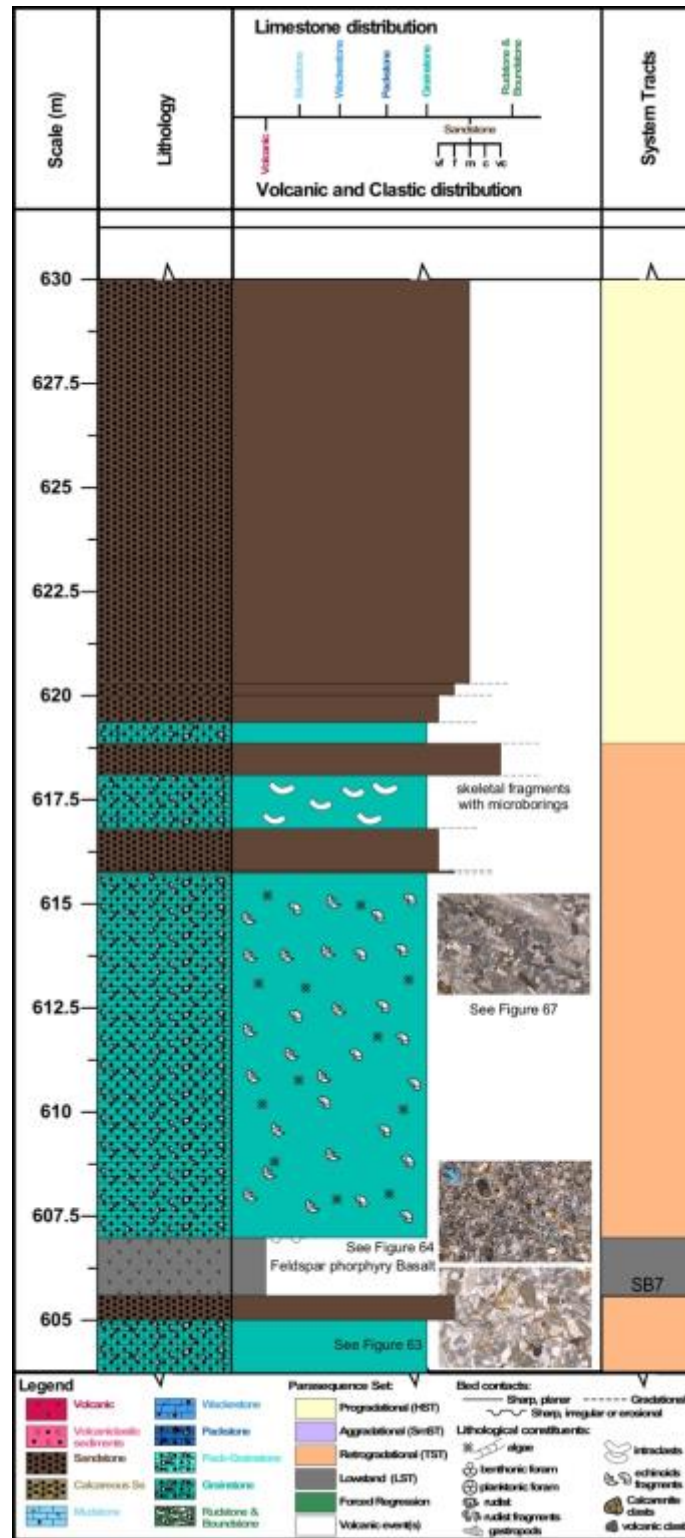


Figure 35: Stratigraphic Column from 577.5 to 603.75 m

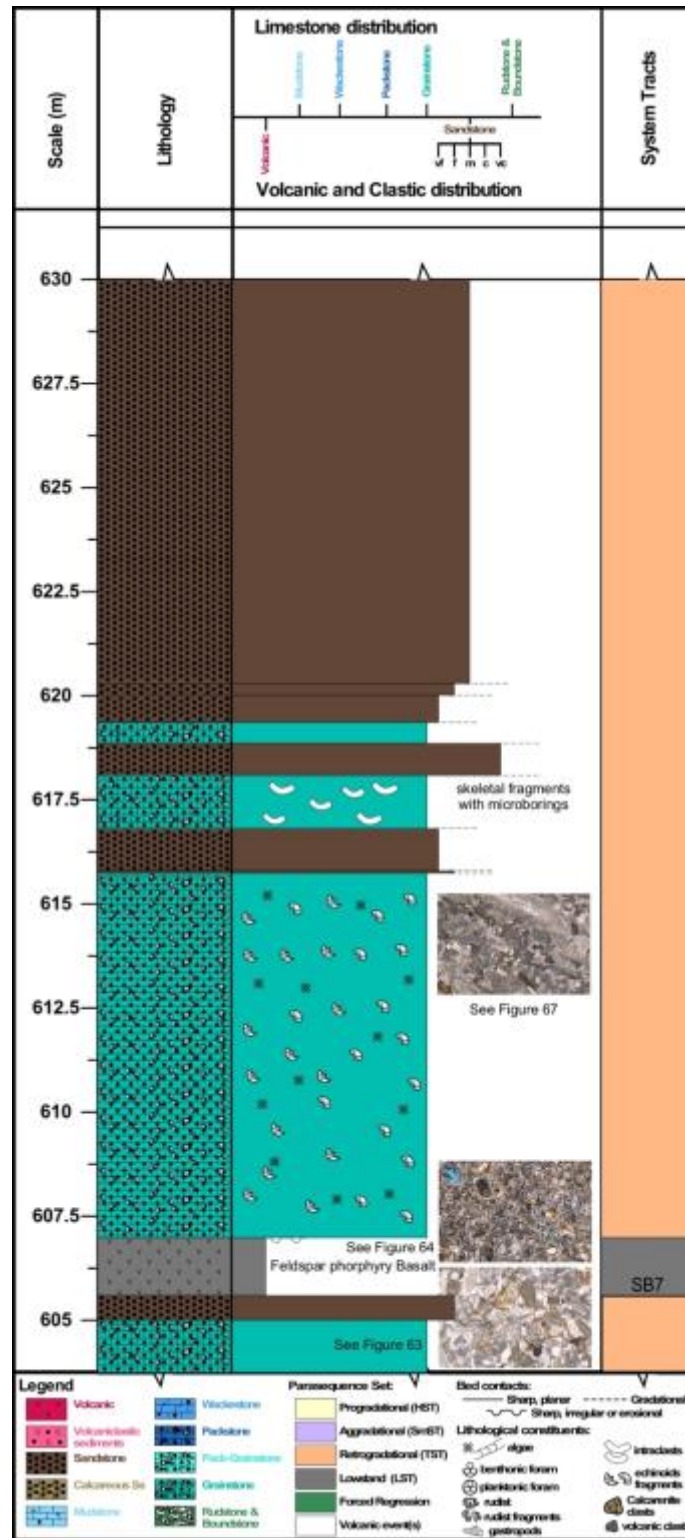


Figure 36: Stratigraphic Column from 603.75 to 630 m

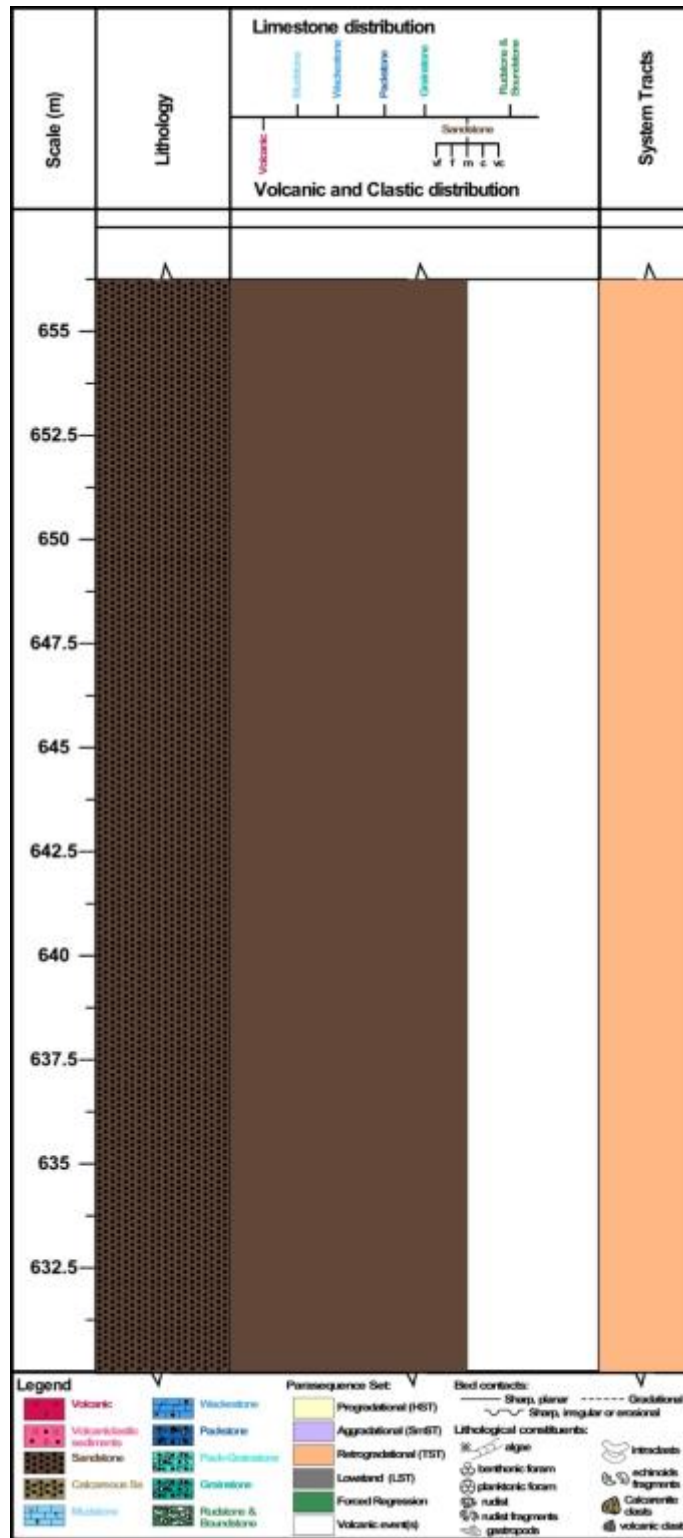


Figure 37: Stratigraphic Column from 630 to 656.25 m

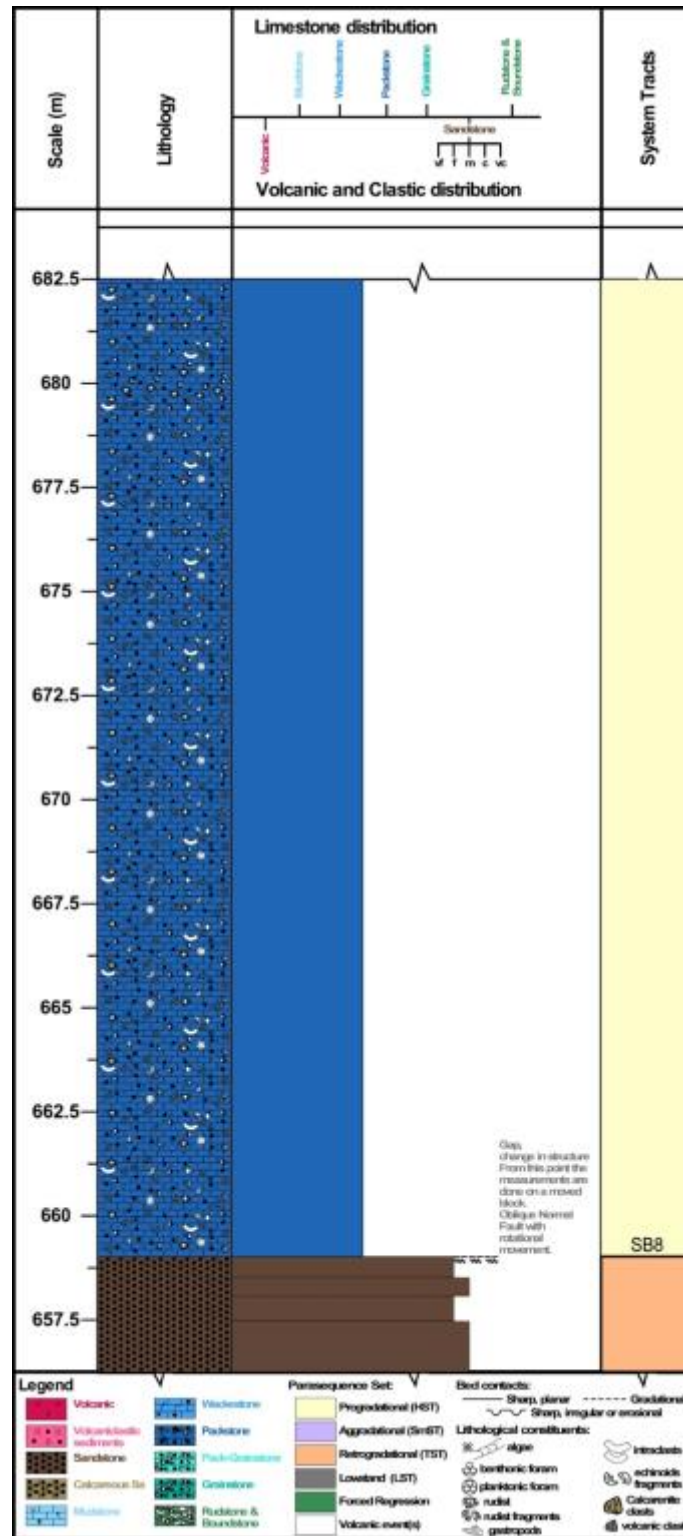


Figure 38: Stratigraphic Column from 656.25 to 682.5 m

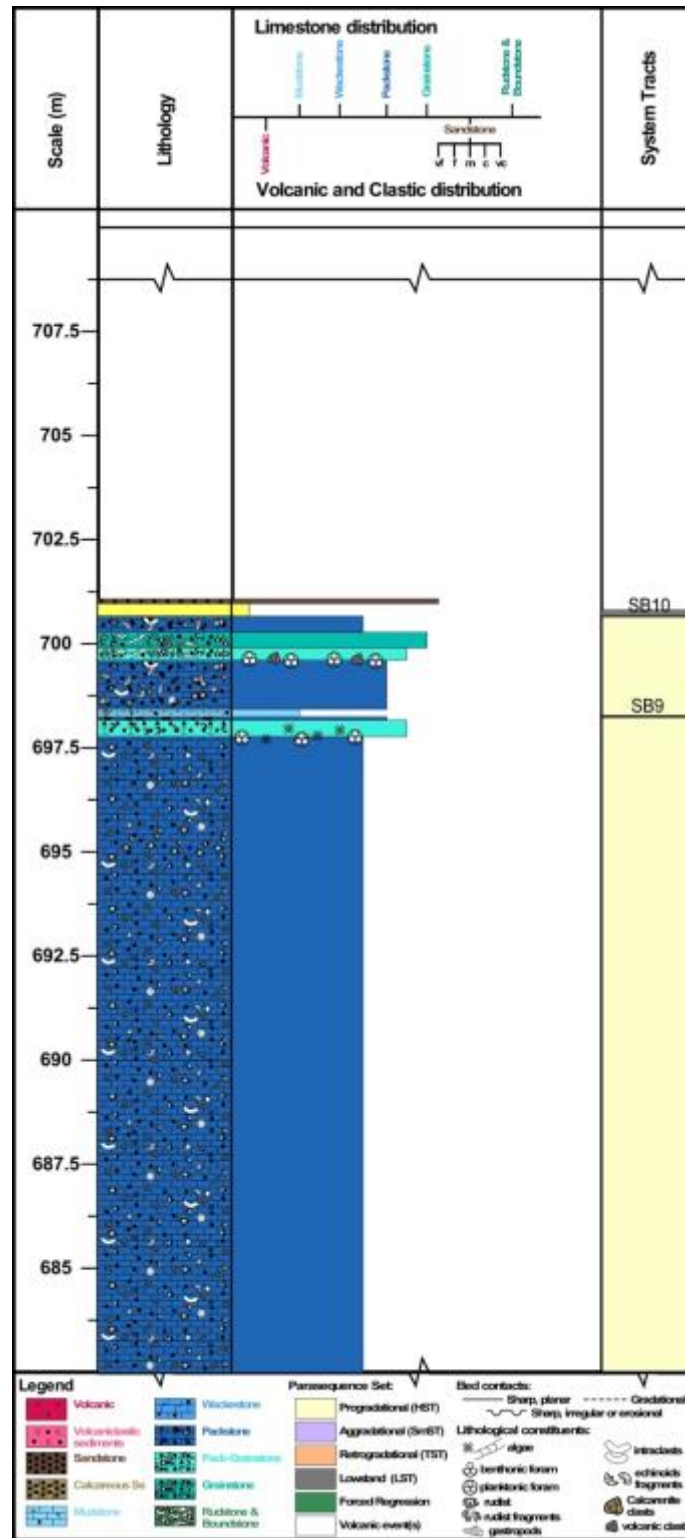


Figure 39: Stratigraphic Column from 682.5 to 708.75 m

Appendix B – Thin Sections

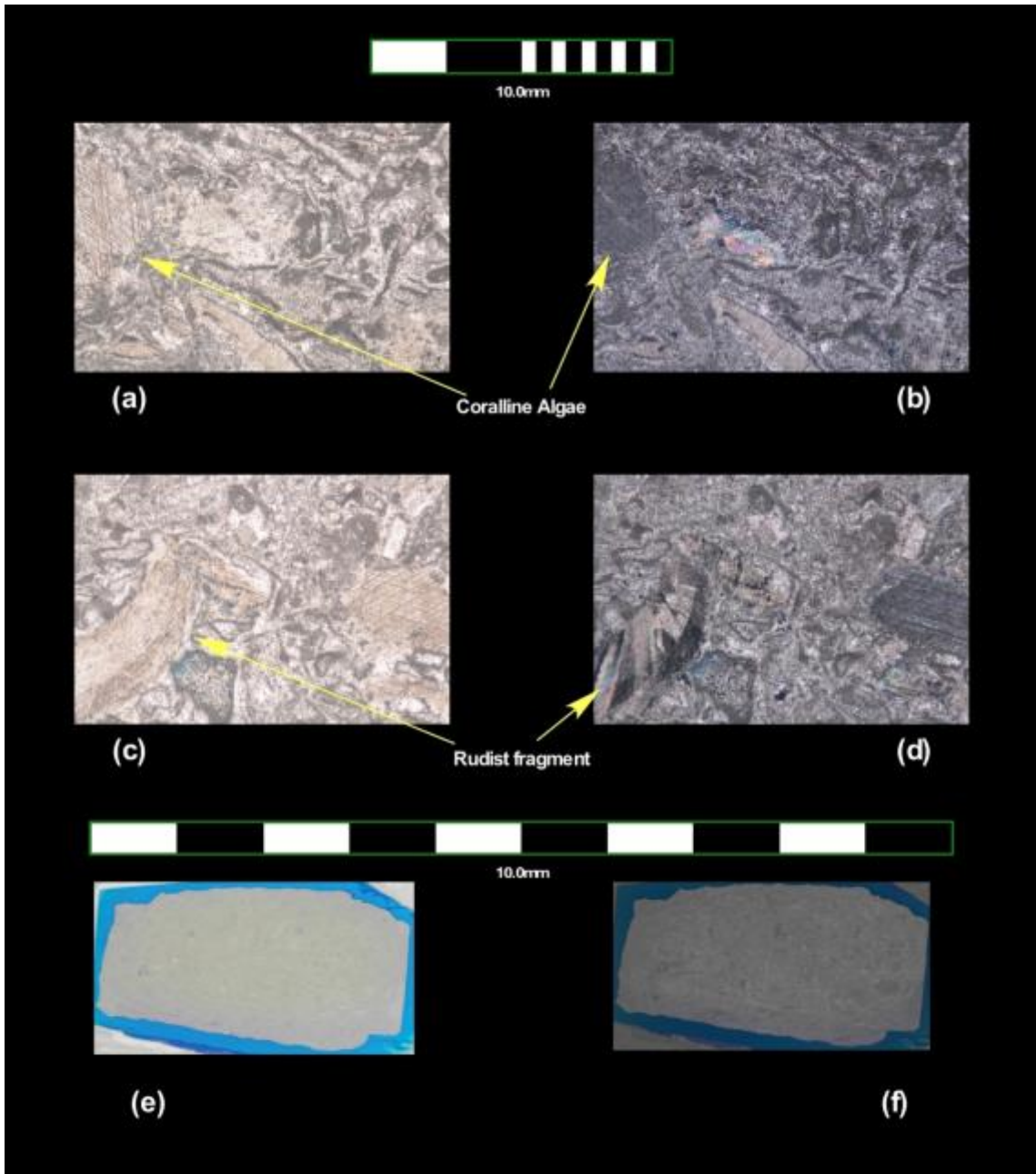


Figure 40: Thin section images of sample from 52.9 m (10/26/11_1), grayish skeletal wack-packstone, some rudists fragments, coralline algae, few mud between grains

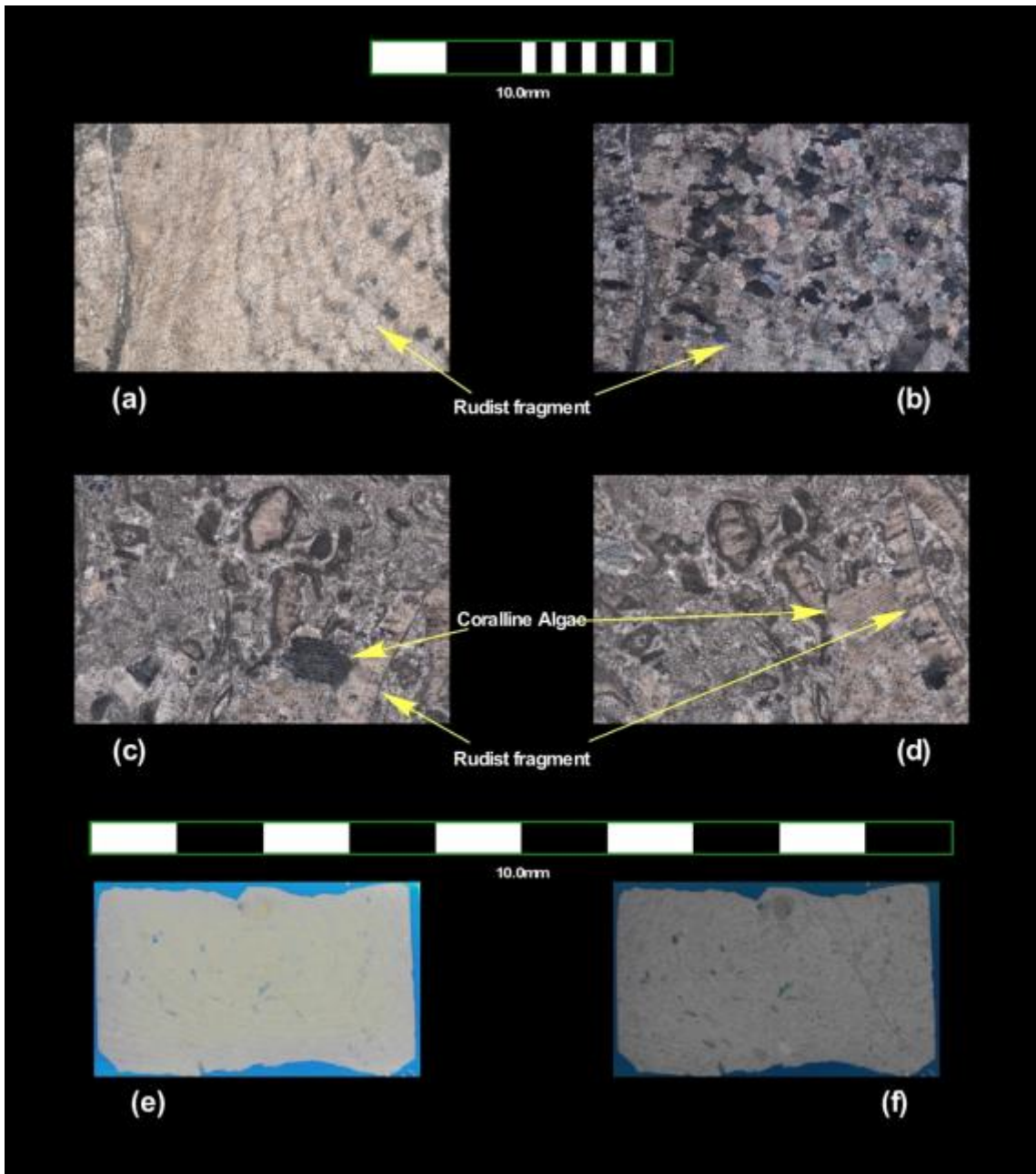


Figure 41: Thin section images of sample from 53.6 m (10/26/11_2), grayish skeletal packstone, some rudists fragments

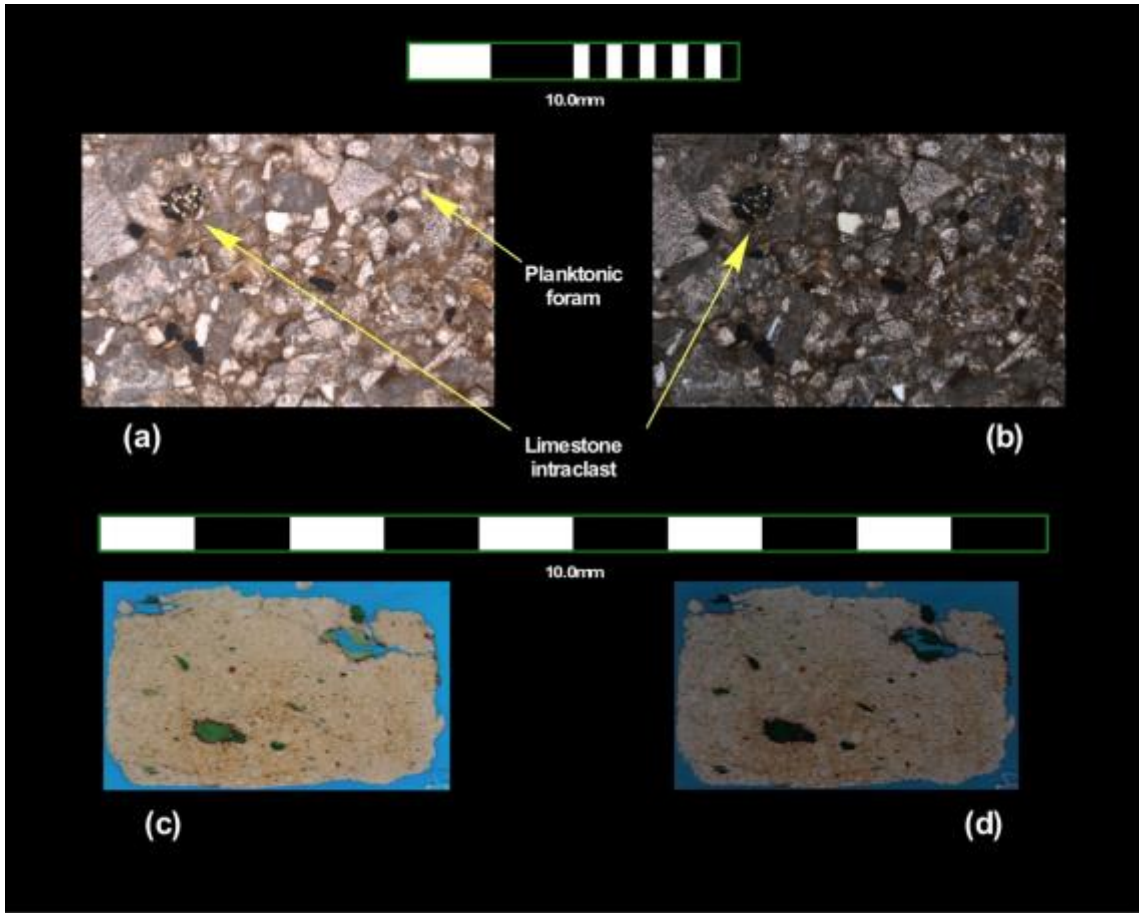


Figure 42: Thin section images of sample from 97.1 m (11/25/11_1), brownish very fine grained volcanic arenite with skeletal fragments, intraclasts and planktonic foraminifera, sub-rounded to sub-angular, some high relieve minerals, micriticized

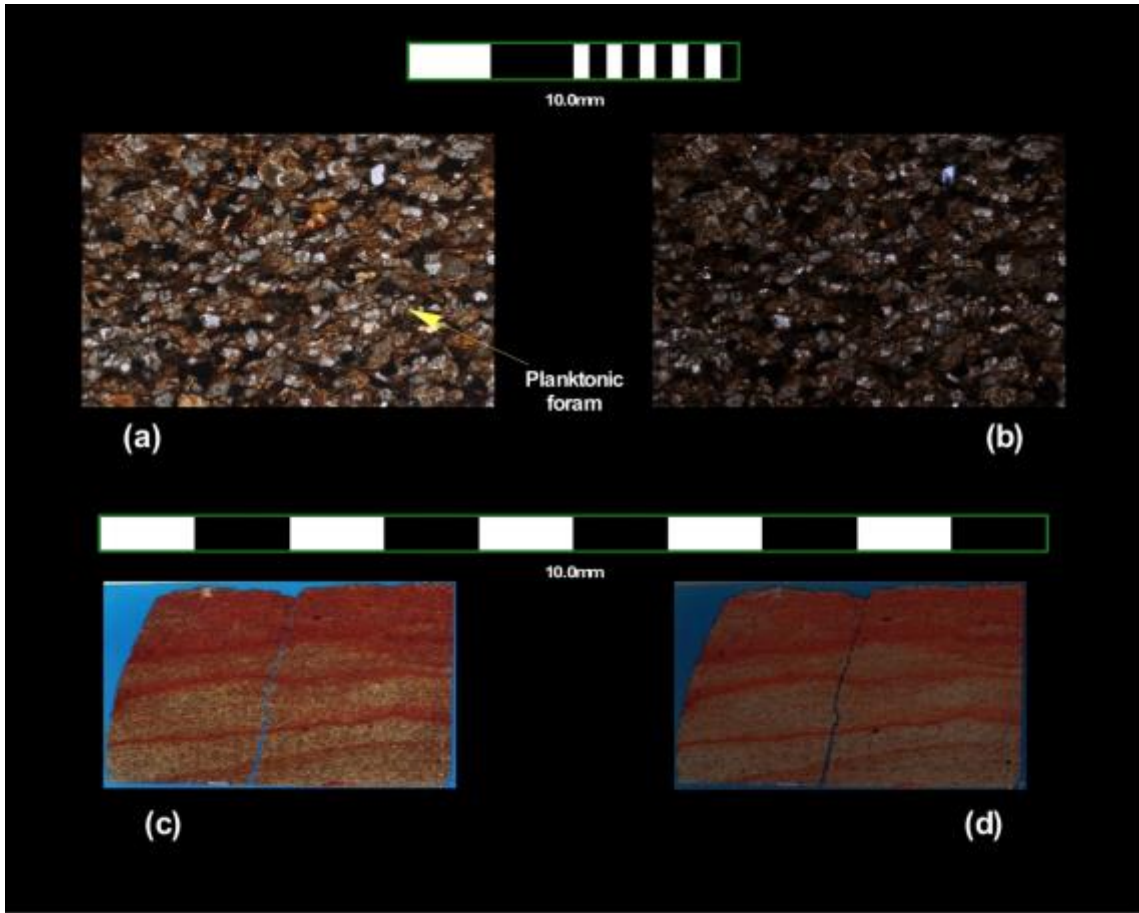


Figure 43: Thin section images of sample from 98.4 m (11/25/11_2), brownish very fine grsined sandstone to siltstone with very few skeletal fragments, rounded to sub-angular

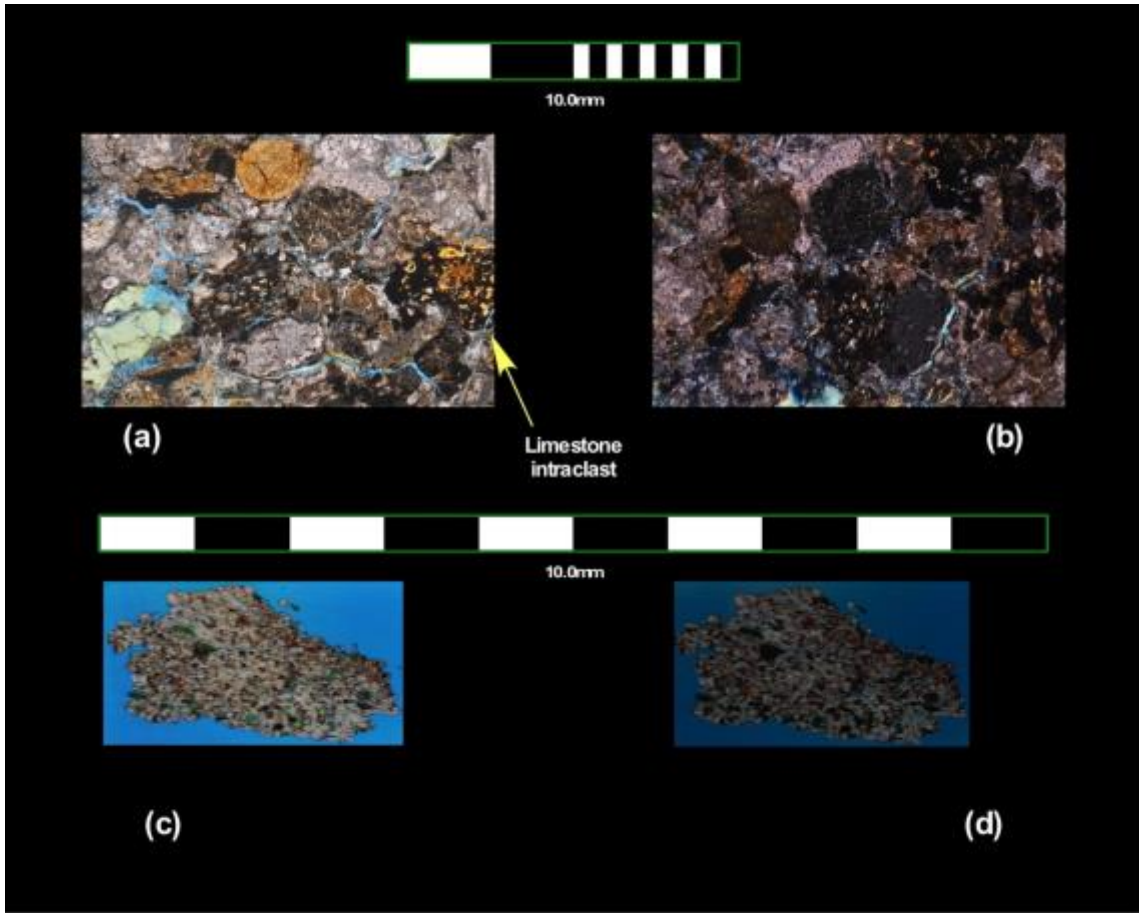


Figure 44: Thin section images of sample from 100.25 m (11/25/11_3), volcanic arenite, intraclasts, volcanic grains, angular to sub-rounded

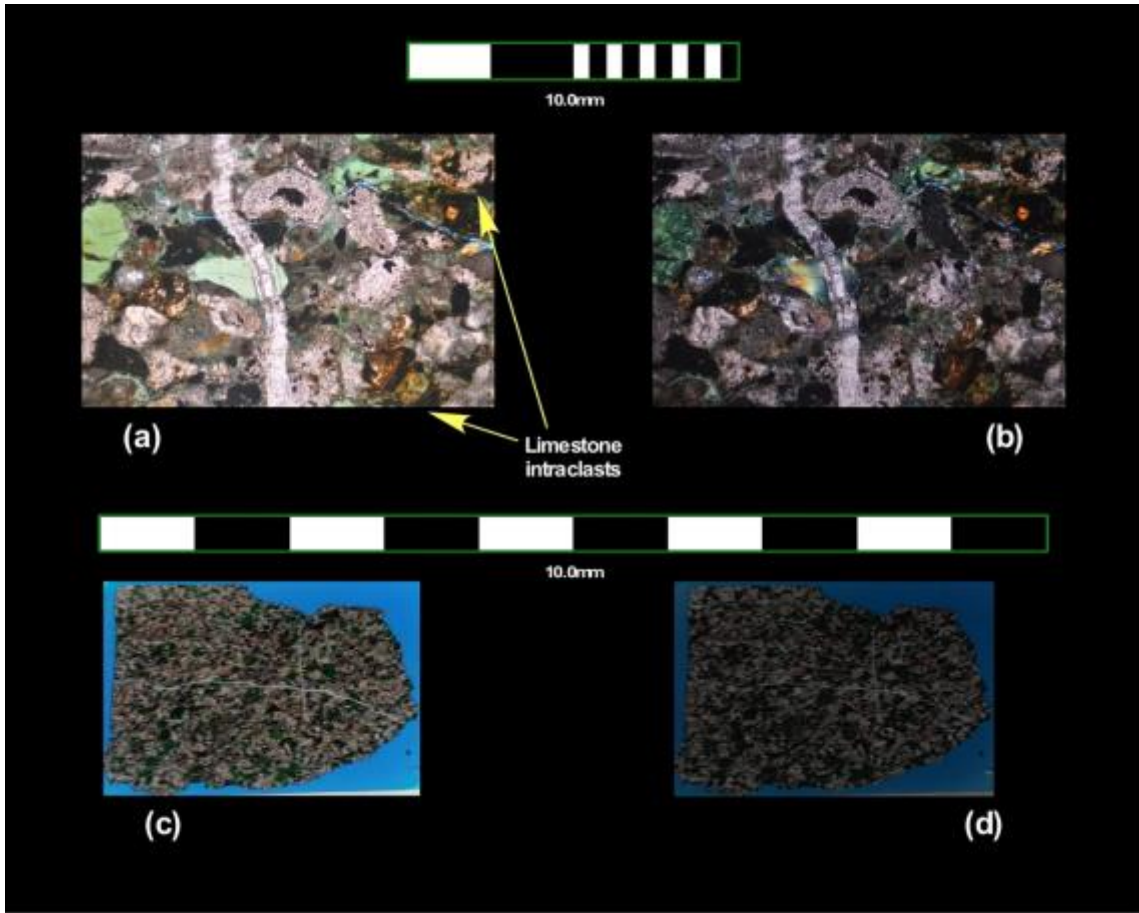


Figure 45: Thin section images of sample from 102.05 m (11/25/11_4), volcanic arenite, intraclasts, volcanic grains, angular to sub-rounded

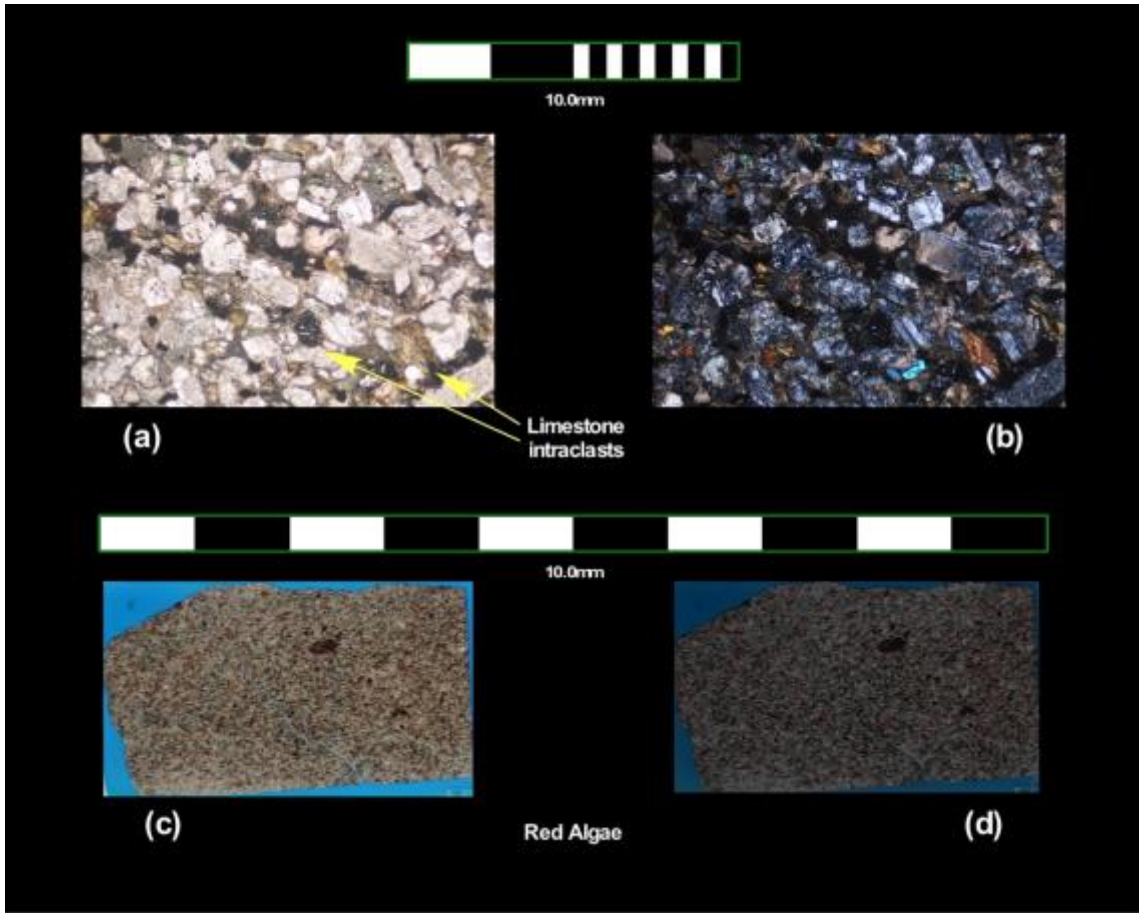


Figure 46: Thin section images of sample from 112.3 m (11/25/11_7), andesitic volcanic flow, feldspars, few intraclasts

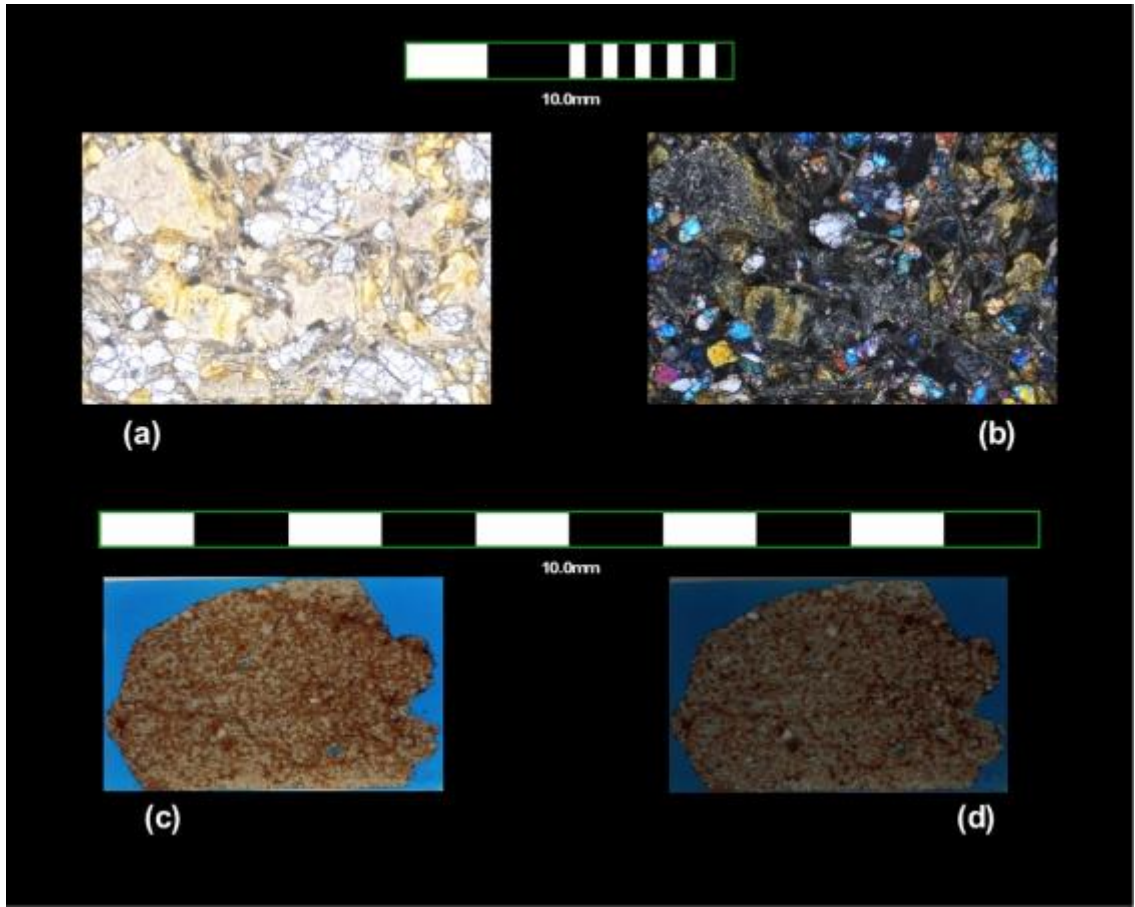


Figure 47: Thin section images of sample from ~223 m (CJ1), columnar joints

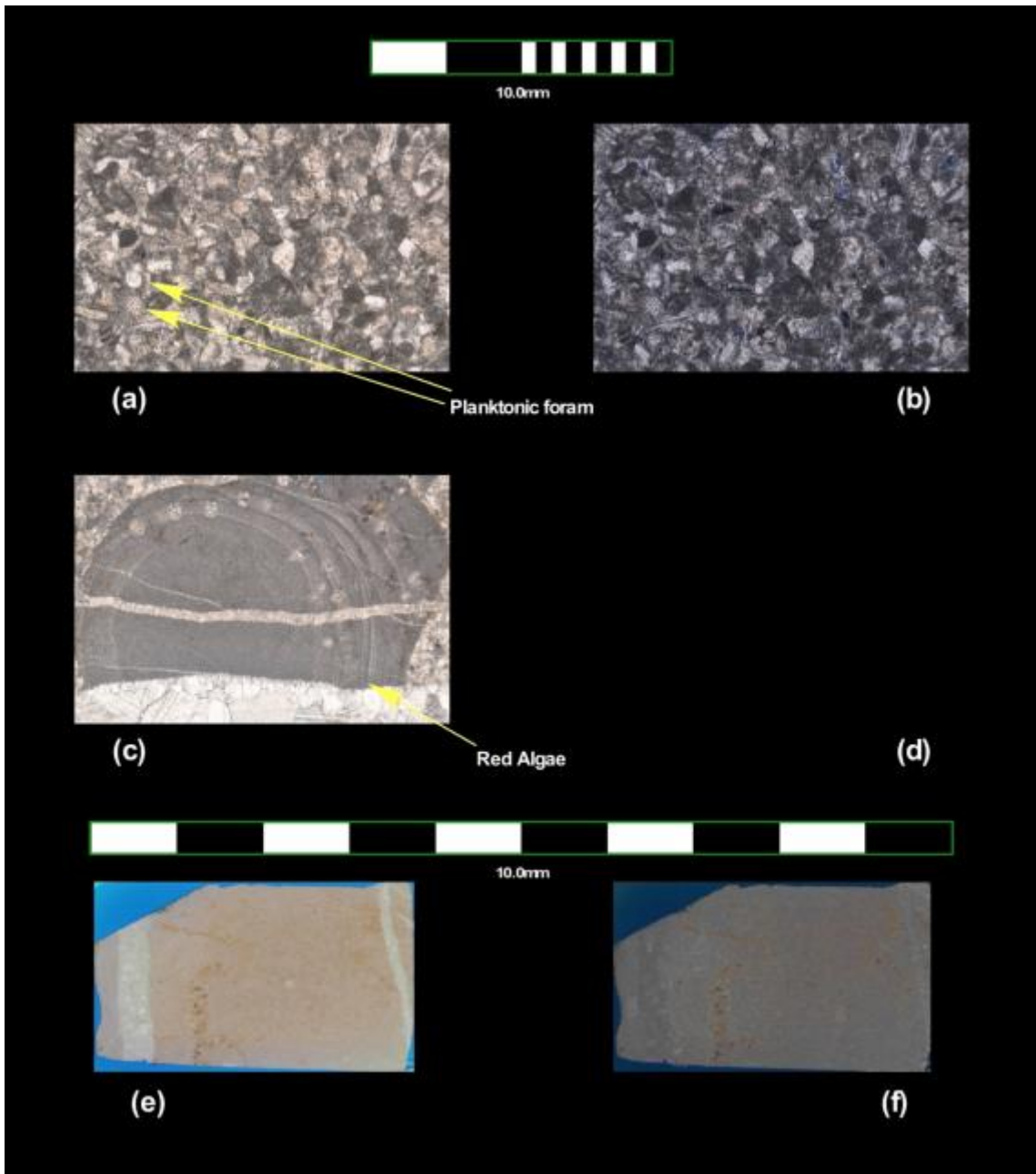


Figure 48: Thin section images of sample from 551.38 m (3/21/12_1), grayish skeletal packstone, red algae present

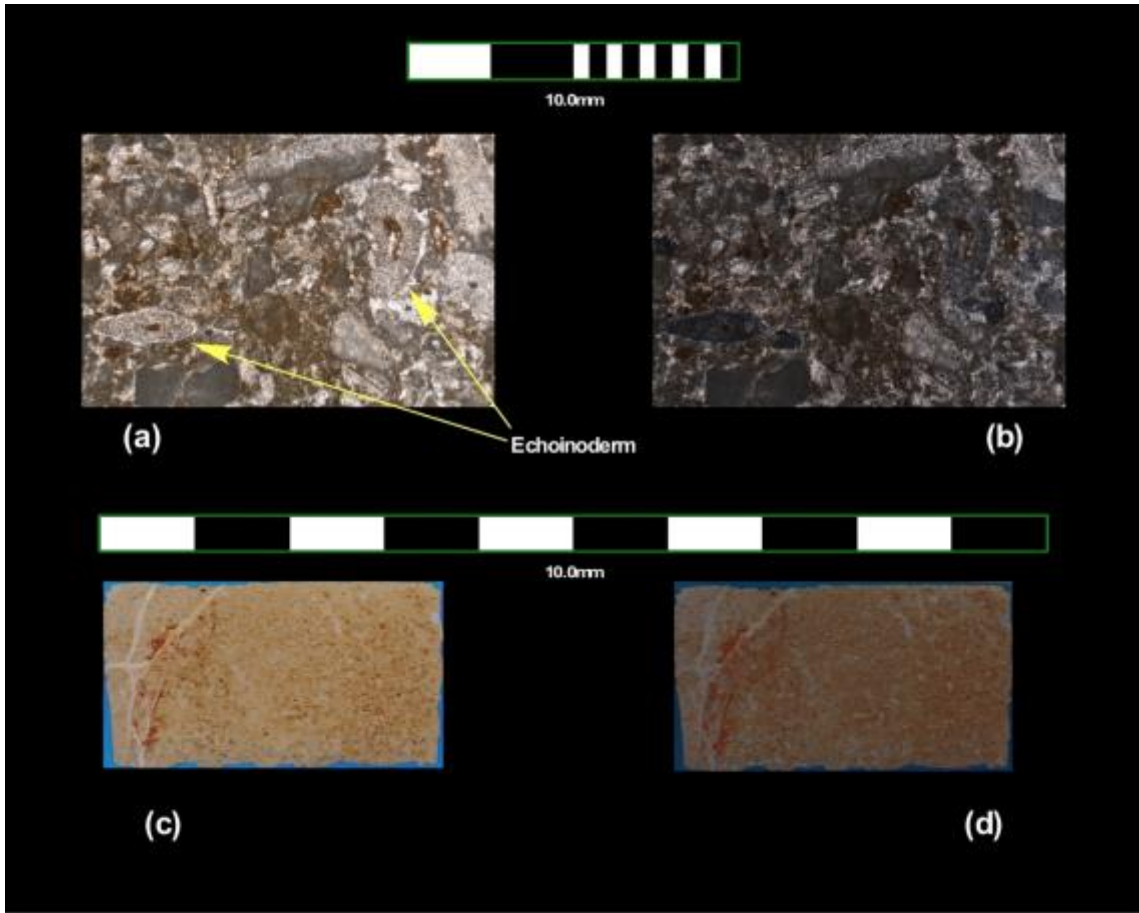


Figure 49: Thin section images of sample from 552.16 m (3/21/12_2), grayish skeletal packstone

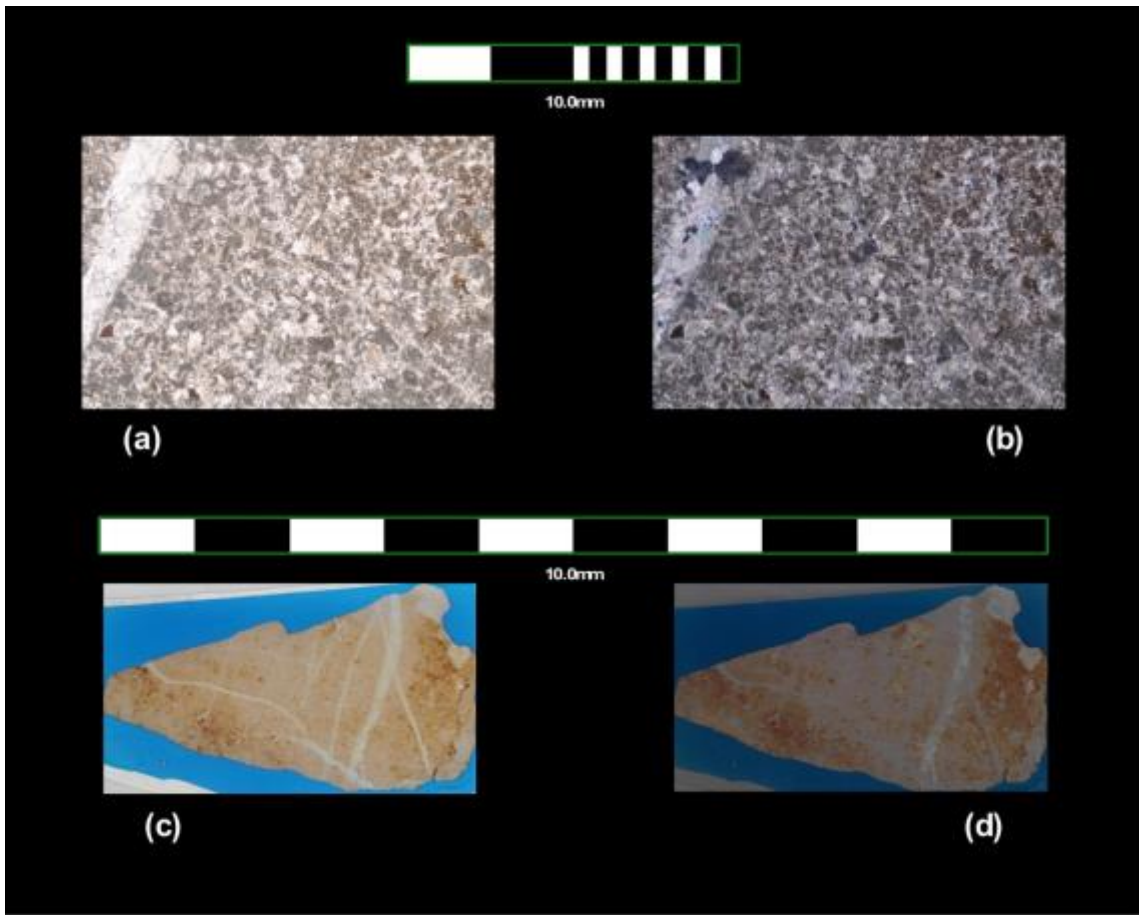


Figure 50: Thin section images of sample from 553.96 m (3/21/12_3), grayish skeletal wack-packstone

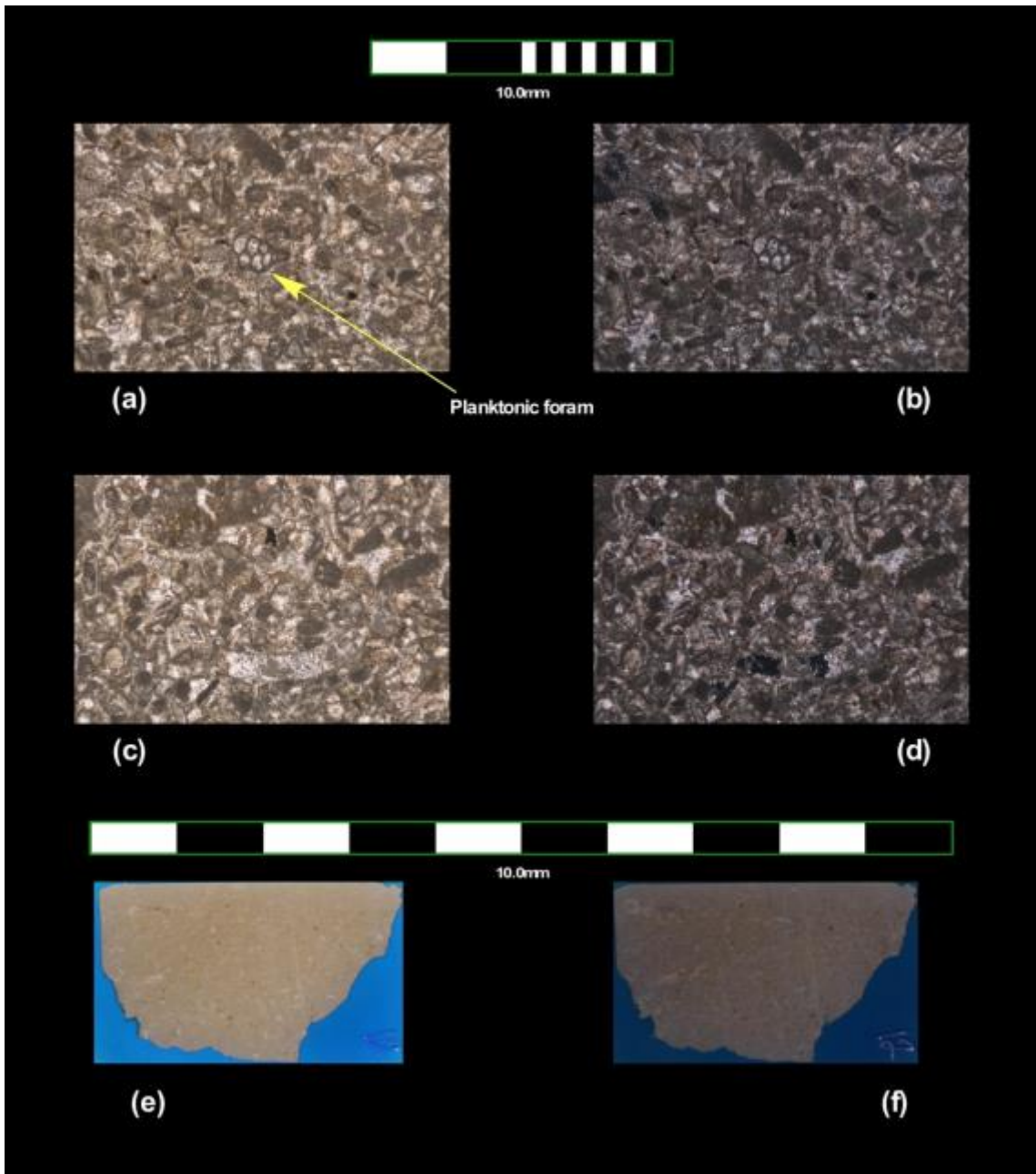


Figure 51: Thin section images of sample from 553.96 m (3/21/12_4), grayish skeletal packstone, few planktonic foraminifera

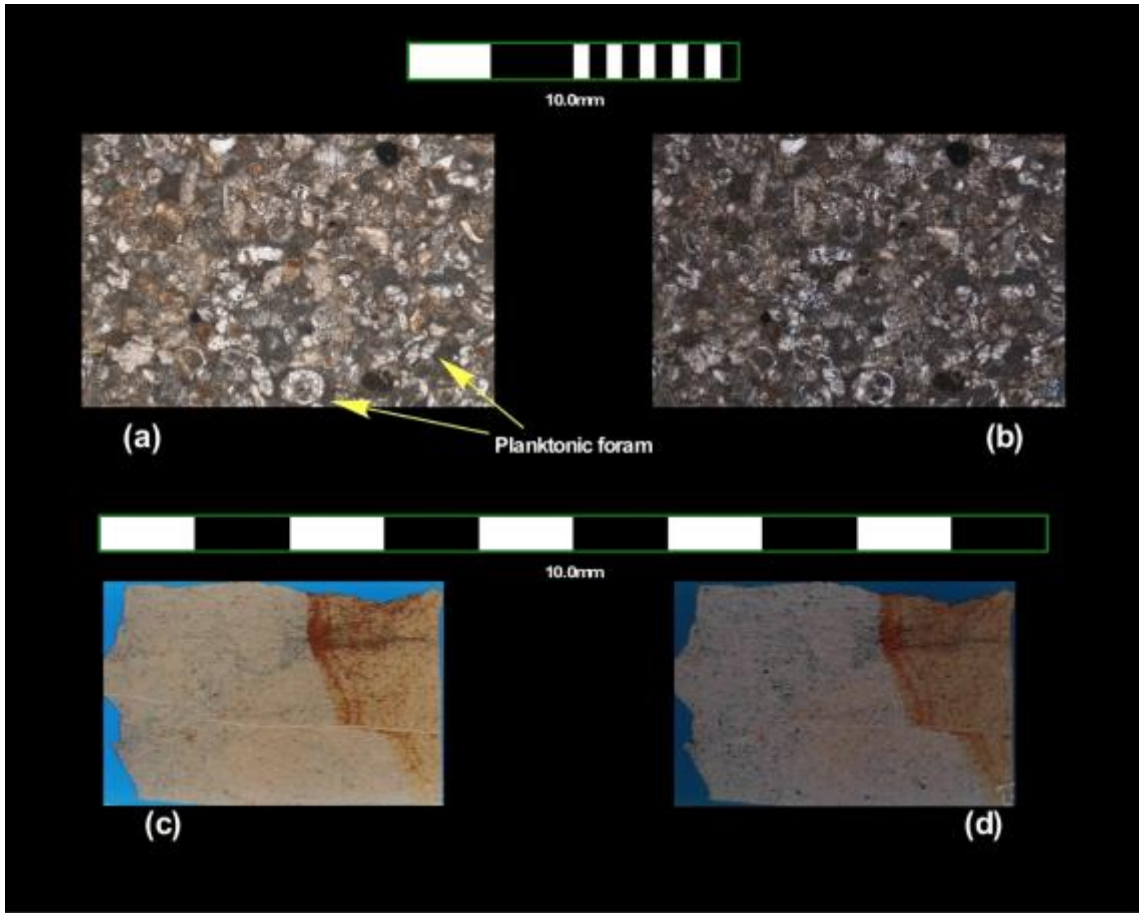


Figure 52: Thin section images of sample from 554.32 m (3/21/12_5), grayish planktonic rich packstone

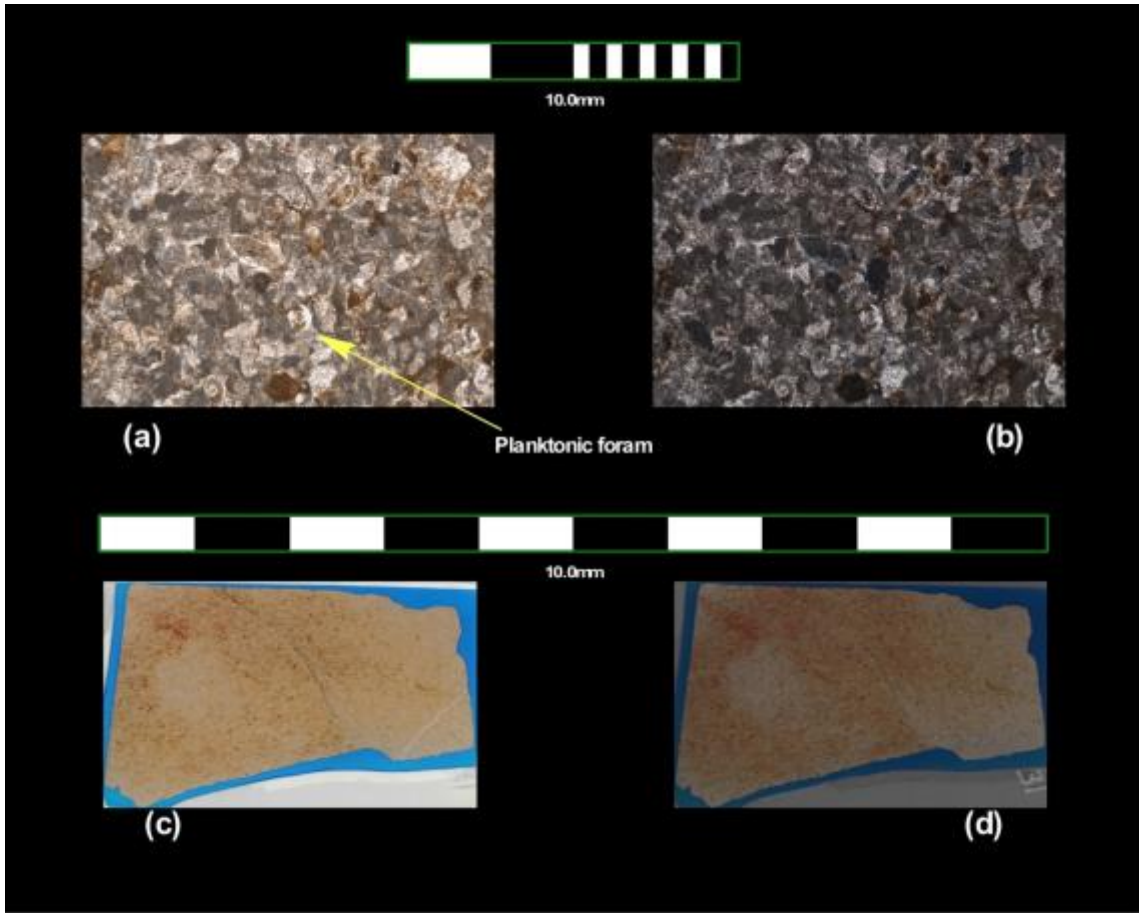


Figure 53: Thin section images of sample from 556.07 m (3/28/12_1), grayish skeletal packstone, few foraminifera

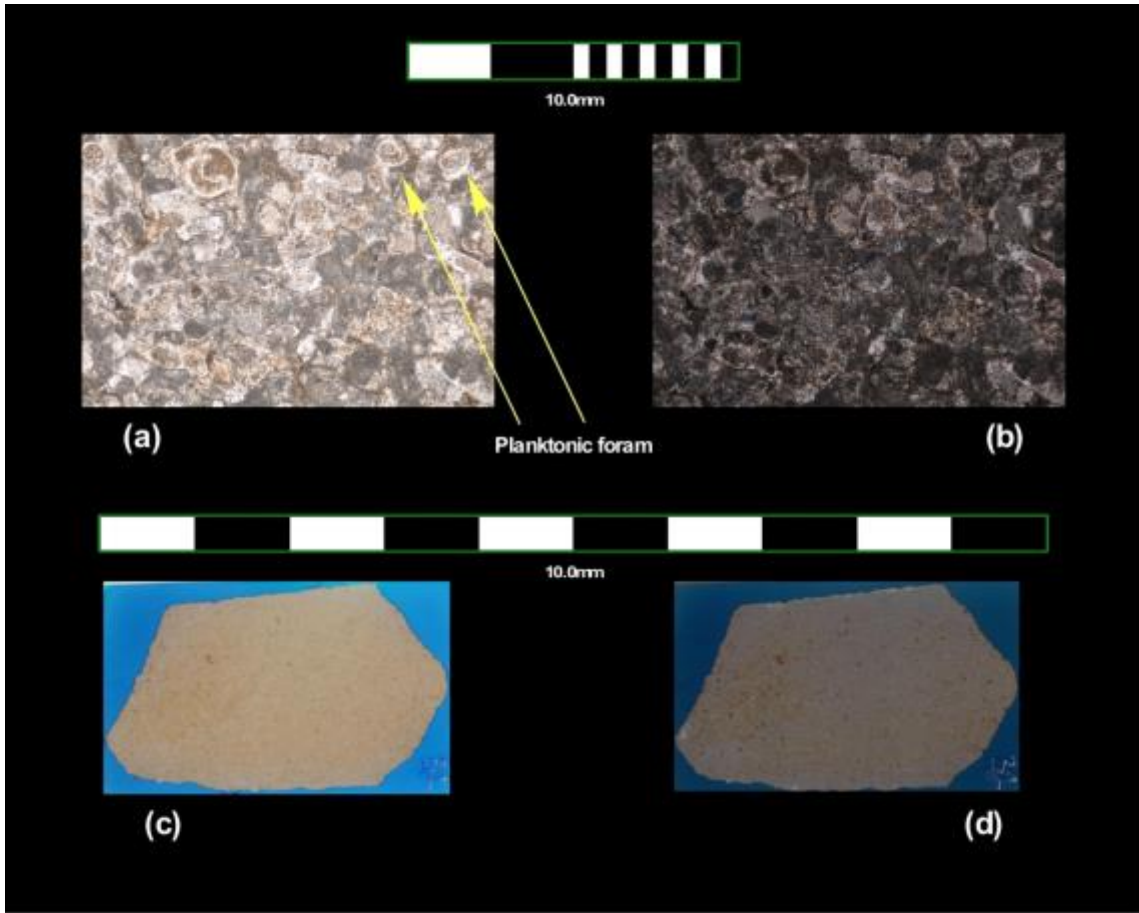


Figure 54: Thin section images of sample from 557.08 m (3/28/12_2), planktonic foraminifera rich packstone, few Echinoderm fragments

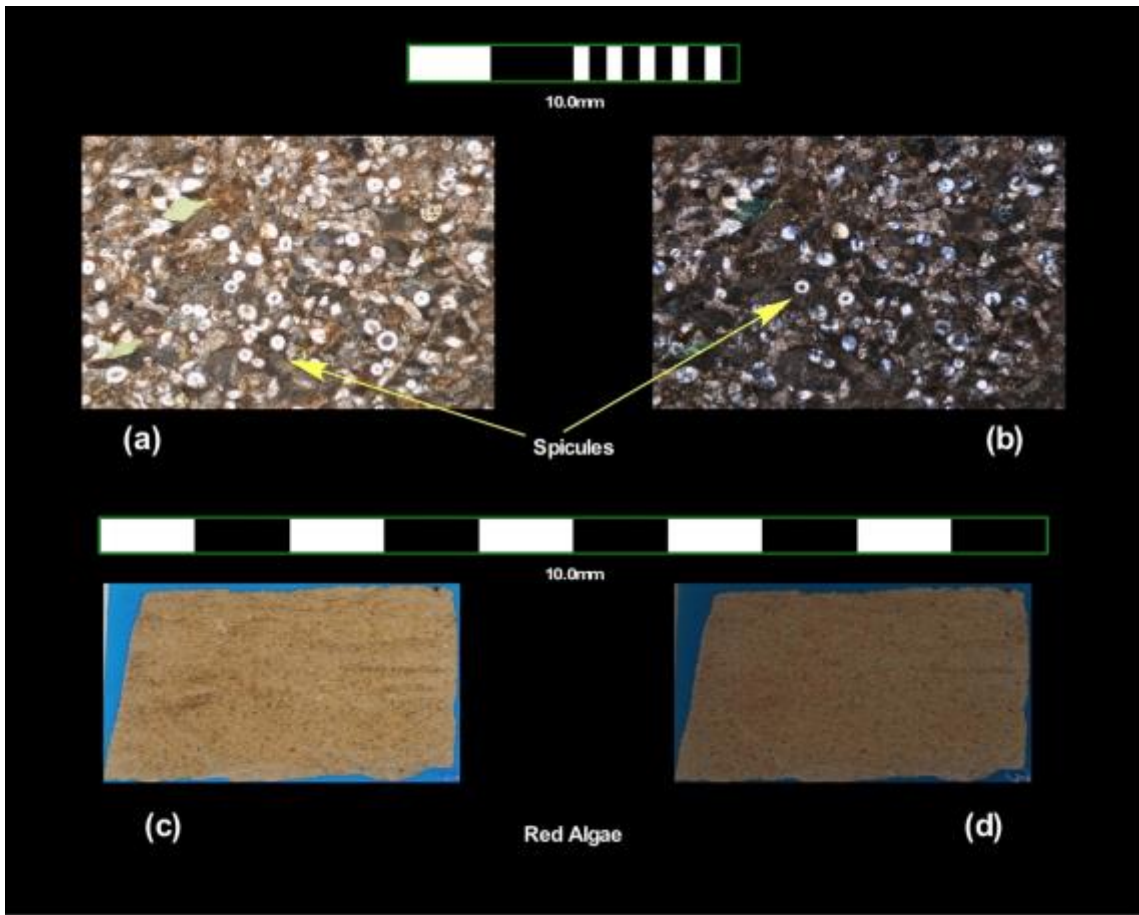


Figure 55: Thin section images of sample from 557.86 m (3/28/12_3), grayish skeletal packstone, spicule rich with lithics

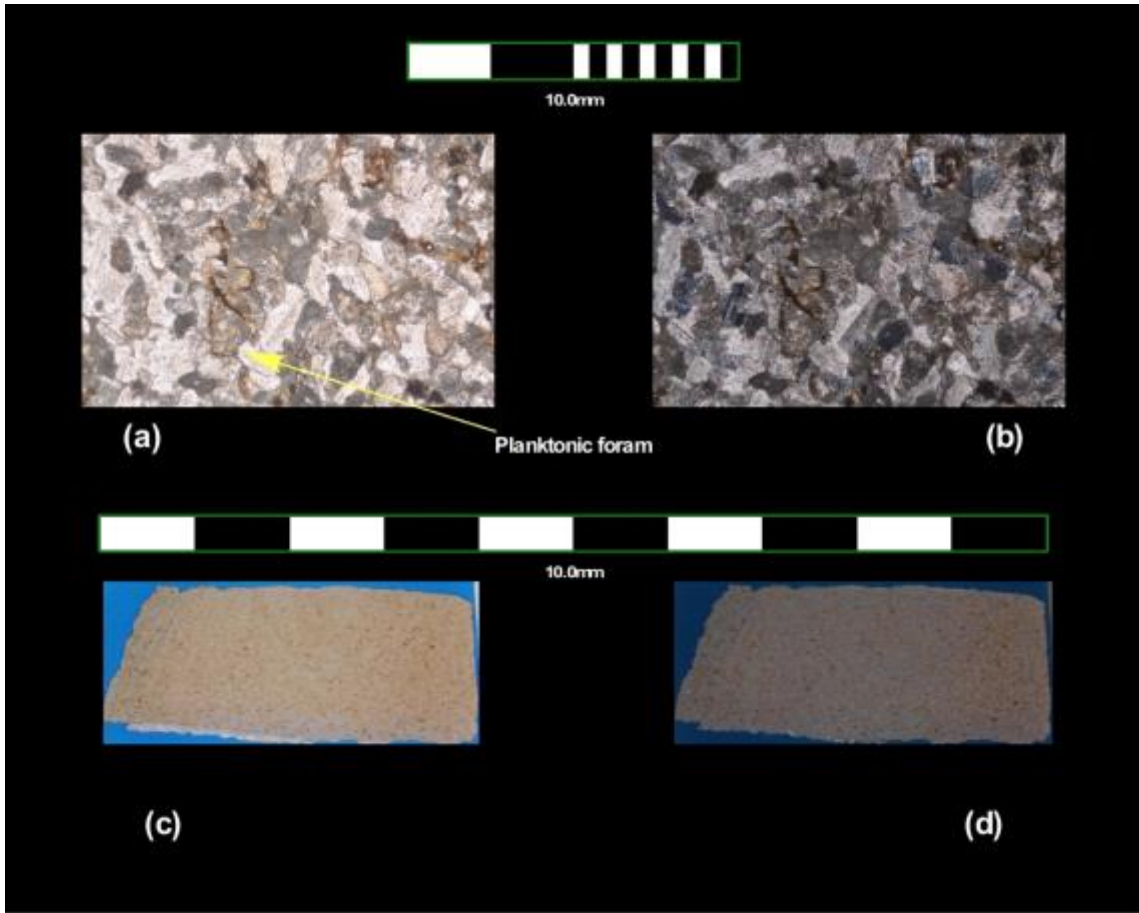


Figure 56: Thin section images of sample from 560.06 m (3/28/12_4), grayish skeletal packstone, few planktonic foraminifera

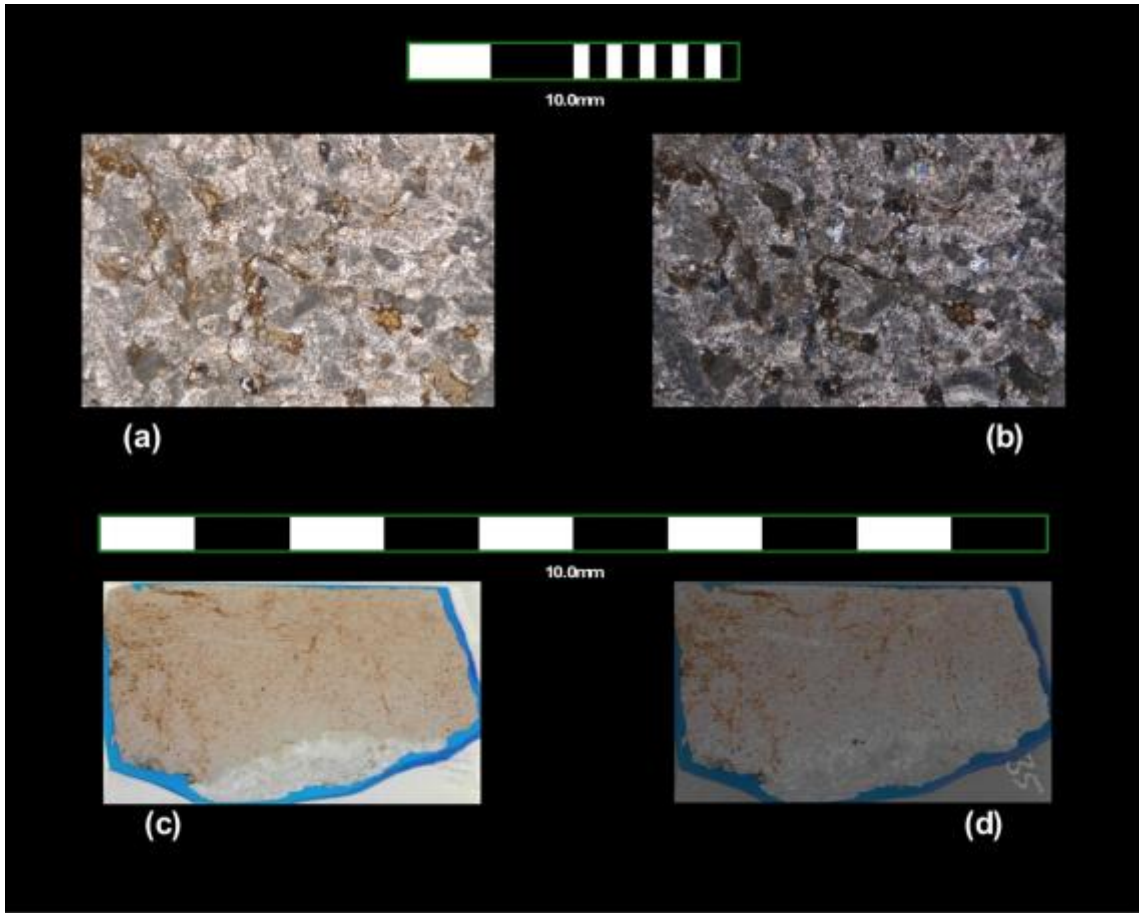


Figure 57: Thin section images of sample from 563.27 m (3/28/12_5), grayish skeletal packstone, some planktonic foraminifera and volcanic grains

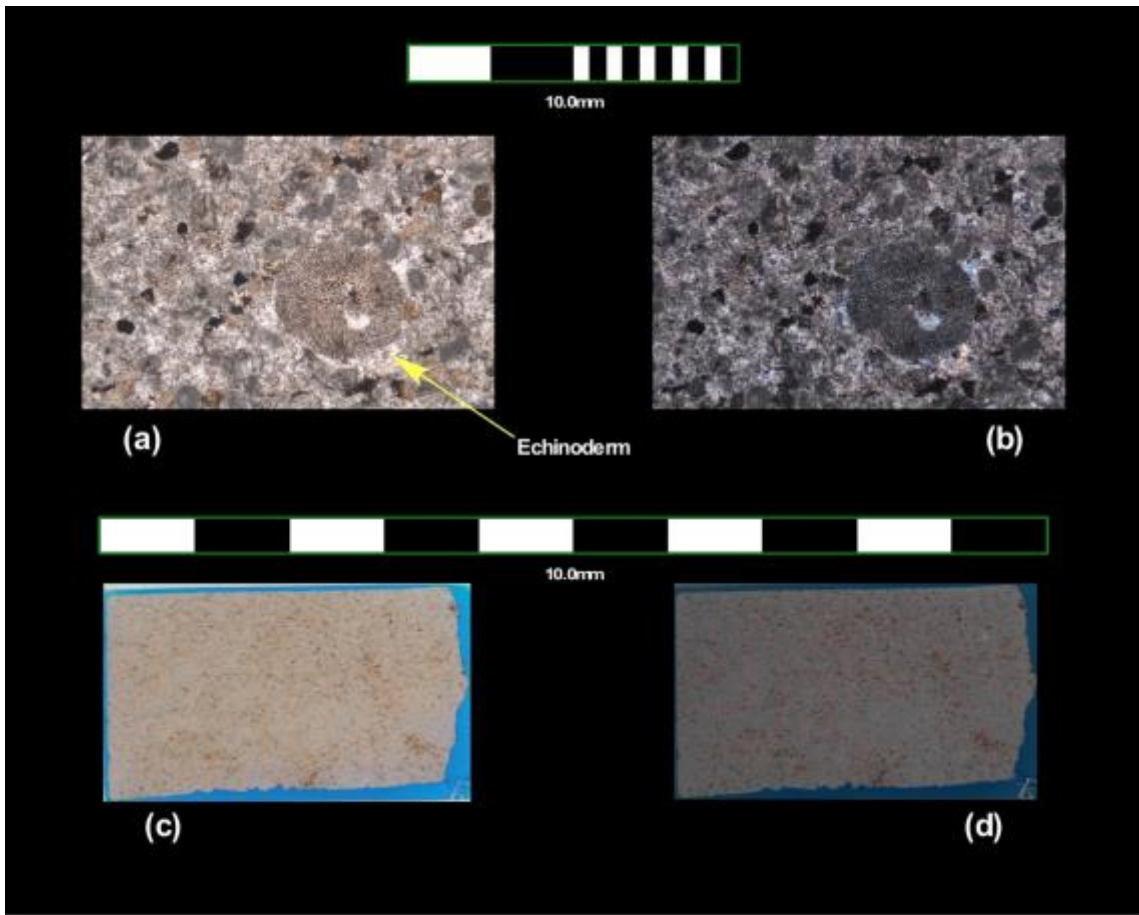


Figure 58: Thin section images of sample from 565.76 m (3/28/12_6), grayish skeletal grainstone, some planktonic foraminifera and volcanic grains

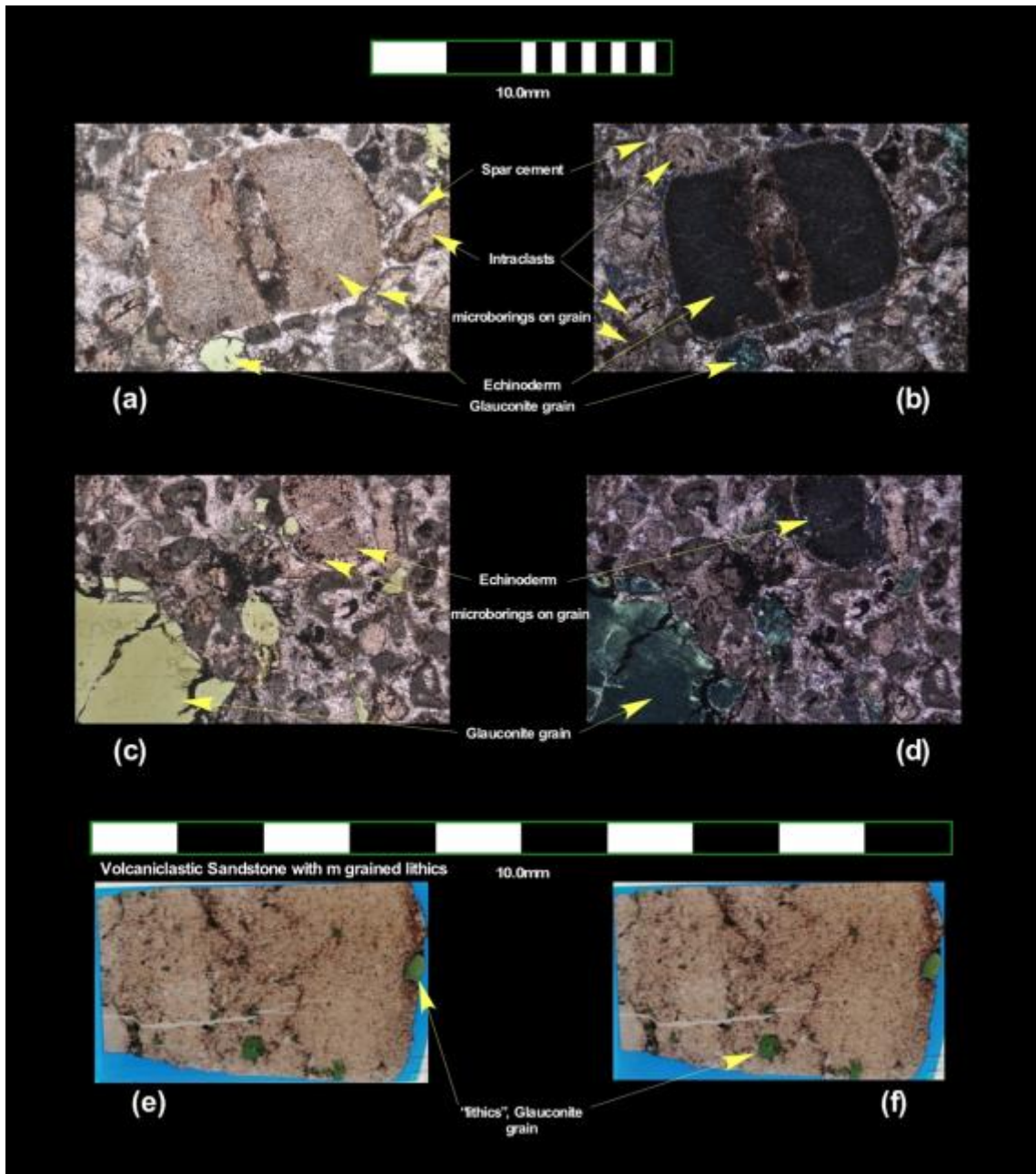


Figure 59: Thin section images of sample from 574.52 m (4/6/12_1), grayish skeletal grainstone, some planktonic foraminifera, spicules and volcanic grains, some skeletal fragments with microborings

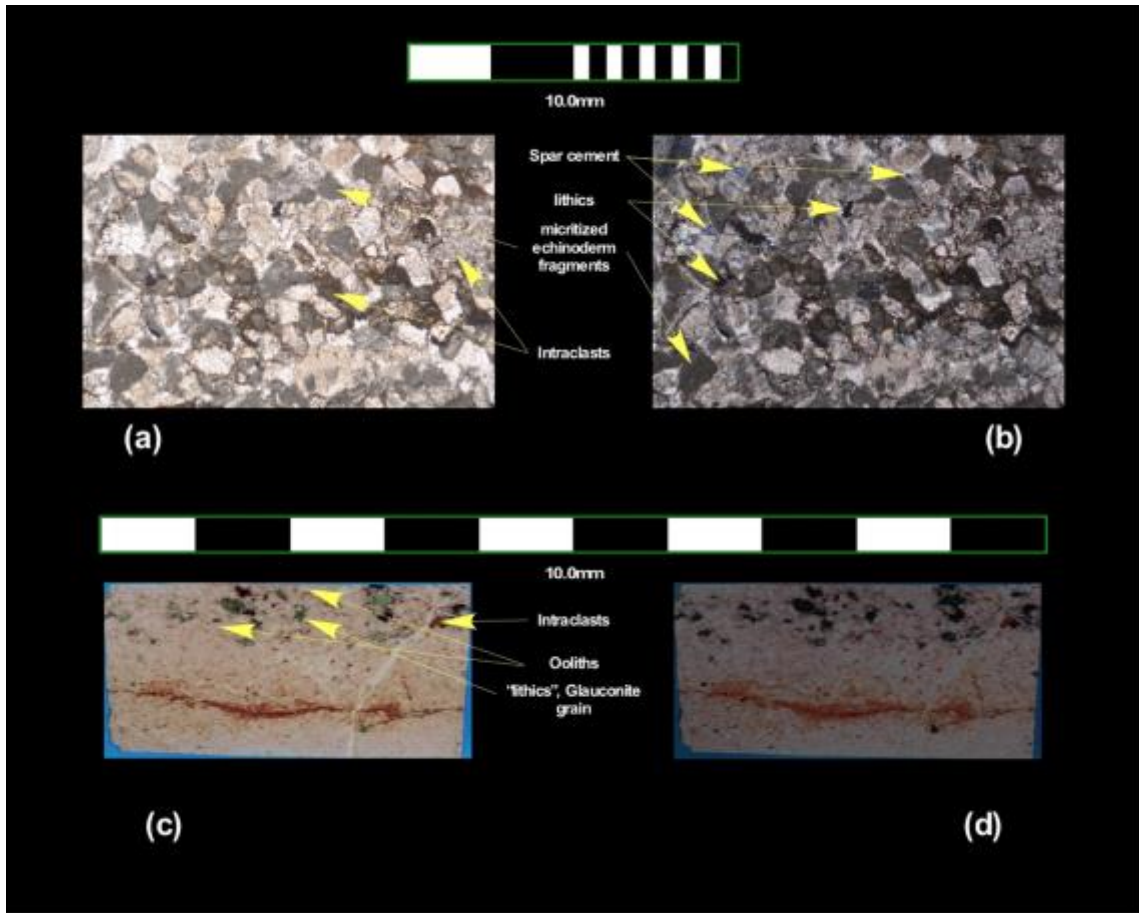


Figure 60: Thin section images of sample from 576.87 m (4/6/12_2), grayish skeletal grainstone, some planktonic foraminifera, spicules and volcanic grains

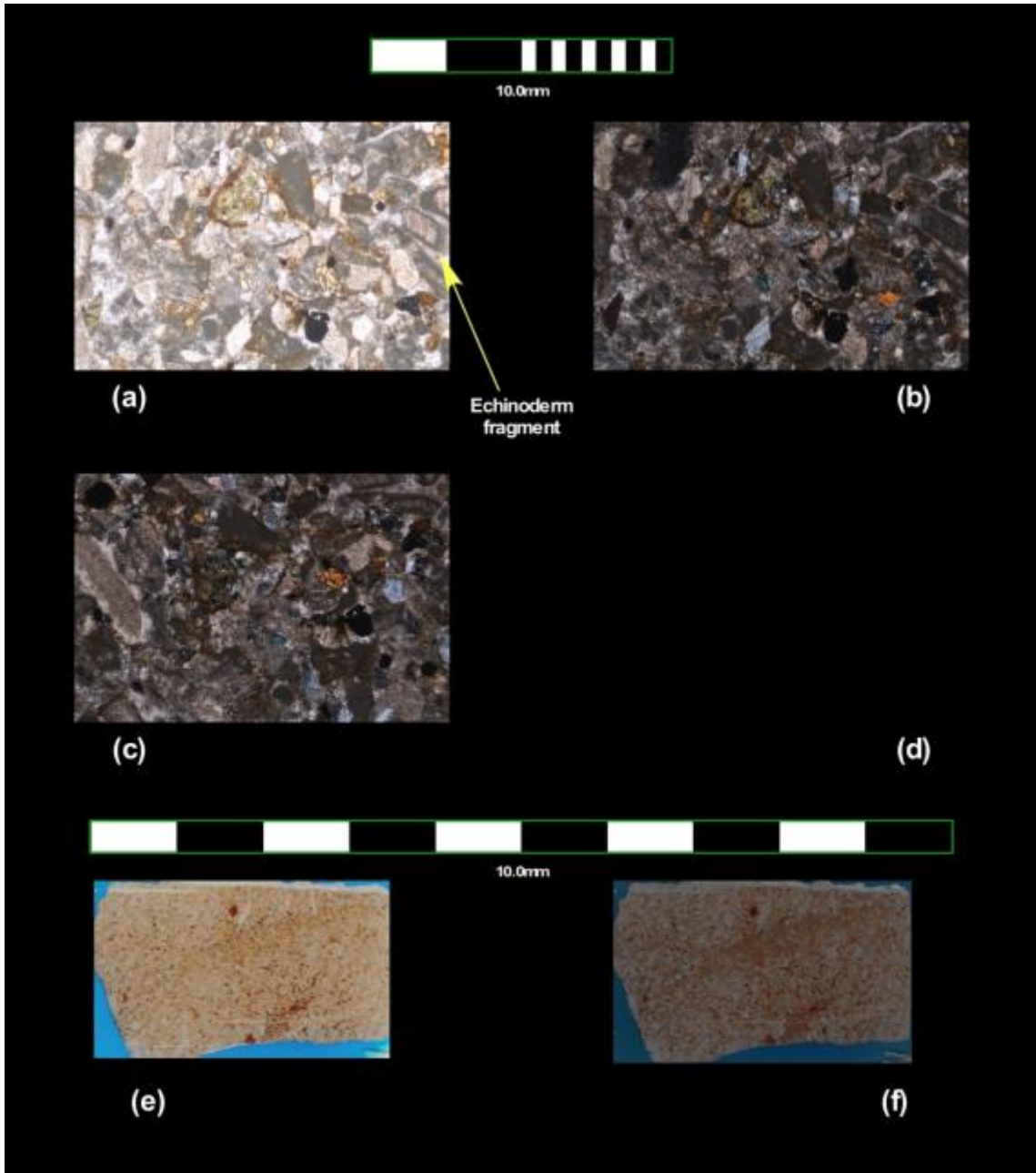


Figure 61: Thin section images of sample from 602.42 m (4/13/12_1), grayish skeletal grain-packstone, some volcanic grains

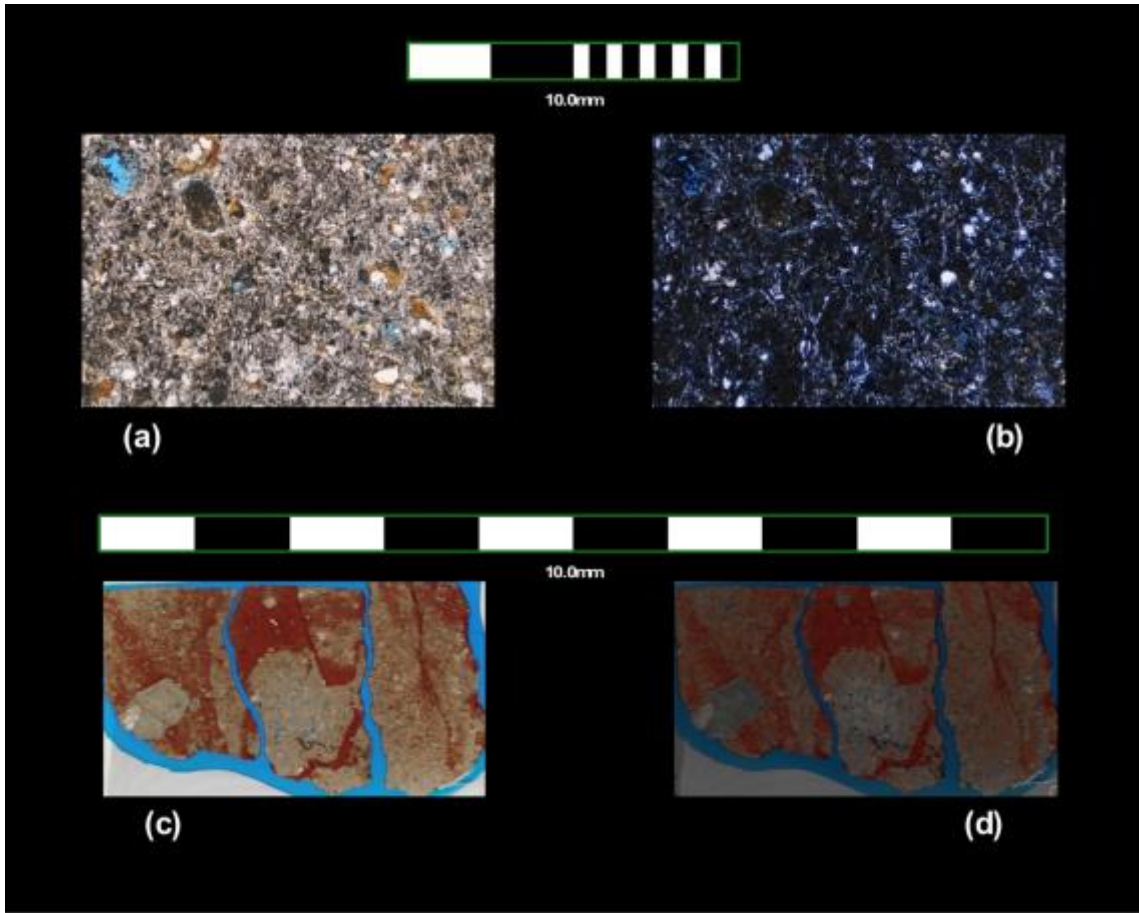


Figure 62: Thin section images of sample from 605.99 m (4/26/12_1), olivine basalt, sub-aerial

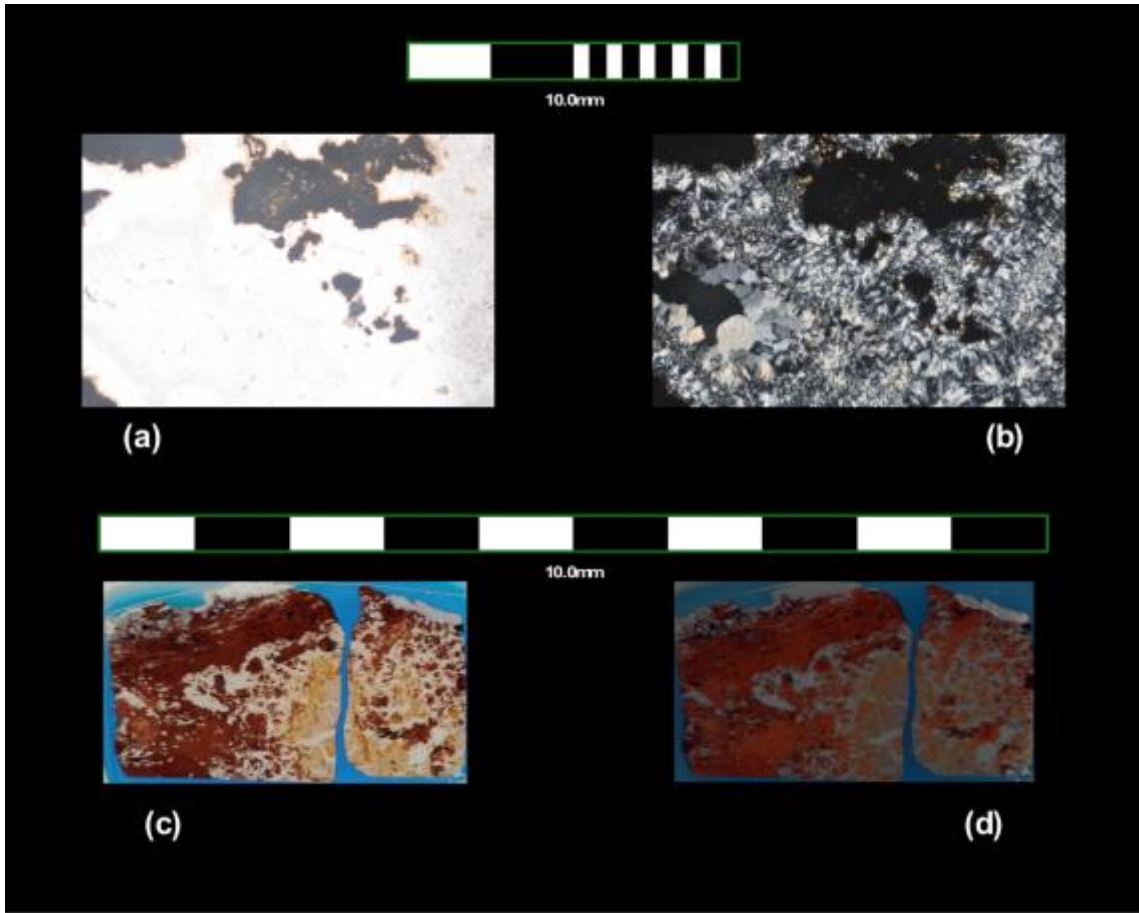


Figure 63: Thin section images of sample from 606.71 m (4/26/12_2), olivine basalt, zeolites, slightly altered

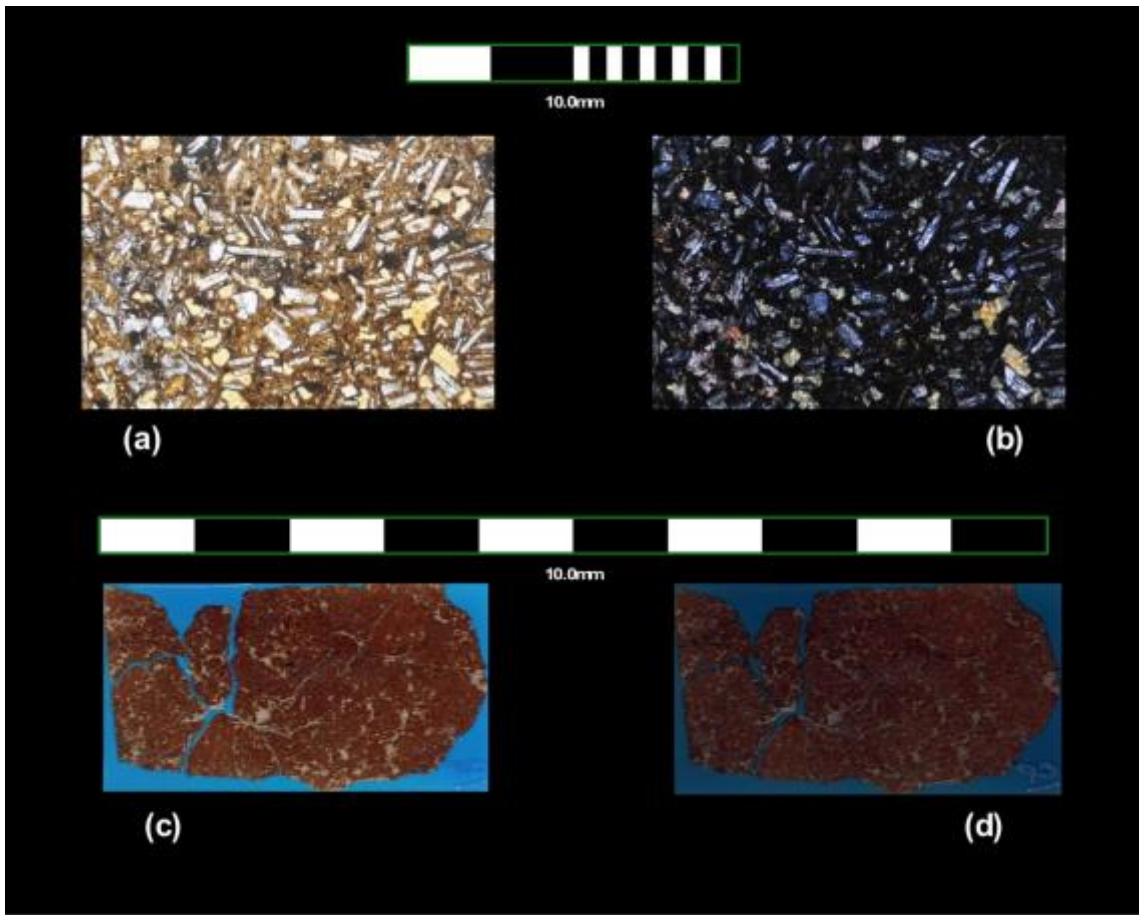


Figure 64: Thin section images of sample from 606.98 m (4/26/12_3), olivine basalt, feldspar porphyry, sub-aerial

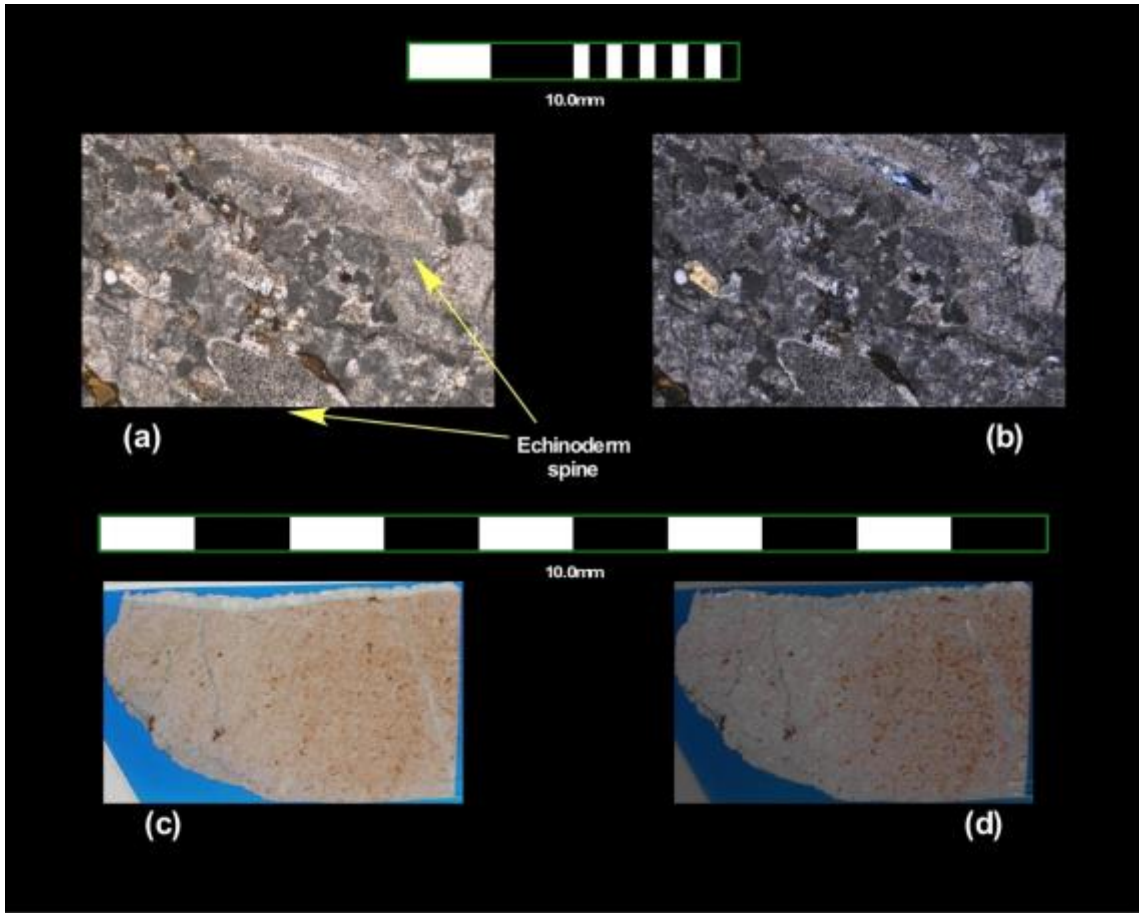


Figure 65: Thin section images of sample from 608.54 m (4/13/12_2), grayish skeletal grain-packstone, some red algae and spicules

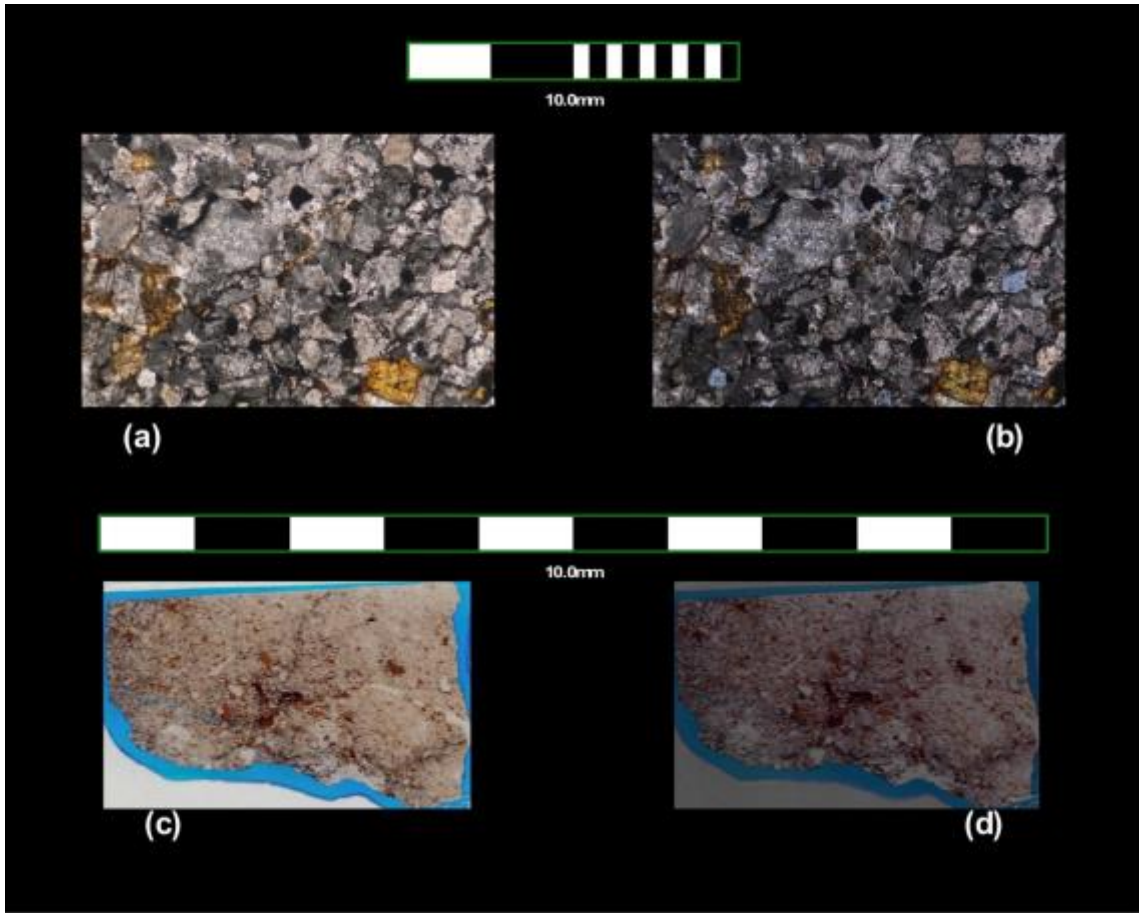


Figure 66: Thin section images of sample from 618.09 m (4/20/12_1), grayish skeletal grainstone, some skeletal fragments with microborings

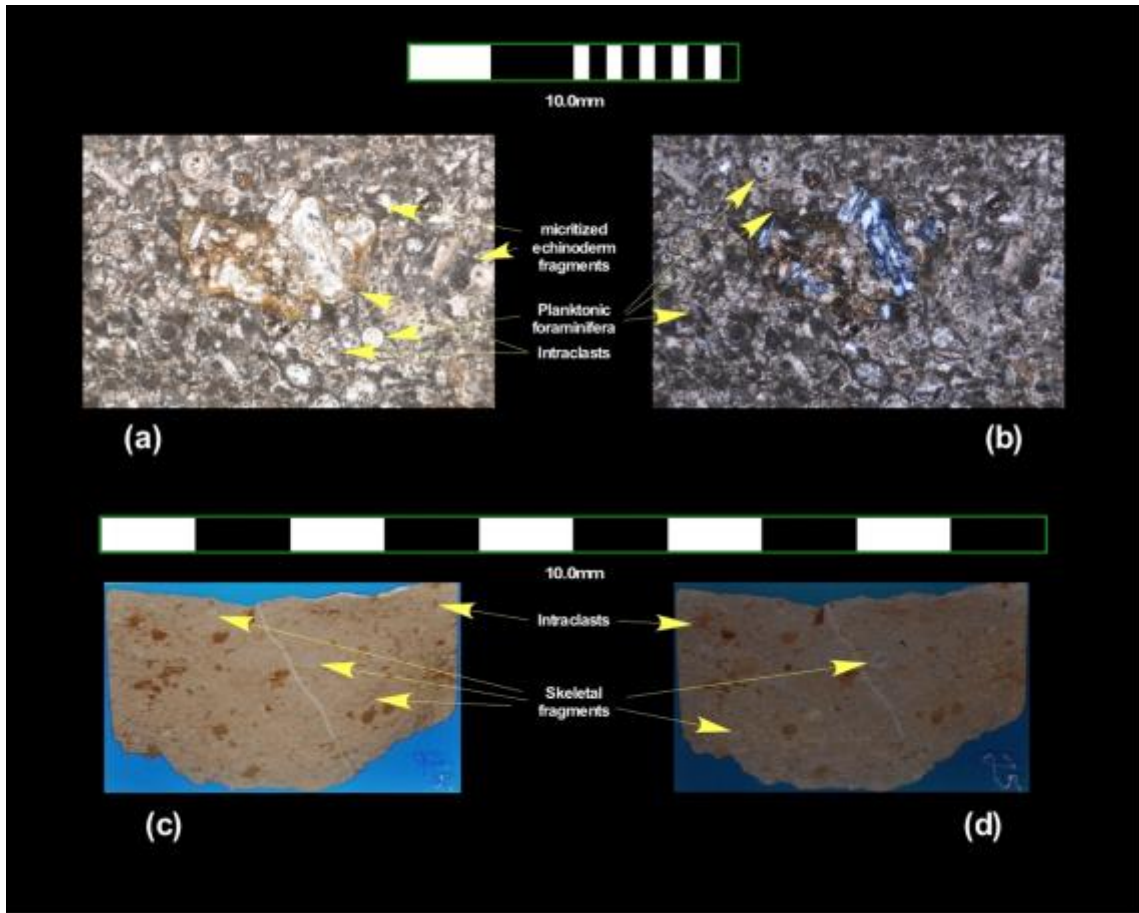


Figure 67: Thin section images of sample from 697.76 m (5/4/12_3b), grayish skeletal packstone, few red algae and few planktonic foraminifera

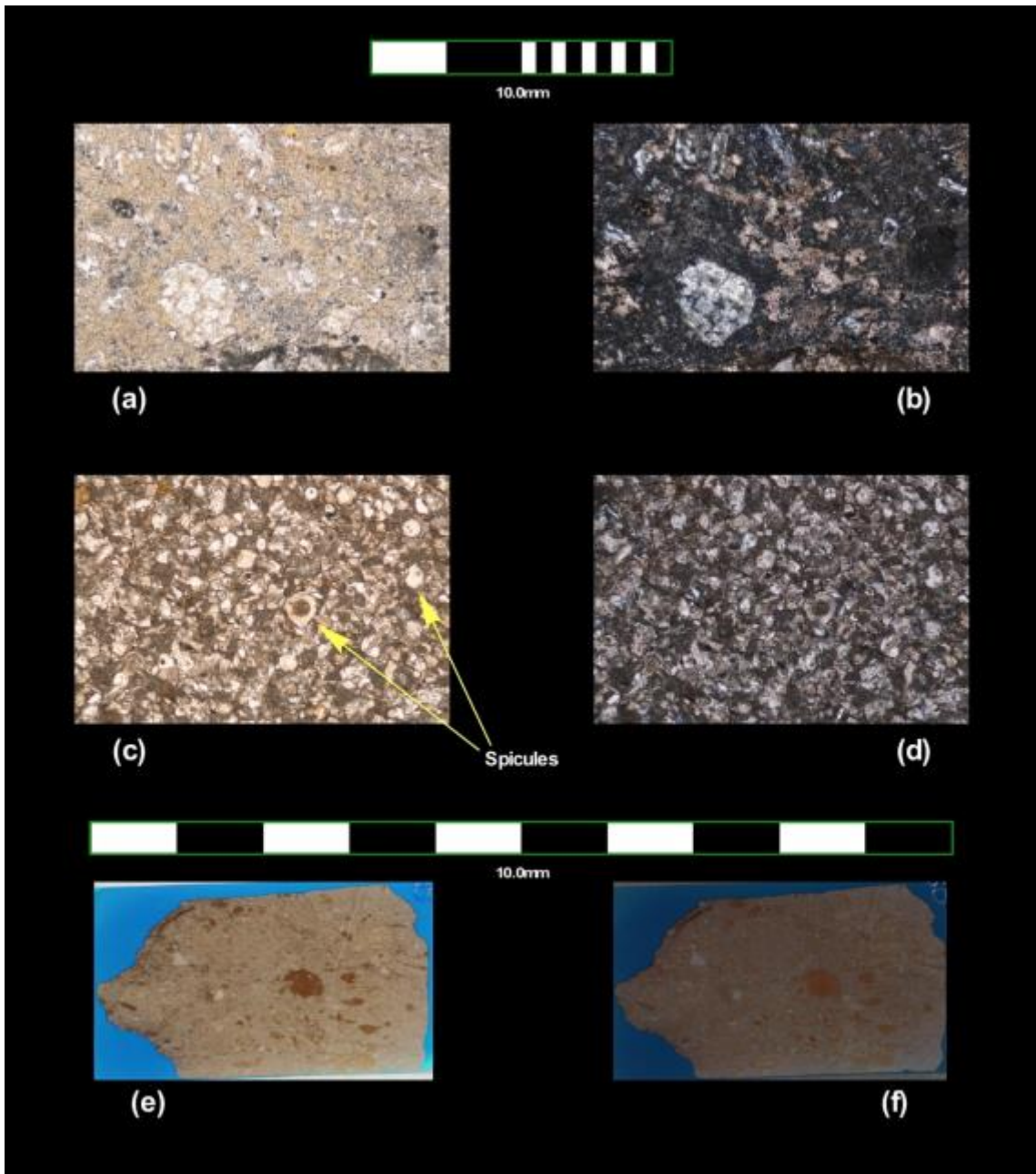


Figure 68: Thin section images of sample from 697.76 m (5/4/12_8), grayish skeletal packstone, few red algae and few planktonic foraminifera

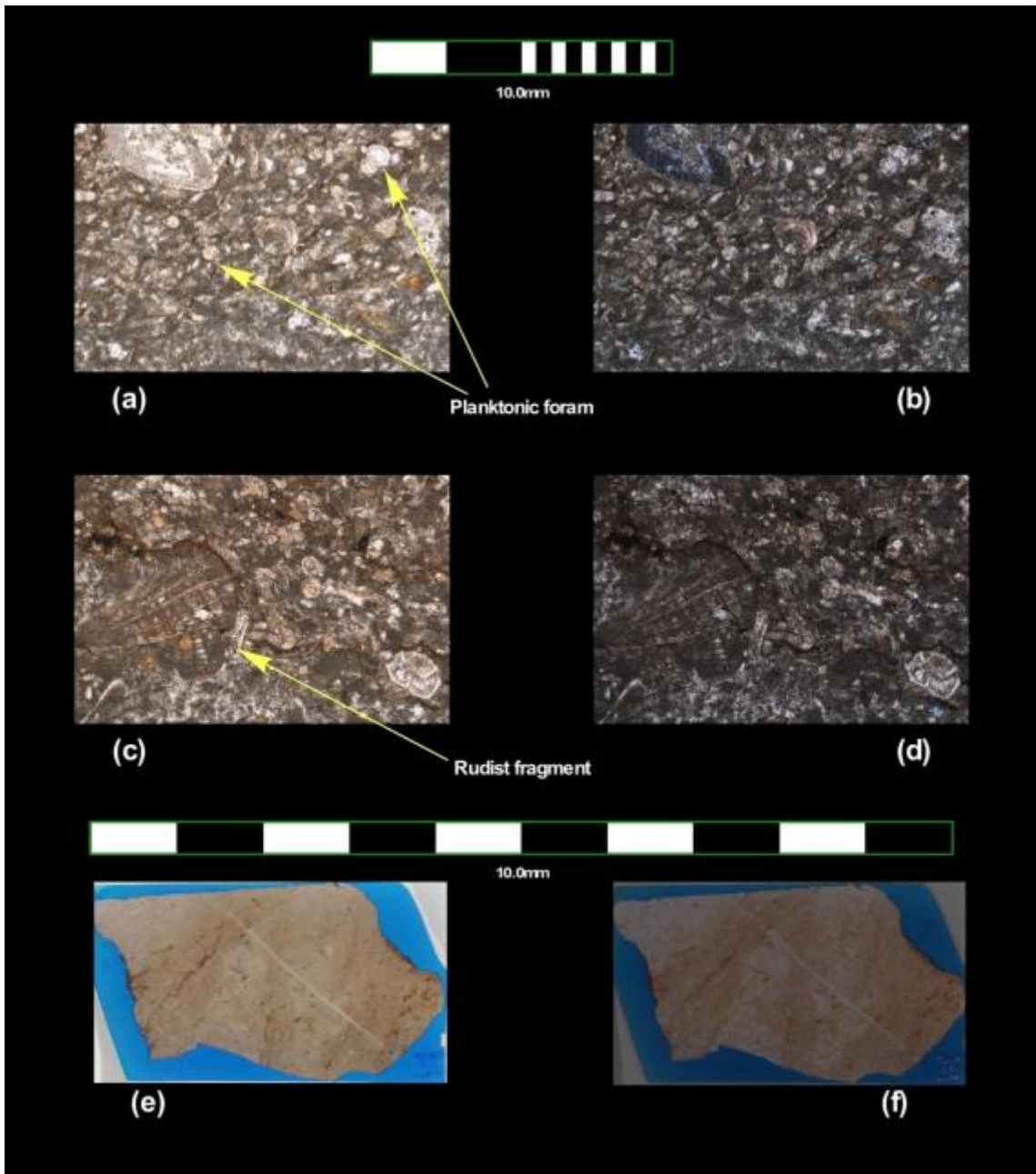


Figure 69: Thin section images of sample from 698.16 m (5/4/12_7), grayish skeletal packstone, some rudists and planktonic foraminifera fragments

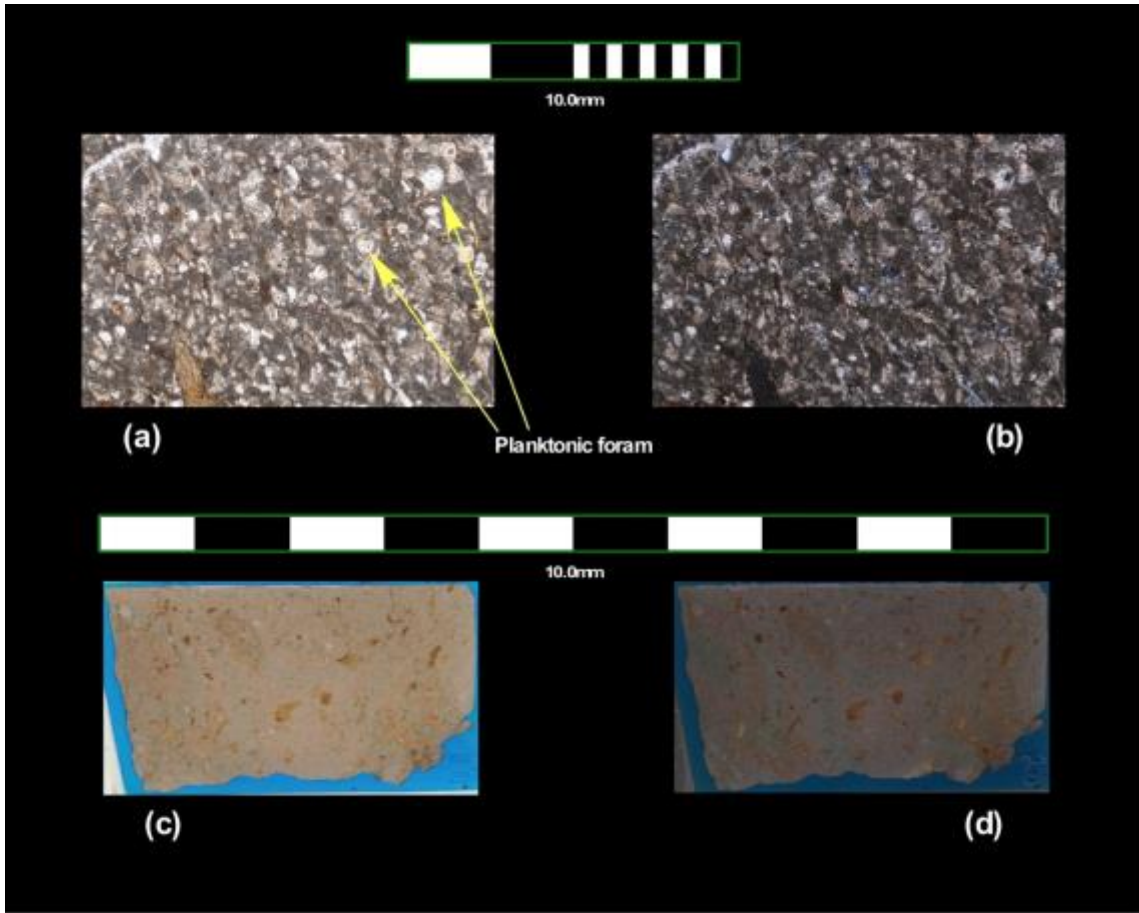


Figure 70: Thin section images of sample from 698.25 m (5/4/12_6), grayish skeletal packstone, some lithics and planktonic foraminifera fragments

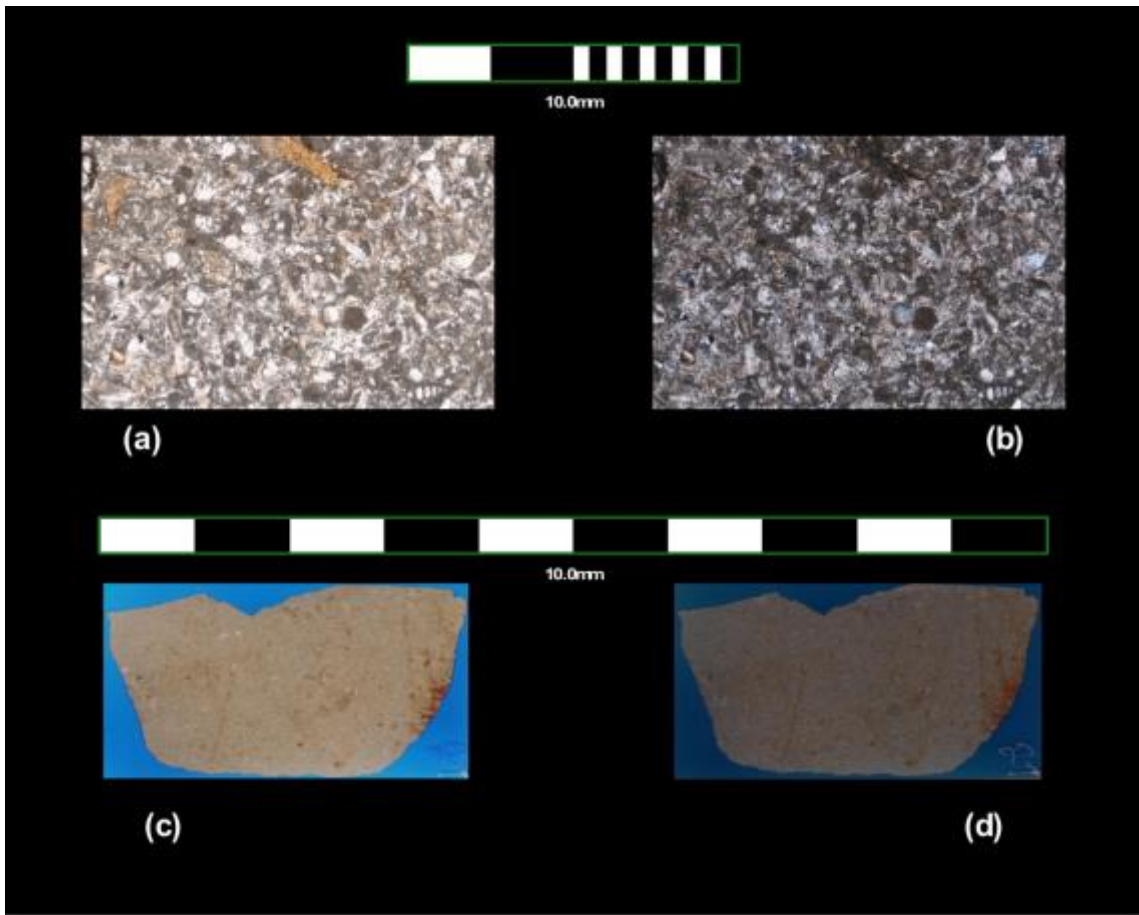


Figure 71: Thin section images of sample from 698.53 m (5/4/12_5), grayish skeletal packstone, some lithics and planktonic foraminifera fragments

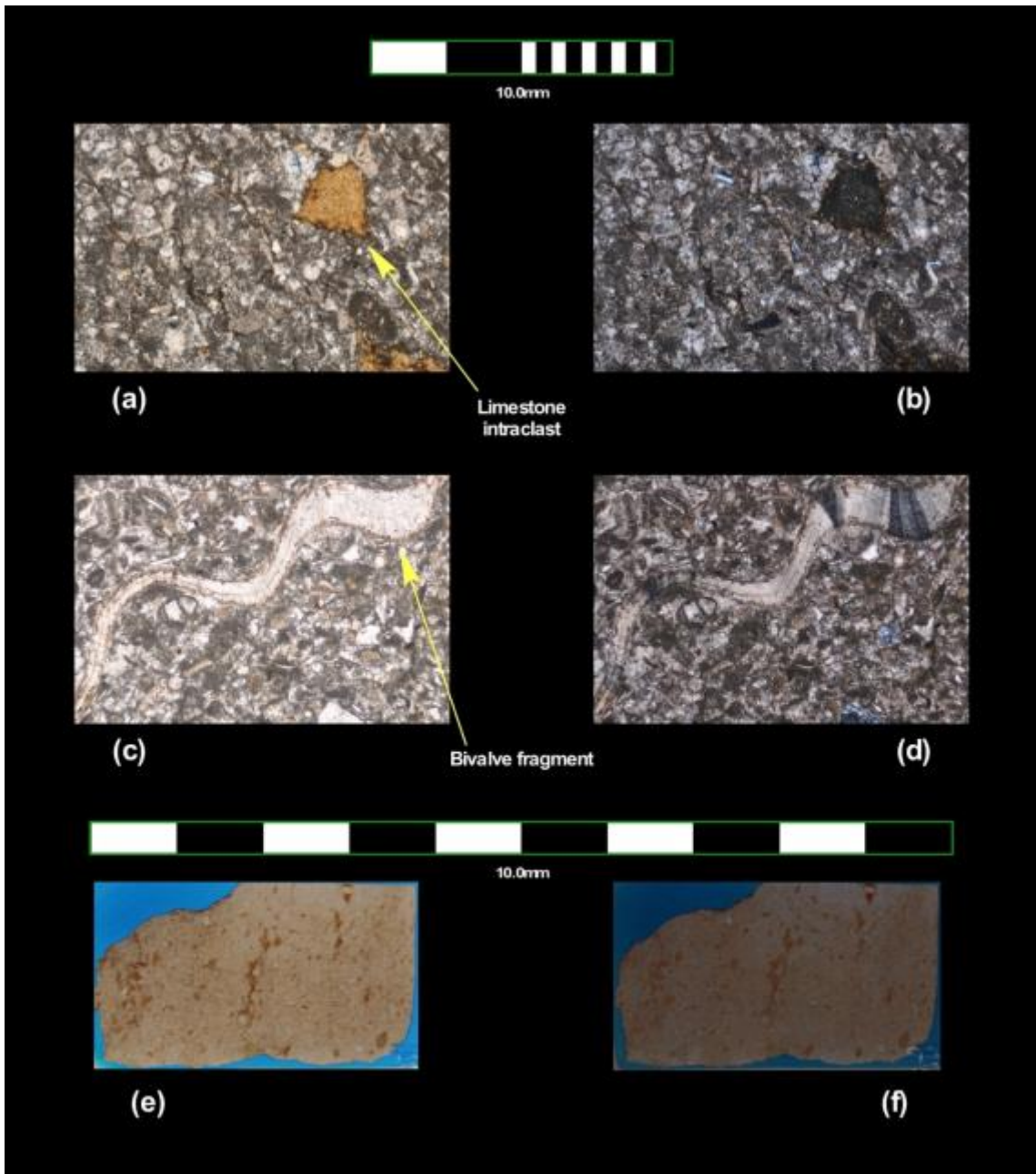


Figure 72: Thin section images of sample from 698.67 m (5/4/12_4), grayish skeletal packstone, some lithics and planktonic foraminifera fragments

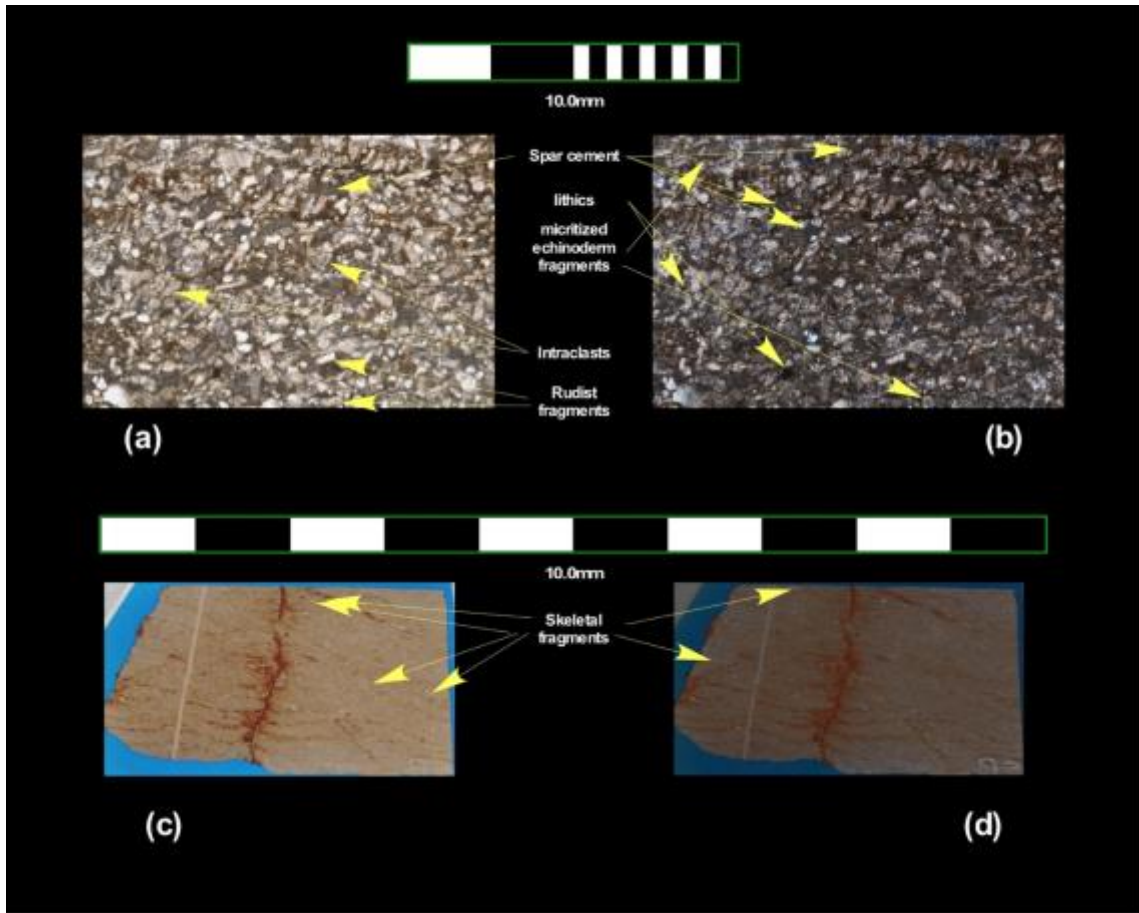


Figure 73: Thin section images of sample from 698.94 m (5/4/12_3), grayish skeletal wack-packstone

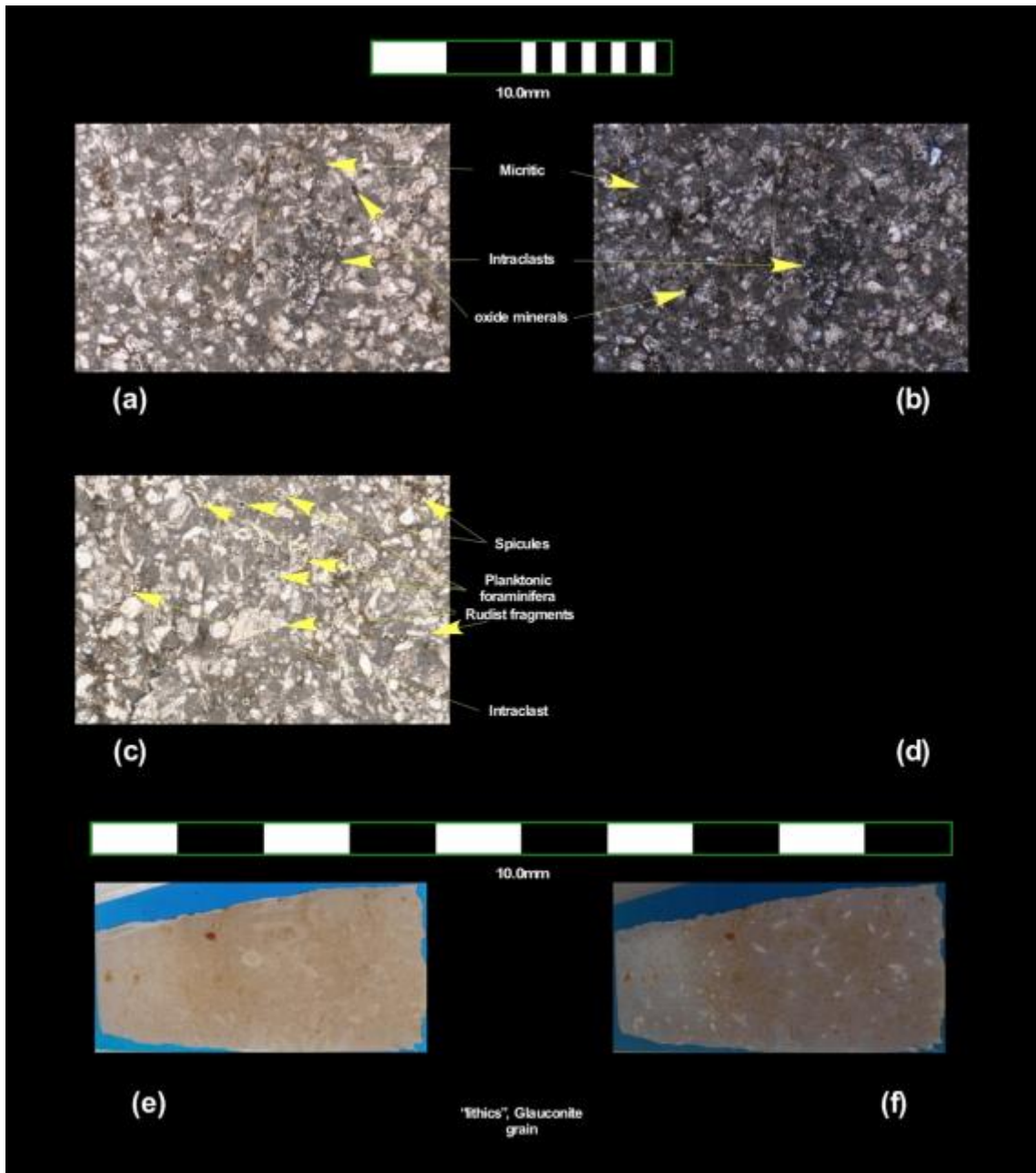


Figure 74: Thin section images of sample from 699.51 m (5/4/12_2), grayish skeletal packstone, some lithics and planktonic foraminifera fragments

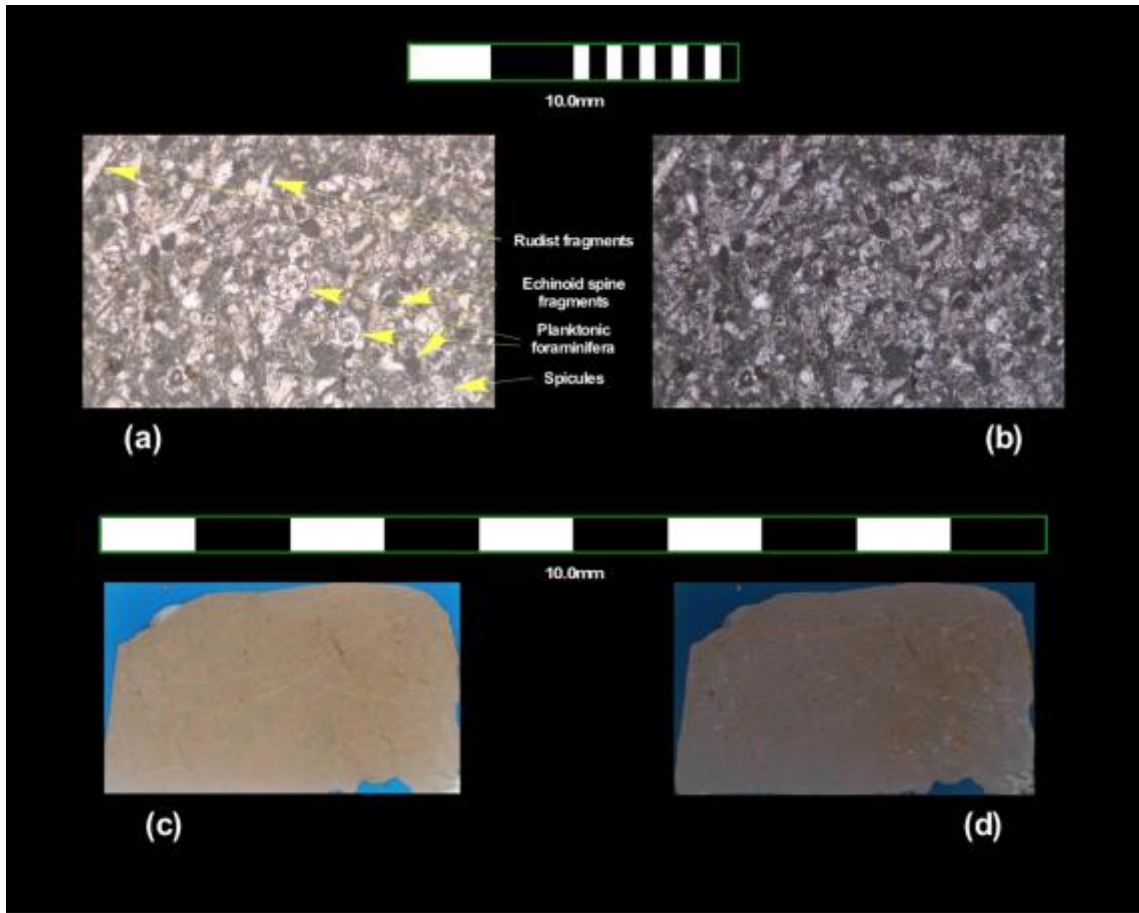


Figure 75: Thin section images of sample from 699.90 m (5/4/12_1), grayish skeletal packstone, some lithics and planktonic foraminifera fragments

Appendix C – Field Photographs



Image 1: Basaltic andesite sub-rounded clasts present near the base of the massive Limestone. Very coarse sand size and gravel size clasts can be seen as well



Image 2: *Barretia* and *Antillosarcolites* sp.



Image 3: *Bournonia* sp. seen in the massive Limestone of the Bahía Fosforescente Member



Image 4: *Stellacaprina* nov. gen. seen in the massive Limestone of the Bahía Fosforescente Member



Image 5: *Durania sp.* seen in the massive Limestone of the Bahía Fosforescente Member



Image 6: *Actaeonella sp.* gastropods seen in the massive Limestone of the Bahía Fosforescente Member



Image 7: View towards the Northeast of the outcrops of the massive Limestone and upper volcanic arenites. This location is an abandoned quarry



Image 8: View of the first deposits on top of the seen in the massive Limestone of the Bahía Fosforescente Member, brown medium grained sandstone with eroded limestone grains and planktonic foraminifera



Image 9: View of the calcarenite block slumped in the brown medium grained sandstone at around 85 m



Image 10: Volcanic arenite with limestone intraclasts. Near the start of the first Lowstand System Tract at 113 m



Image 11: Volcaniclastic event, very coarse sand and pebble size sediments, sub-rounded, little to no matrix at around 300 m



Image 12: Volcaniclastic event, very coarse sand and pebble size sediments, sub-rounded, little to no matrix, sample from 300 m



Image 13: Volcaniclastic event, some local stratification at 385 m



Image 14: View of the change in stratigraphy at 548.68 m



Image 15: View of the rock that outcrops around 564.56 m. The rock was first described as a very fine grained sandstone with lithics but refined with thin sections as alternating skeletal packstone to grainstone with some lithics



Image 16: View of the outcrop where the section from 615.78 m to 621.72 m was measured



Image 17: View of the dark gray fine volcaniclastic sandstone at 615.78 m. At 0.8m higher the reddish altered silicified material, red siliceous mudstone



Image 18: View of the rock at 616.81 m described as a very fine to fine sandstone



Image 19: View of the outcrop at the end of the section. It encompasses from 659.02 m to 700.81 m of the stratigraphic section